Design and Application of Meta-Heuristic Algorithms for Engineering Optimization in Renewable Energy Systems

by

Haichuan YANG

A dissertation

submitted to the Graduate School of Science and Engineering for Education

in Partial Fulfillment of the Requirements

for the Degree of

Doctor of Engineering

Supervisor: Prof. Zheng Tang

Associate Supervisors: Assoc. Prof. Shangce Gao

University of Toyama

Gofuku 3190, Toyama-shi, Toyama 930-8555 Japan

2022

(Submitted October 27, 2022)

Acknowledgements

First of all, I would like to thank my family for their support, which enabled me to maintain high morale in the research process. Secondly, I would like to thank the University of Toyama. It is the superior research conditions provided by the University of Toyama that ensure the advancement of research. Finally, and most importantly, I would like to thank the teachers of the artificial intelligence research laboratory for their earnest teachings, which have created my growth and progress today.

Abstract

Recent shocks such as COVID-19 and the Russia-Ukraine War have shifted the focus of many countries' energy policies to energy security goals. Since the East Asian countries, represented by Japan, are generally well-developed in manufacturing and short on energy, the use of renewable energy has become the focus of research. As an important global optimization technique in artificial intelligence, meta-heuristics have proven to be an effective tool for addressing the engineering optimization problems in renewable energy systems, such as the position optimization problem of wave energy converters (WEC) and the wind farm layout optimization problem (WFLOP). The focus of this study is to investigate and design meta-heuristics in more depth so that they can be better used in the field of renewable energy optimization and can improve energy conversion efficiency. The research is divided into two aspects: one is to develop new meta-heuristics, and the other is to improve existing meta-heuristics into heuristics according to the characteristics of the problem being optimized. Therefore, the spatial information sampling algorithm (SIS) and the improved spherical evolution (ISE) algorithm are proposed successively. The results of SIS and ISE are tested on the WEC and the WFLOP, respectively. In WEC, the energy conversion efficiency of SIS is improved by 22.46%, 107.53%, 99.82%, and 2.54% relative to the existing method for four wave conditions: Tasmania, Adelaide, Perth, and Sydney. The experimental results on WFLOP show that the average conversion rate of ISE is 93.64%, 89.45%, and 97.22% for the three wind conditions of single wind direction, four wind directions, and six wind directions, respectively. The Wilcoxon signed-rank test, Wilcoxon rank-

sum test, and Friedman test results show that SIS and ISE perform significantly better than the other state-of-the-art algorithms in terms of global optimality, avoiding local minima, and solution quality.

Keywords—meta-heuristic algorithms, renewable energy, exploration and exploitation

Contents

List of Figures

List of Tables

Chapter 1

Introduction

Addressing optimization problems is crucial in the study of a wide range of scientific and engineering issues [1–3]. When it is difficult or impossible to find the optimal solution to a problem, such as NP-hard problems [4], a heuristic method [5] is one way of quickly arriving at a viable solution. It is a strategy that provides feasible solutions in a reasonable amount of time and space but does not guarantee the best solution. A meta-heuristic [6] is a generalized heuristic method that can be applied to a broader range of situations than the specific conditions of a particular problem. Obviously, the quality of the solution of the heuristic is superior to that of the meta-heuristic with a high probability in the face of a particular problem.

Since the features of NP-hard problems, especially black-box optimization problems, are difficult to obtain, researchers can only brute force the optimized problem by designing a large number of meta-heuristics. This situation does not always imply a positive meaning. Authors often propose improvements to existing methods and compare them with non-improved versions or similar "novel" methods that show better convergence and properties. The meta-heuristic community already has researchers who argue that applying novel methods or new paradigms proposed for the first time to known problems is not a promising area of research [7, 8]. This situation can also be referred to as the "alchemical dilemma" [9], where people keep improving their meta-heuristics without being able to explain why they are so improved. This

has further led to the selection and improvement of algorithms lacking a theoretical basis and highly dependent on researcher experience, which ultimately pushes up the time and economic costs. This issue is particularly prominent in the field of optimization studies of renewable energy systems. To address this problem, in this study, we propose a spatial information sampling algorithm (SIS) and an improved spherical evolution (ISE) based on exploitation and exploration theory and population interaction network theory. The results of the experiments on the position optimization problem of wave energy converters (WEC) and wind farm layout optimization problem (WFLOP) show that SIS and ISE perform significantly better than the other state-of-the-art algorithms. In WEC, the energy conversion efficiency of SIS is improved by 22.46%, 107.53%, 99.82%, and 2.54% relative to the existing method for four wave conditions: Tasmania, Adelaide, Perth, and Sydney. The experimental results on WFLOP show that the average conversion rate of ISE is 93.64%, 89.45%, and 97.22% for the three wind conditions of single wind direction, four wind directions, and six wind directions, respectively.

The rest of the paper is organized as follows: Two important theories of metaheuristics are introduced in Chapter 2. The engineering optimization problems of renewable energy are introduced in Chapter 3. The proposed spatial information sampling algorithm is introduced in Chapter 4. The spherical evolution and its improvement method are introduced in Chapter 5. The experimental results and analysis are introduced in Chapter 6. The discussions are introduced in Chapter 7. Chapter 8 contains the conclusions and recommendations for future work.

Chapter 2

Two important theories of meta-heuristics

2.1 The balance of exploitation and exploration

In fact, the theoretical research related to meta-heuristics is not a desert, and the balance between exploitation and exploration is one of the most important theories [10]. In meta-heuristics, there are two extremely important properties: exploitation and exploration. According to [11], the term "exploitation" refers to the idea of focusing the search process on a localized but promising area of the solution space, whereas the ability of an algorithm to discover a diverse array of solutions spread across different regions of the search space is emphasized by the term "exploration". The design of meta-heuristics is divided into three operations and four schemes, as shown in Fig. 2.1. In the figure, the design process of meta-heuristics is mainly divided into two steps: 1) The appropriate operations are screened from the three operations as the meta-heuristics parts. 2) Then the appropriate scheme is selected to assemble these parts and finally realize the balance of exploitation and exploration.

According to [11], there are three main ways to realize exploitation and exploration operations: selection, attraction, and perturbation operations. The selection is an operation that emphasizes exploitation and aims to select excellent solutions from the population, integrate them into the next iteration process, or implement

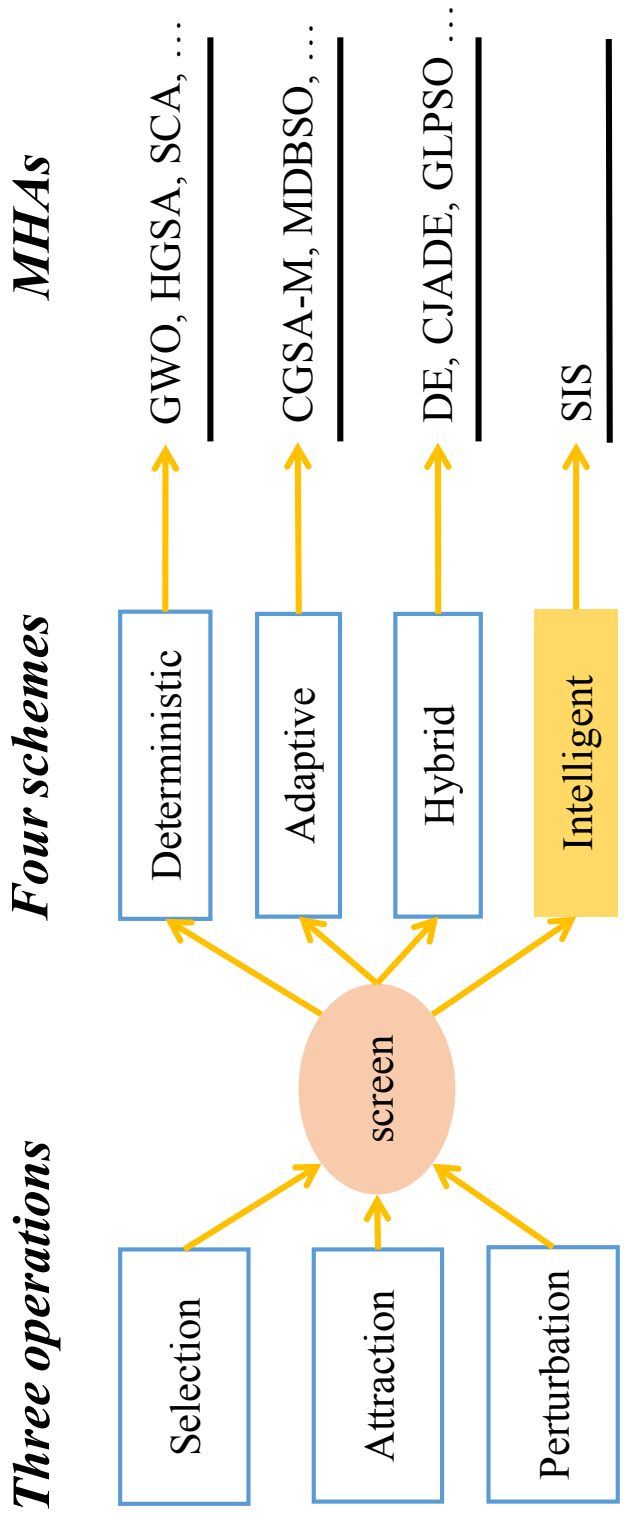

Figure 2.1: Design process and classification of meta-heuristics.

some solution update strategies. Differential evolution (DE) [12] and cuckoo search (CS) [13] are the typical algorithms using such a selection mechanism. Attraction is an operation that emphasizes exploitation and aims to promote other individuals in the population to move closer to the position of the seemingly "good" individuals or move them to the position of the current best individuals found so far to improve the population. Particle swarm optimization (PSO) [14] and grey wolf optimizer (GWO) [15] are typical algorithms using attraction operation. In addition, some algorithms, e.g., the gravitational search algorithm (GSA) [16], also consider the compound attraction effect among multiple individuals. The dynamic neighborhood learning-based gravitational search algorithm (DNLGSA) [17] is an improvement of GSA based on dynamic neighborhood learning technology. In addition, the mutation operation of DE also belongs to this category. The perturbation operation is usually regarded as an exploration-biased operation to modify existing solutions by perturbation, which is often combined with a selection or attraction operation. This perturbation can be implemented on the whole population (e.g., DE and CS) or some individuals in the population (e.g., chaotic maps incorporated grey wolf optimization algorithms (CGWO) [18]). In addition, it should be emphasized that the change in parameters has an important impact on the exploitation and exploration operations. When the change of parameters biases meta-heuristic towards exploitation, it is an attraction operation, and when the change of parameters biases meta-heuristic towards exploration, it is a perturbation operation.

In essence, the balance of exploitation and exploration of meta-heuristics is realized by combining selection, attraction, or perturbation operations. According to [19], we divide the main combination methods into the following three types: deterministic, adaptive, and hybrid schemes. The deterministic scheme determines when to exploit and when to explore before the algorithm runs. For example, the parameters in GWO

and the hierarchical gravitational search algorithm (HGSA) [20] change along with the increment of iteration times so that exploration and exploitation can be carried out in the early and late iterations, respectively. In addition, there are also examples where two mutation operations are performed randomly to perform exploitation and exploration operations, such as the sine cosine algorithm (SCA) [21]. The adaptive scheme performs exploitation and exploration adaptively according to the change in population fitness value or diversity value in the iterative process. For example, the multiple chaoses embedded gravitational search algorithm (CGSA-M) [22] adapts the hyper-parameters according to the change in fitness value, and the multiple diversity-driven brainstorm optimization (MDBSO) [23] uses both fitness and diversity as the basis for adjusting the balance. The hybrid scheme not only combines the selection, attraction, or perturbation operations but also introduces the deterministic scheme or adaptive scheme into one algorithm. It should be emphasized that most meta-heuristics adopt more than one operation at a time, and DE is the most representative example. The mutation, crossover, and selection operations of DE correspond to attraction, perturbation, and selection operations in this paper, and they are combined in a deterministic scheme. An outstanding variant of DE, chaotic local search-based differential evolution (CJADE) [24], adds the adaptive scheme to adjust the algorithm's hyper-parameters on the basis of the hybrid scheme and adds chaotic maps as a perturbation operation, which greatly improves the performance of the algorithm. Genetic learning particle swarm optimization (GLPSO) [25] is another example of combining attraction, perturbation, and selection operations. Alternatively, there is a typical hybrid scheme, such as [26]. In this case, two algorithms with different capabilities are mixed, with the exploitation-biased algorithm performing selection and attraction operations and the exploration-biased algorithm performing perturbation operations.

Although there are already deterministic and adaptive schemes (the hybrid scheme is a mixture of the above two schemes) to achieve the balance of exploitation and exploration, it remains difficult to judge when to exploit and when to explore [19]. The reasons are as follows: 1) The deterministic scheme is relatively simple. This scheme is highly subjective and directly based on the designer's experience. It ignores the information feedback during the operation of the algorithm, which makes it difficult for the algorithm to adjust the strategy along with the changes in the search stage, thus limiting the performance of the algorithm. 2) The design of an adaptive scheme is relatively complex. The adaptive scheme either depends on a threshold or adjusts according to the historical information of fitness value during the operation of the algorithm. The determination of the threshold is difficult and requires repeated experiments. Furthermore, the adaptive scheme based on historical information needs to analyze the change in fitness value in advance and then design an appropriate adaptive scheme according to the analysis results. The above process not only takes a lot of time but also requires the rich experience of designers, and the universality of the algorithm is weakened because the designer obtains information about the optimized problem in the analysis process. Based on the above discussion, it can be concluded that deterministic and adaptive schemes are both prior experience-based schemes that restrict the acquisition and application of information by the algorithm itself, causing the algorithm to stray from the path of "intelligence".

In order to address the above problems, an intelligent scheme is proposed in this study. In the intelligent scheme, the perturbation operation is performed when the current optimal individual appears in the population's periphery. Otherwise, the attraction operation is carried out. Thus, an SIS algorithm that uses an intelligent scheme is proposed. In SIS, the characteristics of the solution space are described by comprehensively comparing and processing the information obtained by individuals

in different positions in the solution space. Then, the attraction scheme or perturbation scheme in the intelligent scheme is automatically activated according to the obtained information. Specifically, the perturbation operation is performed when the current optimal individual appears in the population's periphery. Otherwise, the attraction operation is carried out. The differences between the intelligent scheme of SIS and other schemes are: 1) Difference with the deterministic scheme: Through the processing of solution space information by the intelligent scheme, the algorithm in the running process is adjusted based on the feedback information. Thus, the performance of the algorithm is effectively improved. 2) Difference with the adaptive scheme: The implementation of the intelligent scheme does not require a pre-defined threshold, nor does it require designers to record, analyze, or process any historical fitness value during the iteration. It only needs the algorithm to be adjusted based on the information of solution space. Through this scheme, the dependence of the algorithm on the designer's experience is reduced, and the autonomy and flexibility of the algorithm in a variety of environments are improved.

The main highlights and contributions of SIS can be summarized as follows:

1) In SIS, the ergodicity and specificity of the chaotic map [27,28] are fully utilized to construct a population with a unique internal-external structure, and an intelligent scheme is proposed accordingly.

2) Through the intelligent scheme, the SIS is able to obtain information about the location of the population in the solution space and activate exploitation and exploration operations autonomously by analyzing the obtained information.

3) Through the intelligent scheme, SIS achieves an efficient balance of exploitation and exploration in a smarter way, thus significantly reducing the complexity of the algorithm in the design process and enhancing the flexibility of the algorithm in dealing with various types of complex optimization problems.

4) To validate the performance of SIS, we test it on 30, 50, and 100 dimensions of the CEC2017 benchmark functions, the CEC2011 real-world problems, the artificial neuron training problem, and the position optimization problem of wave energy converters. Experimental results prove that SIS has higher flexibility and competitiveness in solving different problems in comparison with other state-of-the-art algorithms.

SIS is tested on extensive benchmark functions and the position optimization problem of wave energy converters. The result proves that SIS is competitive with the mainstream state-of-the-art algorithms in dealing with a variety of optimization problems.

Although the theories of exploitation and exploration have been very well developed, there are still two drawbacks. One is that the exploitation and exploration of algorithms are difficult to define, and although there are many algorithms claiming that they achieve a balance between exploitation and exploration, there is rarely mathematical proof. The second is that the so-called exploitation and exploration is a tool to describe the nature of the algorithm itself, which is difficult to combine with the problem being optimized.

2.2 Population interaction network

To compensate for the shortcomings of the exploitation and exploration theory, we used the population interaction networks (PIN) to analyze the meta-heuristics . The PIN is proposed based on complex systems. A complex system consists of many components that may interact with each other [29]. In many cases, it is useful to represent such a system as a network, with the nodes representing the components and the links representing their interactions. They can reflect some characteristics of various networks, such as small-world with Poisson degree distribution [30] and scale-free networks with power-law degree distribution [31]. These qualities make

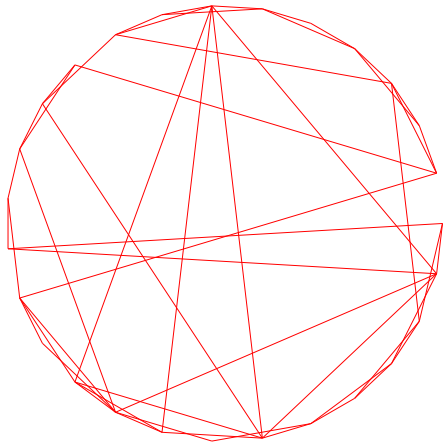

(a) Small-world networks with Poisson degree distribution.

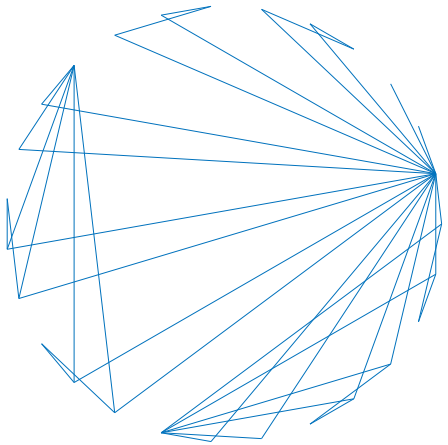

(b) Scale-free networks with power-law (i.e., scale-free) degree distribution.

Figure 2.2: Two typical complex networks.

it easier to comprehend complex network laws and provide explanations for specific real-world phenomena. Thus, as an efficient theoretical tool, complex networks can analyze the essence of research objectives and improve their robustness [32] in many scientific researches [33], such as traffic networks [34], Internet-of-things networks [35], and social networks [36].

By counting and fitting the number of information interactions between population individuals during the iteration of the algorithm, algorithms with two kinds of degree distributions are obtained: algorithms with a Poisson distribution and algorithms with a power-law distribution. According to [30], scale-free networks with power-law distribution increases the likelihood of finding nodes with a lot of links compared to small-world networks with Poisson distribution, as shown in Fig. 2.2. Furthermore, according to our related research on exploitation and exploration [37], "good" individuals with extensive connections in meta-heuristics are more likely to be involved in exploitation-biased attraction operations. Consequently, it can be said that algorithms with the Poisson distribution are more exploration-biased, whereas those with the power-law distribution are more exploitation-biased.

Subsequently, the NP-hard or black-box problems are optimized using these two types of algorithms. When the exploitation-biased algorithm achieves a higher quality solution, it means that this problem is more likely to be a single-peaked problem and that the exploitation capability of the algorithm should be enhanced. When the exploration-biased algorithm achieves better quality solutions, it means that this problem may be more inclined to be a multi-peaked problem and the exploration capability of the algorithm should be strengthened. Based on the above inference, we believe that the emergence of different meta-heuristics makes sense overall. Meta-heuristics with different complex network structures can be used as an effective tool to analyze the features of the problem being optimized. In other words, based on the

PIN, we make an attempt to improve the meta-heuristic into a heuristic, thus further improving the performance of the algorithm on specific problems.

In our previous study of PIN [38], we analyzed the performance of DE and its improved algorithms on the IEEE CEC2017 benchmark function [39]. The conclusion is that biased exploitation algorithms with power-law distributions are more advantageous in CEC2017. In this study, we further validate the role of PIN in the wind farm layout optimization problem (WFLOP). Since this problem is an NP-hard optimization problem containing a large number of constraints [40], it is very difficult to analyze its properties directly. Alternatively, in this study, the PIN is used to analyze the properties of the WFLOP. Then, the spherical evolution (SE) [41] is filtered out and further improved. Extensive experiments are conducted based on various wind scenarios with a single wind direction, four wind directions, and six wind directions under 13 different constraints. Comparative results show that the proposed improved spherical evolution (ISE) performs significantly better than other state-of-the-art algorithms.

The main contributions of this study can be summarized as:

1) In this study, we analyze and categorize the properties of some representative meta-heuristics using complex networks for the first time. This scheme (PIN) can give more insights into the algorithm design for the WFLOP, aiming to improve the optimization efficiency and reduce the time and economic cost of the optimization process.

2) Using PIN, we improve the SE algorithm to address the WFLOP problem. Experimental results prove that ISE outperforms its competitors by a wide margin.

3) This efficient way of improving the meta-heuristic into a heuristic will bring new inspiration to the research in field of optimization algorithms.

Note: Fig. 2.3 displays the PIN of meta-heuristics. In Fig. 2.3 (1), X_i'' is an

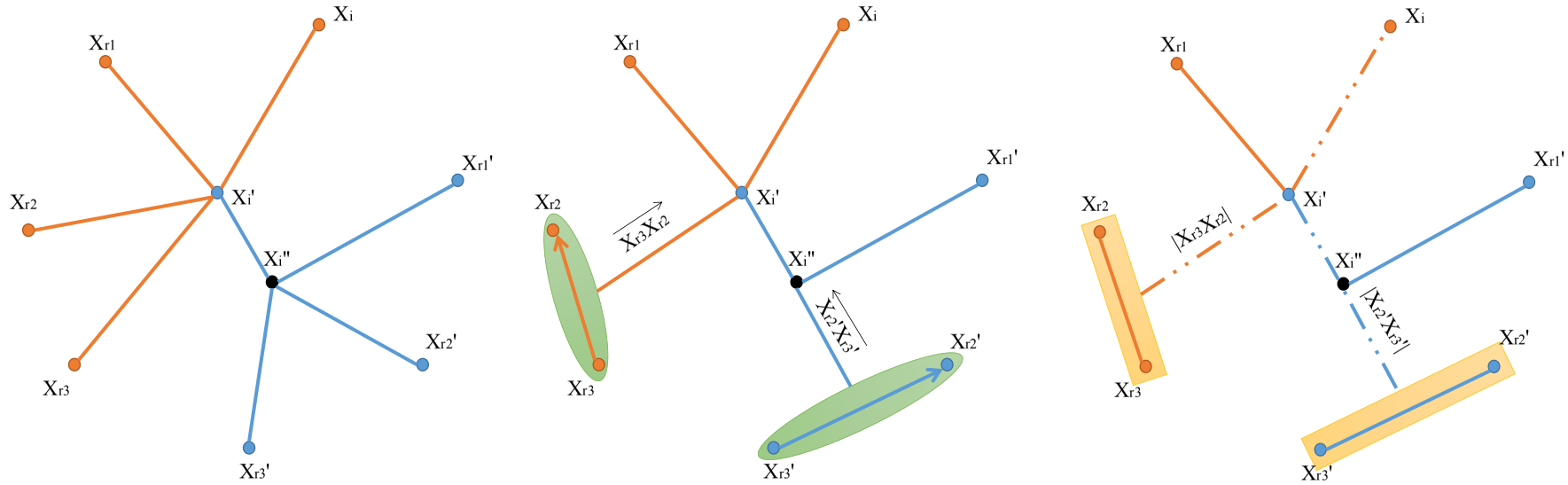

(1) Conceptual diagram of population interaction network in MHAs.

(2) The population interaction network of DE.

(3) The population interaction network of SE.

Figure 2.3: The population interaction networks of meta-heuristics.

offspring of X_i'. The yellow lines represent the network connections of X_i' to its parents X_{r1}, X_{r2}, X_{r3}, and X_i during the update process, and the blue lines represent the network connections of X_i'' to its parents X_{r1}', X_{r2}', X_{r3}', and X_i' during the update process. As a result, at one iteration, the newly generated individuals X_i' and X_{r1}', X_{r2}', X_{r3}', and X_i are related. Subsequently, node X_i' and the four edges (degree) associated with it are recorded in the PIN. Two distribution models are then used to fit the frequency distributions of the recorded data, including Poisson and power-law models.

The Poisson distribution is applied using the maximum likelihood estimation.

1) The Poisson distribution's probability density function can be shown as $p(x_i|\lambda) = \frac{\lambda^{x_i}}{x_i!}e^{-\lambda}$;

2) The likelihood function is $P(X|\lambda) = \prod_{i=1}^{N} p(x_i|\lambda)$;

3) The log-likelihood function is $lnP(X|\lambda) = ln\lambda^{\sum_{i=1}^{N} x_i} - ln\prod_{i=1}^{N} x_i! - n\lambda$;

4) We set $\frac{\partial P(X|\lambda)}{\partial \lambda} = 0$. Then, $\lambda = \frac{1}{N}\sum_{i=1}^{N} x_i$.

According to [42], the power-law model can be constructed. It is written as $P(i) \propto i^{-\alpha}$. where $P(i)$ represents the probability distribution of variable i and i falls within the interval $(1, n]$. α represents the power index, which is described as follows:

$$\alpha = \frac{lnP(i_1) - lnP(i_2)}{lni_2 - lni_1} \tag{2.1}$$

where i_1 and i_2 are two integers from the interval $(1, n]$. In SE and DE, $i_1 = 25$ and $i_2 = 5$. The reason is that nodes with less than 5 edges or greater than 25 edges are almost unrepresentative. Thus, we exclude them to calculate the power index α. It is important to note that the PIN only includes individuals who interact with one another. Although their edges and nodes are recorded, no operation's precise

form is ever recorded. The PIN can therefore be used to study a wide range of meta-heuristics.

Chapter 3

Engineering optimization problems of renewable energy

3.1 The position optimization problem of wave energy converters

Renewable energy will be critical in meeting global energy demand in the future. Because of the high energy density of waves, wave energy is one of the most promising forms of renewable energy currently available [43]. Wave farms consist of multiple buoys in order to be commercially viable. Our research looks into the design of a wave farm made up of an array of fully submerged tri-series buoys [44] that mimic the hydrodynamic behavior of fully submerged three-tether wave energy converters (WECs) in irregular directional waves. In a wave farm, the position of the buoys largely determines the output. However, due to the complicated hydrodynamic interactions between converters, optimizing buoy placement becomes more difficult as the number of converters grows, and evaluating each layout is time-consuming. These problems necessitate the use of search MHAs that can accurately optimize buoy configurations with a small number of evaluations. Fig. 3.1 depicts the WECs. The inclined taut tethers connect a fully submerged spherical buoy to three independent power take-off units in this converter. The power take-off system's tripod configu-

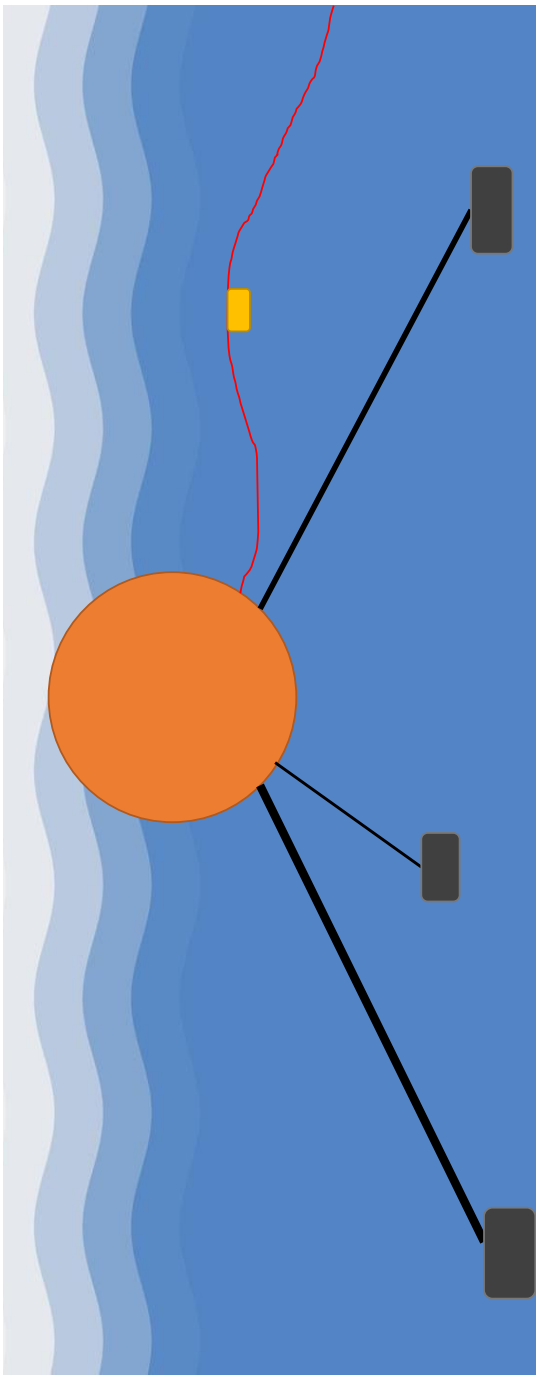

Figure 3.1: wave energy converter.

ration allows power to be absorbed from all three translational degrees of freedom: surge, sway, and heave [45].

The optimization problem can be viewed as optimizing a set of N WECs positions to achieve the maximum total output value P^* in a bounded wave field Ω.

$$P^* = argmax_{x,y} P(x_i, y_i) \tag{3.1}$$

where $P(x, y)$ is the sum of the mean power output by buoys placed at x and y coordinates in a given area. The number of buoys is $N = 4$. Each buoy i's position is expressed as the coordinate: $[x_i, y_i]$, so a 4-buoy array is represented as $[(x_1, y_1), (x_2, y_2), ..., (x_4, y_4)]$ and the decision variable size is $2 \times N$.

3.2 Wind farm layout optimization

The effective use of wind power is an important means to ensure energy security as it is an important part of renewable energy [46]. Due to a single wind turbine's limited energy output, wind power generation typically takes the form of a wind farm, where many wind turbines are installed on a large scale to maximize the wind power at a specific site. However, clustered wind turbines introduce the issue of a wake effect [47] from upstream turbines to downstream turbines, reducing downstream turbine power output. In order to attenuate the wake effect and enhance the power output of wind farms, the wind farm layout optimization problem (WFLOP) [48] has become a current research hot spot. WFLOP is to maximize conversion efficiency in a wind farm by minimizing the power loss due to the wake effect between wind turbines. It is realized by optimizing the positioning of the wind turbines. Usually, the conversion efficiency is not the only factor to be considered and its maximization should be combined with the minimization of costs [48] since wind turbine planning

Table 3.1: Nomenclature used in Chapter 3.2.

Symbol	description
P_1, P_2, P_3	Three different wind profiles
θ	The wind direction
I	The number of square cells
i	The index labels to indicate the index of each cell
X_i, Y_i	The column and row indexes of 2-dimensional coordinate system
S_c, S_r	The number of cells in a column and a row
M_s	The matrix of all cells in a standard 2-dimensional coordinate system
M_a	The matrix of all cells in an actual location coordinate system
C	The cell width
D_c	The dimension of the original D after the dimensionality reduction operation
M_a^θ	The matrix of all cells in an actual location coordinate system with a wind direction
v_0	The ambient wind speed
v_1	The wake wind speed just behind the wind turbine
v_2	The wake velocity at downwind distance d
r_0	The rotor radius of the wind turbine
r_1	The the wake effect radius at downwind distance d
α	The dimensionless scalar
h	The wind turbine's hub height
s	The surface roughness of the wind farm area
v_i	The actual wind speed at wind turbine i under multiple wake effects
$v_{i,j}$	The wind speed of turbine i only taking consideration of the wind turbine j's wake effect
A	The indices set of all the wind turbines in the upwind direction of turbine i
W	The output power of $GE1.5sle$ wind turbine
X	The feasible layout for a wind farm
n	The total number of wind turbines
$E(\cdot)$	The sum of the power
$T(\cdot)$	The total cost
η	The conversion efficiency
$r(v)$	The wind turbine's rate power output at wind speed v

is an economical project. When dealing with the WFLOP, two major types of wind farm layout models are typically used: the grid-based model and the unrestricted coordinate model [49]. The former only allows wind turbines to be placed in a limited number of locations, while the latter allows wind turbines to be positioned anywhere in the wind farm, subject to some constraints. Although the unconstrained coordinate model can be optimized with a slightly improved fitness and leads to a slight increase in the optimal number of turbines, the grid-based model is more widely used since it is computationally efficient [49].

In recent decades, meta-heuristics have proven to be an effective tool for addressing WFLOP problems [50]. Among meta-heuristics, genetic algorithms (GAs) [51,52] and their improved versions [53, 54] are the most dominant and typical ones. According to [40], GAs are used in more than 75% of WFLOP studies. In addition, there are also many other algorithms that are widely used, such as particle swarm optimization [55, 56], ant colony optimization [57], lazy greedy algorithm [58], and multi-objective evolutionary algorithms [59]. However, the rift between the research fields of WFLOP and meta-heuristics has continued to expand [60]. On the one hand, with the continuous research on meta-heuristics, a large number of new algorithms have emerged [18, 61–65]. On the other hand, each WFLOP has different features due to their differences in wind speed, type of wind turbines, wind directions, and constraints in different regions, and this has led to a large number of wind farm layout problem models [40, 66–71]. According to the "No-Free-Lunch Theorem" [72], it is unrealistic to expect to find the most suitable algorithm for all the WFLOPs. The issue of how to filter and improve the existing algorithms so that they can better address WFLOP has become a major challenge for research.

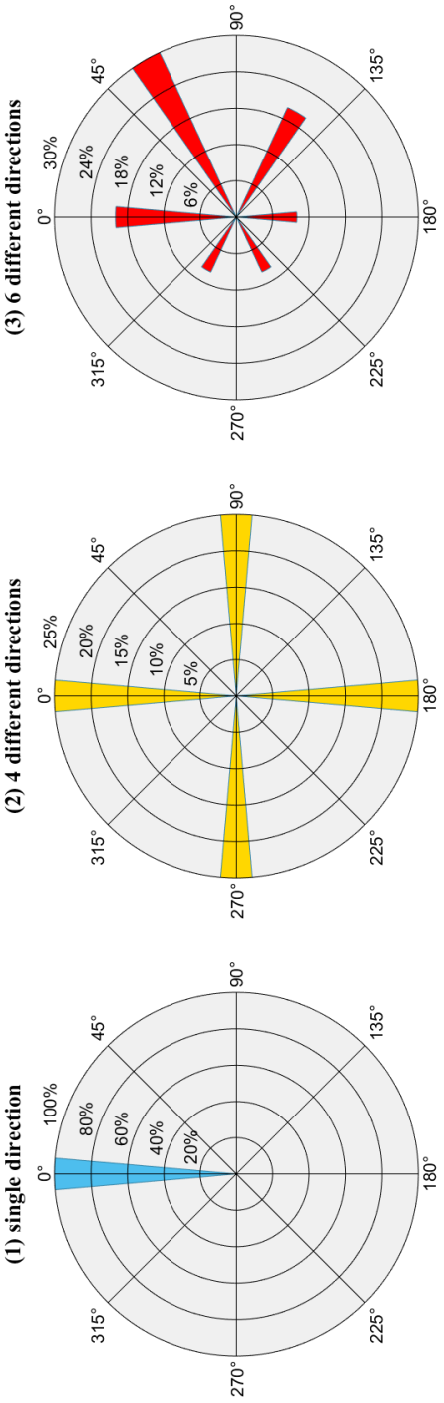

Figure 3.2: 3 types of wind conditions.

3.2.1 The wind condition model

Within wind farm layout problem models, there are usually five sub-models: the wind condition model, the wake effect model, the wind turbine model, the wind farm land model, and the wind farm cost model. In this study, we use the wind farm layout problem model with consideration of participation among landowners proposed in [71]. This model takes into account land use constraints well and thus has good implications for the optimization of wind farms in different regions. Table 3.1 lists the nomenclatures used in Chapter 3.2.

3.2.2 The wind condition model

In the model of [71], we chose three different wind profiles, including a single direction, four, and six different directions with a speed of $13m/s$. They are denoted as P_1, P_2, and P_3 respectively. Wind distribution P_1 have a single wind direction with $\theta = 0$, as summarized in Fig. 3.2 (1). Wind profile P_2 has 4 wind directions, $\left\{0, \frac{\pi}{2}, \pi, \frac{3\pi}{2}\right\}$, each with a probability of occurrence of 25%, as given in Fig. 3.2 (2). Wind distribution P_3 has 6 wind directions, $\left\{0, \frac{\pi}{3}, \frac{2\pi}{3}, \pi, \frac{4\pi}{3}, \frac{5\pi}{3}\right\}$, with the corresponding probability being 20%, 30%, 20%, 10%, 10% and 10% respectively, as prescribed in Fig. 3.2 (3).

3.2.3 The wind farm land model

The study in [71] takes into account the possibility that some areas of the wind farm land are inaccessible to wind turbines, as shown by the shaded region in Fig. 3.3. It should be noted that Fig. 3.3 is only one of 13 types of wind farm land. Each farmland is divided into I ($I = 144$) square cells, where the light green cells are the cells where wind turbines may be placed, the blue cells are the cells where wind turbines are actually placed, and the shaded cells are the unavailable cells. The numbers in Fig. 3.3 are index labels i to indicate the index of each cell. The index label is converted

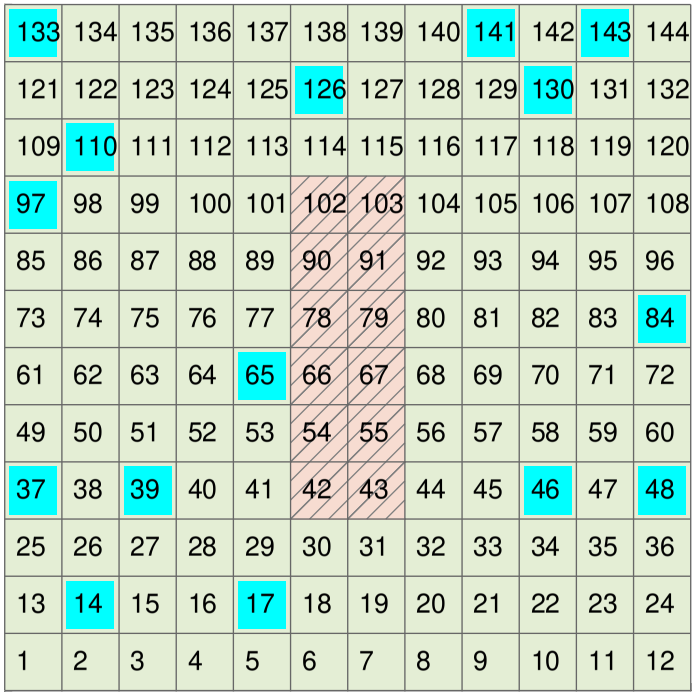

Figure 3.3: Example of a wind farm layout with restrictions placed by the landowner.

into a 2-dimensional ($2D$) coordinate system and used to label the location of each cell in the wind farm. The $2D$ coordinate system is created in three steps. Step 1: Create standard $2D$ coordinate system (X_i, Y_i). In $2D$ coordinate system, X_i is created as column index $(0, 1, \cdots, S_c - 1)$, Y_i is created as row index $(0, 1, \cdots, S_r - 1)$, where $S_c = 12$ is the number of cells in a column and $S_r = 12$ is the number of cells in a row. All cells in a standard $2D$ coordinate system can be represented as a matrix M_s. M_s is denoted as:

$$M_s = \begin{bmatrix} X_1 & X_2 & \cdots & X_i & \cdots & X_I \\ Y_1 & Y_2 & \cdots & Y_i & \cdots & Y_I \end{bmatrix} \tag{3.2}$$

(X_i, Y_i) can be calculated using the index labels i as:

$$X_i = i - S_c \left\lfloor \frac{i-1}{S_c} \right\rfloor - 1, \quad Y_i = \left\lfloor \frac{i-1}{S_c} \right\rfloor \tag{3.3}$$

Step 2: Based on the standard $2D$ coordinate system, the actual location coordinate system is created, and the unit is m. All cells in the actual location coordinate system can be represented as a matrix M_a. M_a is denoted as:

$$M_a = \begin{bmatrix} x_1 & x_2 & \cdots & x_i & \cdots & x_I \\ y_1 & y_2 & \cdots & y_i & \cdots & y_I \end{bmatrix} \tag{3.4}$$

(x_i, y_i) can be calculated using the index labels i as:

$$x_i = \left(i - S_c \left\lfloor \frac{i-1}{S_c} \right\rfloor - 0.5 \right) C, \quad y_i = \left(\left\lfloor \frac{i-1}{S_c} \right\rfloor + 0.5 \right) C \tag{3.5}$$

where C is the cell width.

Step 3: The rotation of the actual location coordinates system, also referred to as the rotated actual location coordinates system, is based on the various wind directions

θ. All cells in the rotated actual location coordinate system can be represented as a matrix M_a^θ. M_a^θ is denoted as:

$$M_a^\theta = \begin{bmatrix} x_1^\theta & x_2^\theta & \cdots & x_i^\theta & \cdots & x_I^\theta \\ y_1^\theta & y_2^\theta & \cdots & y_i^\theta & \cdots & y_I^\theta \end{bmatrix} \tag{3.6}$$

$\left(x_i^\theta, y_i^\theta\right)$ can be calculated using (x_i, y_i) as:

$$\begin{bmatrix} x_i^\theta \\ y_i^\theta \end{bmatrix} = \begin{bmatrix} cos\theta & -sin\theta \\ sin\theta & cos\theta \end{bmatrix} \begin{bmatrix} x_i \\ y_i \end{bmatrix} \tag{3.7}$$

3.2.4 The wake effect model

In the model of [71], the classical wake effect model is used. It is assumed that the momentum is conserved [73]. According to the law of conservation of momentum, the radius of the wake behind the turbine should increase linearly with downwind distance [74]. Fig. 3.4 displays the wake effect behind a wind turbine facing an ambient wind speed of v_0, where v_1 is the wake wind speed behind the wind turbine, which can be approximated as $\frac{1}{3}v_0$ [75]. r_0 is the rotor radius of the wind turbine, r_1 and v_2 represent the wake effect radius and wake velocity respectively at downwind distance d. d has different values for different wind directions θ. The decay constant, α determines how quickly the wake expands with distance. Eq. 3.8 is the expression for the law of conservation of momentum for wind turbines.

$$\pi {r_0}^2 v_1 + \pi \left({r_1}^2 - {r_0}^2\right) v_0 = \pi {r_1}^2 v_2 \tag{3.8}$$

v_2 can be derived as:

$$v_2 = v_0 \left[1 - \frac{2}{3}\left(\frac{r_0}{r_1}\right)^2\right] \tag{3.9}$$

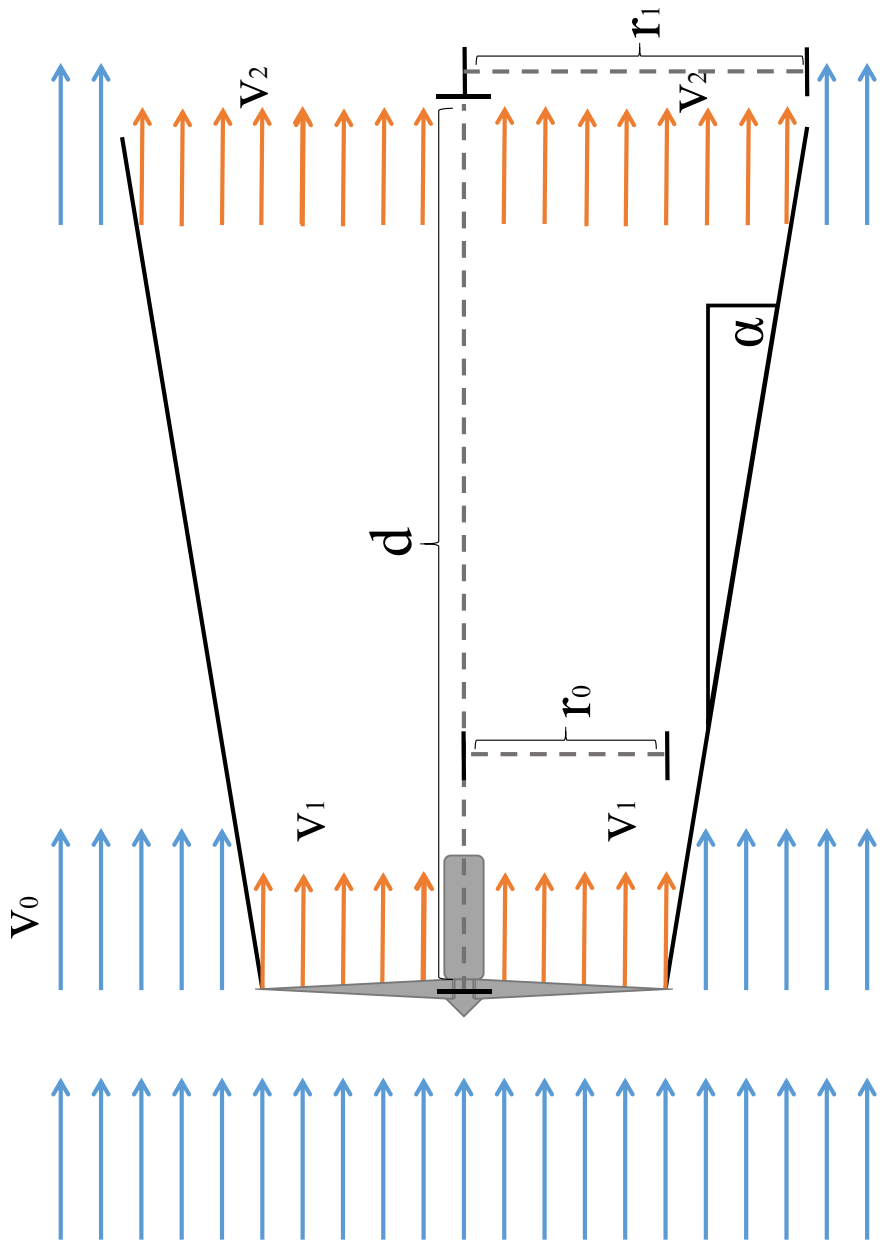

Figure 3.4: The wake effect behind a wind turbine facing ambient wind speed.

The wake effect radius is $r_1 = r_0 + \alpha d$, and the dimensionless scalar α is given as:

$$\alpha = \frac{0.5}{ln\left(\frac{h}{s}\right)} \tag{3.10}$$

where h is the wind turbine's hub height and, s represents the surface roughness of the wind farm area. When the ground is sand, s is set at $0.25mm$ [71].

When a wind turbine i is effected by the wake effects of multiple upwind turbines [51]. Let A represent the collection of wind turbine indices upwind of turbine i and the following can be derived:

$$\left(1 - \frac{v_i}{v_0}\right)^2 = \sum_{j=1}^{A} \left(1 - \frac{v_{i,j}}{v_0}\right)^2 \tag{3.11}$$

where v_i indicates the actual wind speed at wind turbine i, $v_{i,j}$ is the wind speed of turbine i only taking consideration of the wind turbine j's wake effect using Eq. 3.9. The actual wind speed v_i is:

$$v_i = v_0 \left[1 - \sqrt{\sum_{j=1}^{A} \left(1 - \frac{v_{i,j}}{v_0}\right)^2}\right] \tag{3.12}$$

3.2.5 The wind turbine model

In this section, the type of wind turbines are $GE1.5sle$. The diameter of the wind turbine is $77m$, the hub height h is $88m$. The output power of $GE1.5sle$ is calculated according to Eq. 3.13:

$$W\left(v_i\right) = \begin{cases} 0, & \text{if } v_i < 2 \\ 0.3v_i^2, & \text{if } 2 \leq v_i < 12.8 \\ 629.1, & \text{if } 12.8 \leq v_i < 18 \\ 0, & \text{if } 18 \leq v_i \end{cases} \tag{3.13}$$

Fig. 3.5 is the power curve of $GE1.5sle$.

3.2.6 The wind farm layout optimization problem's objective function

To maximize power production, WFLOP seeks to determine the best location for each wind turbine. In order to provide the wind turbines in the downwind direction with a better wind input speed, an ideal layout should minimize the wake effect to the lowest possible level. In [71], the objective function of Mosetti et al. [51] is used as:

$$Objective = \min_{n,X} \frac{T(n)}{E(n,X)} \tag{3.14}$$

where X is a feasible layout for a wind farm and n is the total number of wind turbines. In meta-heuristics, X is the individual of the algorithm. $E(n,X)$ denotes the sum of the power generated by the n wind turbines that are arranged in accordance with X's layout. $T(n)$ is the total cost of n wind turbines on the wind farm. $E(n,X)$ and $T(n)$ can be calculated as:

$$E(n,X) = \sum_{1}^{n} \sum_{\theta,v} p(\theta,v)\, o_i(\theta,v,X), \quad T(n) = n\left(\frac{2}{3} + \frac{1}{3}e^{-0.00174n^2}\right) \tag{3.15}$$

where θ is the wind direction with the wind speed v. $p(\theta,v)$ is the probability distribution of θ and v. $o_i(\theta,v,X)$ is the power output of wind turbine i under layout X with θ and v. Since the cost is constant for any given n, when dealing with issues involving a specific number of wind turbines, the objective function is equivalent to maximizing the anticipated overall power output of the wind farm, denoted by:

$$Objective = \max_{X} E(X), \quad E(X) = \sum_{1}^{n} \sum_{\theta,v} p(\theta,v)\, o_i(\theta,v,X) \tag{3.16}$$

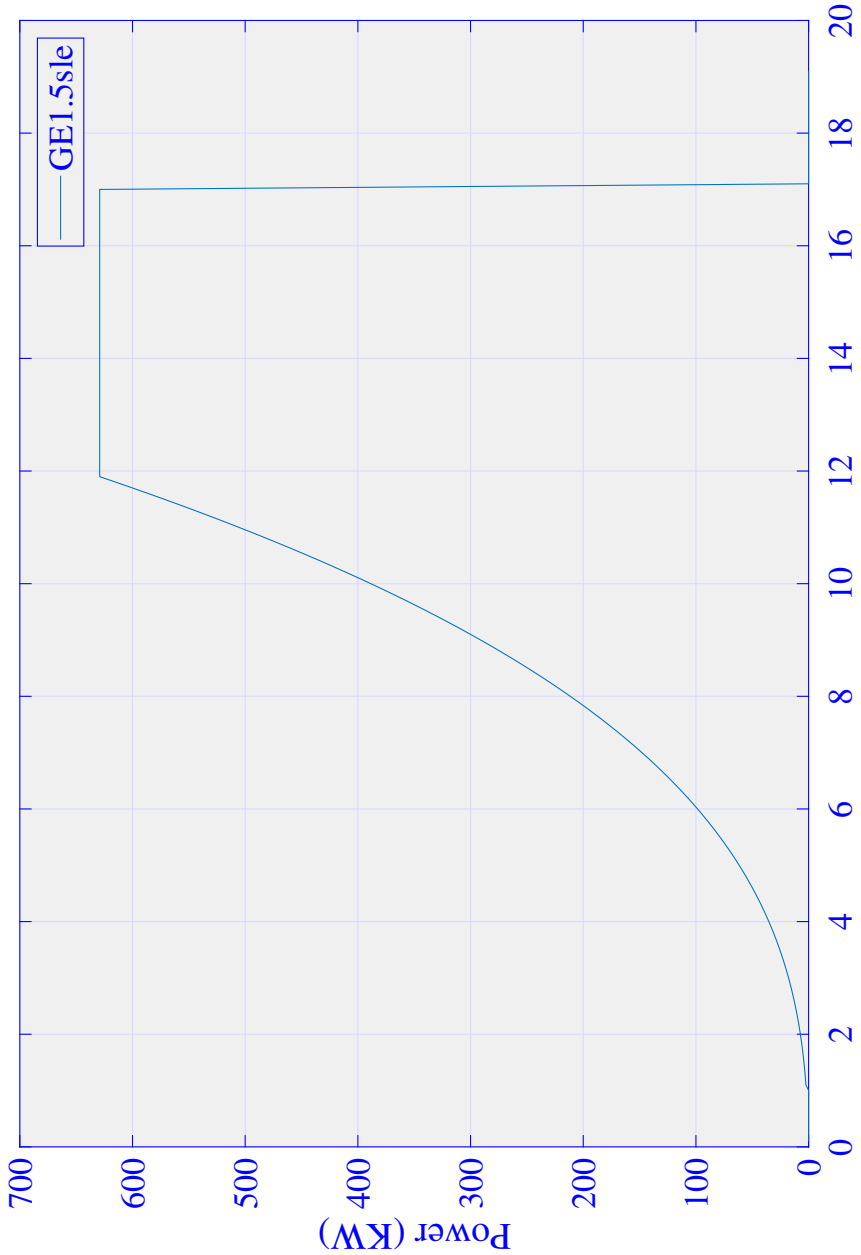

Figure 3.5: The output power of $GE1.5sle$.

Each layout's performance is measured using the conversion efficiency η for simple quantification.

$$\eta = \frac{E\left(n, X\right)}{n \sum_{\theta, v} p\left(\theta, v\right) r\left(v\right)} \tag{3.17}$$

where $r\left(v\right)$ is a wind turbine's rate power output at wind speed v, without accounting for the wake effect. To compare two layouts, conversion efficiency η is used as the criterion. The layout with a higher η is regarded as superior.

Chapter 4

Spatial information sampling algorithm

4.1 Basic idea of spatial information sampling algorithm

Table 4.1 lists the nomenclatures used in Section 2. In this study, we regard the problem to be optimized as a space in which the SIS population swims to find the global best. The entire SIS population is referred to as X, and it is divided into two sub-populations, L and R, with individuals in L distributed along the population's periphery and R distributed evenly.

Remark 1: In order to distinguish individuals at different positions in the population, we standardize the spatial shape of the population and make it hypercube distributed in the solution space. The specific distribution method is introduced in section 2.2.

When the current optimal individual is observed in L, it indicates that the search space covered by the population is not large enough, and the better individual may still be outside the current range. Then the perturbation operation of the intelligent scheme is activated: when the next generation of X is generated, the current optimal individual is regarded as the center, and the distance between individuals is expanded. As a result, SIS's exploration ability is enhanced. The mechanism of perturbation operation is shown in Fig. 4.1, where the contour line is represented by the circle in

Table 4.1: Nomenclature used in chapter 4

Symbol	description
N	The number of individuals in the population
D	The number of dimensions of the optimization problem
t	The number of iterations
i	The index of individuals
d	The index of dimensions
x_i^t	The i-th individual in population in the t-th iteration
$f(\cdot)$	The fitness function
o^t	The optimal individual in the t-th iteration
N_0	The number of nodes in each dimension
δx^t	The distance between each individual in the same dimension in the t-th iteration
U_d	The upper limits of the solution space in the d-dimension
F_d	The lower limits of the solution space in the d-dimension
X	The name of population
R	The name of sub-population generated by the random sequence
L	The name of sub-population generated by the logistic map
$r_{i,d}$	The ith data generated by the random sequence in the d-dimension
$l_{i,d}$	The ith data generated by the Logistic map in the d-dimension
b	The parameter for adjusting the distance between individuals
R_m	The individual with the best fitness value in R
L_m	The individual with the best fitness value in L

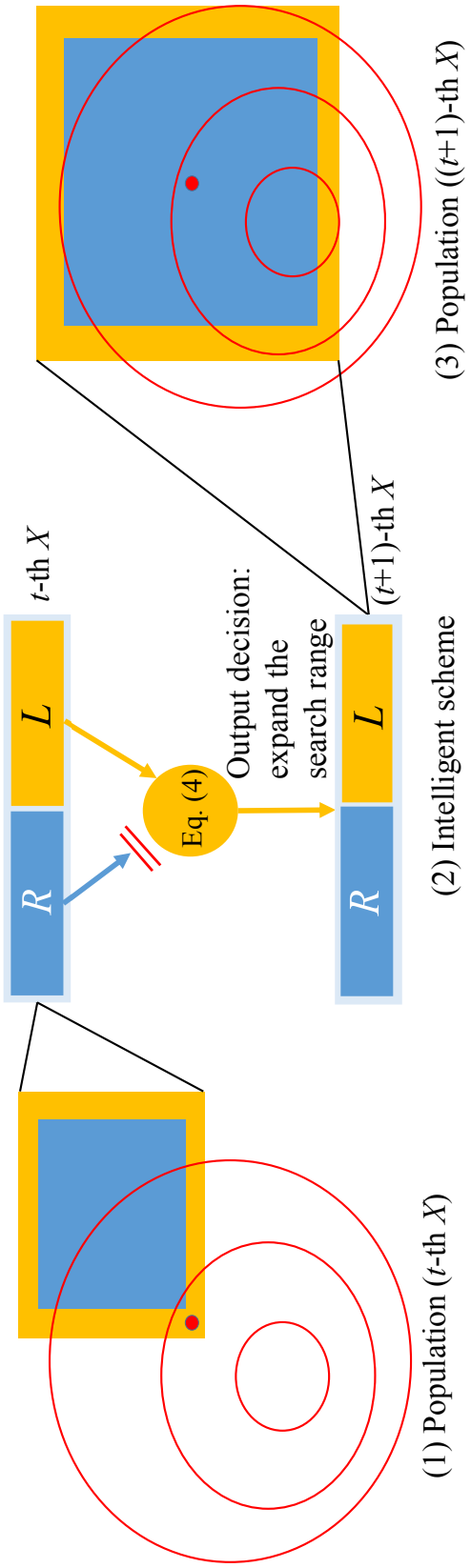

Figure 4.1: Perturbation operation of SIS.

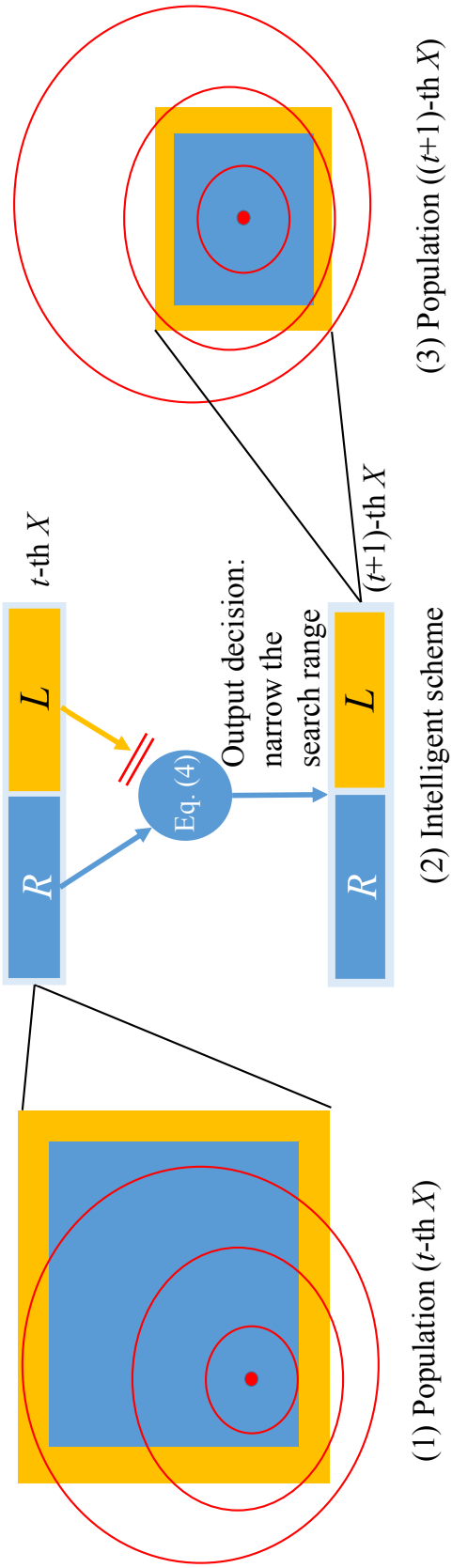

Figure 4.2: Attraction operation of SIS.

the figure, and the smaller the circle, the better the fitness value. The square is in the range of X, the yellow part is L and the blue part is R. The red dot represents the current optimal individual.

When the current optimal individual is observed in R, it indicates that the population may have covered a promising search area. Then the attraction operation of the intelligent scheme is activated: when the next generation of X is generated, the current optimal individual is regarded as the center, and the distance between individuals is reduced. As a result, SIS's exploitation ability is enhanced. The mechanism of attraction operation is shown in Fig. 4.2. Through the above operations of the intelligent scheme, the perception of the solution space is realized, and the flexibility and autonomy of SIS are enhanced.

Remark 2: In X, the individuals in L are responsible for searching for the current optimal individuals in the periphery of the population, while the individuals in R are responsible for searching for the current optimal individuals within the population. The two sub-populations have a clear division of labor and are indispensable.

4.2 Basic components of spatial information sampling algorithm

SIS is mainly composed of two parts: algorithm initialization and population construction, and their specific definitions are as follows:

Part 1: Algorithm initialization in SIS is the process of generating initial individuals in the solution space and also includes the assignment of initial parameters. First, N individuals are randomly initialized. Individuals in a D-dimensional solution space are represented by $x_i^t = [x_{i,1}, x_{i,2}, ..., x_{i,D}]$, where t is the iteration number and $i = [1, 2, ..., N]$, and the population X is formed by x_i. All individuals in the population are evaluated by the fitness function $f(\cdot)$, and the optimal one is represented as o.

In each dimension, the number of nodes is set as $N_0 = \sqrt[D]{N}$. $\delta x^t = [\delta x_1, \delta x_2, ..., \delta x_D]$ denotes a discrete step, representing the distance between each individual in each dimension. When initialized, δx^t is defined as:

$$\delta x^t = \frac{U_d - F_d}{N_0}, \quad t = 1, \quad d = [1, 2, ..., D] \tag{4.1}$$

where U_d and F_d are the upper and lower limits of the solution space in the d-dimension, respectively.

Part 2: The purpose of population construction is to construct a population to make SIS mark the position of the current optimal individual in the population. The population X is divided into two sub-populations, each with $N/2$ individuals. The sub-population generated by the random sequence is called R. The other one generated by the Logistic map [76] (a kind of chaotic map) is referred to as L. The generation process of individuals x_i in R and L is written as:

$$\begin{cases} x_{i,d}^{t+1} = (2 \cdot r_{i,d} - 1) \cdot \delta x_d^t + o^t & x_i \in R \\ x_{i,d}^{t+1} = (2 \cdot l_{i,d} - 1) \cdot \delta x_d^t + o^t & x_i \in L \end{cases} \tag{4.2}$$

where $i = [1, 2, ..., N/2]$. $r_{i,d}$ is generated by the random sequence and $l_{i,d}$ is generated by the Logistic map, shown as:

$$l_{i+1,d} = r \cdot l_{i,d} \cdot (1 - l_{i,d}), \quad i = [1, 2, ..., N/2] \tag{4.3}$$

where $l_{i,d}$ denotes the ith data generated by Logistic map in the d-dimension, $l_t \in (0, 1)$, $l_0 \in (0, 1)$ and $l_0 \notin \{0, 0.25, 0.5, 0.75, 1.0\}$, and we set r=4 according to [76].

Remark 3: The reason we use the chaotic map is that certain rules can be derived from a comprehensive and long-term analysis of the chaotic map, including ergodicity [27] and pseudo-randomness [28]. The distribution characteristic of the one-

```
begin
    /*Algorithm initialization */
    Initialize parameter b and randomly initialize N individuals
    Calculate δx^1 by Eq. (4.1)
    f(X) = evaluate(X)
    Find out the optimal individual o in the population
    while Terminal Condition do
        /*Population construction*/
        for i = 1 : N/2 do
            for d = 1 : D do
                Eq. (4.2)
            end
        end
        Boundary detection
        /*Intelligent scheme */
        f(X) = evaluate(X)
        Looking for the individual R_m and L_m with the best fitness value in R and L
        Through Eq. (4.4), update δx and o
    end
end
```

Algorithm 1: Pseudocode of SIS

dimensional sequence produced by the Logistic map is that the points are more likely to be distributed near the boundaries of 0 and 1. Based on the above characteristics, we construct a hypercube point set with a dense peripheral distribution and a sparse inner distribution in high-dimensional space to generate the sub-population L.

4.3 The realization of intelligent scheme

Without loss of generality, the optimization of a minimization problem is considered. After generating X, the fitness values of all individuals are calculated, and thereafter those with the best value in R and L are denoted by R_m and L_m, respectively. Since individuals in L are more likely to be distributed at the periphery of population, when $f(L_m) < f(R_m)$, the current range of search space is not big enough, and individuals with better fitness values may be found outside the current range. Therefore, the perturbation operation of the intelligent scheme is activated and δx^{t+1} is increased.

When $f(L_m) > f(R_m)$, the optimal individual may have been covered by the current search range, and the search range needs to be reduced for exploitation. Therefore, the attraction operation of the intelligent scheme is activated and δx^{t+1} is reduced. δx^{t+1} and o^{t+1} can be calculated as:

$$(c)\begin{cases}(a)\begin{cases}\delta x^{t+1} = (1+b)\cdot \delta x^{t} \\ o^{t+1} = L_m\end{cases} & \text{if } f(R_m) > f(L_m) \\ (b)\begin{cases}\delta x^{t+1} = (1-b)\cdot \delta x^{t} \\ o^{t+1} = R_m\end{cases} & \text{if } f(R_m) < f(L_m)\end{cases} \tag{4.4}$$

where b is the parameter for adjusting the distance between individuals. Repeat the operation from Eq. (4.2) to Eq. (4.4) until the iteration termination condition is met. The pseudo-code of SIS is given in Algorithm 1.

Remark 4: The two-dimensional schematic diagram of SIS in the iterative process is shown in Fig. 4.3. Figs. (a), (b) and (c) in Fig. 4.3 are consistent with the operations represented by Eqs. (a), (b) and (c) in Eq. (4.4). The contour line is the same as Fig. 4.1. The square is the range of the population X, and the red dot represents the current optimal individual. The numbers in the figure represent the number of iterations t. The perturbation operation is represented in Fig. 4.3 (a). When the global optimal area is not found, the population will move towards a better fitness value. Simultaneously, according to Eq. (4.4) (a), the search range of the population is continuously expanded. The attraction operation is represented in Fig. 4.3 (b). When the search range of the population encompasses the global optimal area, the search range begins to converge due to Eq. (4.4) (b). The whole optimization process of SIS is represented in Fig. 4.3 (c). Through Figs. 4.1, 4.2 and 4.3, we can find

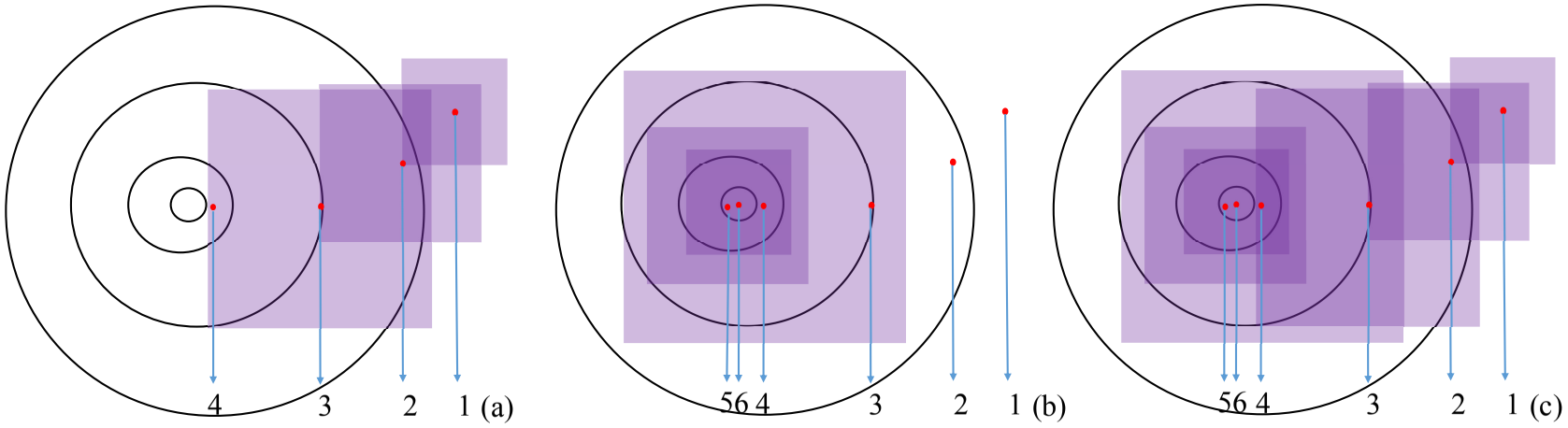

Figure 4.3: Two-dimensional schematic diagram of SIS in the iterative process.

that in the intelligent scheme, the solution space is observed and described by SIS according to the information obtained from individuals in different locations, and the exploitation or exploration operation can be chosen by SIS autonomously.

Chapter 5

Spherical evolution and its improvement method

5.1 Spherical evolution

According to Tang [41], the search operation of meta-heuristics has some common characteristics or patterns, which can be represented as:

$$X'_{i,j} = X_{r1,j} + \sum_{k=1}^{n} S\left(X_{r2,j}, X_{r3,j}, \cdots, X_{N,j}\right) \tag{5.1}$$

where X' is the offspring individual, X represents individuals of the parent generation. n denotes the number of updating units. $(r1, r2, \cdots, N)$ represents the index of the individual, and they are determined by the specific algorithm. $S\left(X_{r2,j}, X_{r3,j}, \cdots, X_{N,j}\right)$ represents the updating units in the search operator and decides the search style.

SE contains an initialization operation, a search operation, an evaluation operation, and a selection operation. Table 5.1 lists the nomenclatures used in Section 5. The initialization operation is the process of generating initial individuals in the solution space and also includes the assignment of initial parameters. First, N individuals are randomly initialized. Individuals in a D-dimensional solution space are represented by $X_i = [X_{i,1}, X_{i,2}, ..., X_{i,j}, ..., X_{i,D}]$. D is the total number n of wind turbines in this paper. i represents the index of the individual and j represents the index

Table 5.1: Nomenclature used in chapter 5.

Symbol	description
N	The number of individuals in the population
D	The number of dimensions of WFLOP
i	The index of individuals
j	The index of dimensions
X_i	The i-th individual in parent population
X_i'	The i-th individual in offspring population
$f(\cdot)$	The evaluation function
U_i	The temporary offspring individual
$r1, r2, r3$	The index of individuals
X_{r1}, X_{r2}, X_{r3}	The $r1, r2, r3$-th individual in parent population
D_c	The dimension of the original D after the dimensionality reduction operation
θ	The random number of uniform distribution between $[0, 2\pi]$
$*$	The set of all dimensions after dimensionality reduction
F	The scale factor
i_o	The index of individuals in the population ranked from best to worst
r_a	The normally distributed random number

of the dimension, and $i = [1, 2, ..., N]$, $j = [1, 2, ..., D]$. All individuals in the population are evaluated by the evaluation operation function $f(\cdot)$. $f(\cdot)$ is the conversion efficiency calculated by Eq. (3.17).

In high dimensions, the updating units of SE can be represented as:

$$U_{i,j} = X_{r1,j} + \begin{cases} F \cdot \left\| X_{r2,*} - X_{r3,*} \right\|_2 \cdot \prod_{k=j}^{D_c-1} \sin\left(\theta_j\right), & \text{if } j = 1 \\ F \cdot \left\| X_{r2,*} - X_{r3,*} \right\|_2 \cdot \cos\left(\theta_{j-1}\right) \cdot \prod_{k=j}^{D_c-1} \sin\left(\theta_j\right), & \text{if } 1 < j \leq D_c - 1 \\ F \cdot \left\| X_{r2,*} - X_{r3,*} \right\|_2 \cdot \cos\left(\theta_{j-1}\right), & \text{if } j = D_c \end{cases} \tag{5.2}$$

In two dimensions, the updating units of SE can be represented as:

$$U_{i,j} = X_{r1,j} + \begin{cases} F \cdot \left\| X_{r2,*} - X_{r3,*} \right\|_2 \cdot \sin\left(\theta_j\right), & \text{if } j = 1 \\ F \cdot \left\| X_{r2,*} - X_{r3,*} \right\|_2 \cdot \cos\left(\theta_j\right), & \text{if } j = 2 \end{cases} \tag{5.3}$$

In a single dimension, the updating units of SE can be represented as:

$$U_{i,j} = X_{r1,j} + F \cdot \left\| X_{r2,*} - X_{r3,*} \right\|_2 \cdot \cos\left(\theta_j\right) \tag{5.4}$$

where U_i is a temporary offspring individual. $(r1, r2, r3)$ represents the index of the individual, and they are random integers between 1 and N. F denotes a scale factor that can appropriately adjust the search radius length. In SE, the worse the individual's solution, the greater the value of F. $\left\| X_{r2,*} - X_{r3,*} \right\|_2$ denotes the radius of sphere computed by Euclidean norm in high dimensions. D_c is the dimension of the original D after the dimensionality reduction operation. $* = \{1, 2, ...D_c\}$ is the set of all dimensions after dimensionality reduction. θ is generated by a random number of uniform distribution between $[0, 2\pi]$.

Once the search operation is executed, the fitness values of the total individuals in U are evaluated. U_i is compared with the original population X_i with a greedy se-

lection strategy, and individuals who outperformed remaining in the next generation. The selection operation is formulated as:

$$X_i' = \begin{cases} U_i, & \text{if } f(U_i) > f(X_i) \\ X_i, & \text{if } otherwise \end{cases} \tag{5.5}$$

The maximum value optimization case is used here. After performing the selection operation, the algorithm proceeds to the next iteration of the search operation.

5.2 improved spherical evolution

Subsequently, we make more exploration-oriented improvements to the SE in two main ways. In the original SE, the update formula for F is:

$$F_{i_o} = \frac{i_o}{N} + 0.1r_a \tag{5.6}$$

where i_o is the index of individuals in the population ranked from best to worst according to their fitness value. The smaller the value of i_o, the better the $f(X_{i_o})$ of X_{i_o}, r_a is the normally distributed random number. When F is greater than 1 or less than 0, F will be remade. The value of F does not exceed 1, which indicates that the search range of the algorithm is shrinking, which weakens the SE exploration ability. To enhance the exploration of SE, we increase the value of F so that $F = 10$. In addition, we reduce the number of individuals N in the population of SE from 100 to 5. The reason for this operation is that when the population size declines, the amount of information contained in the individuals in the population decreases, thus reducing the information interaction and further enhancing SE exploration. The final experimental results confirm that the ISE performs far better than the original algorithm on the WFLOP. The pseudo-code of ISE to solve the WFLOP is given in

Algorithm 2.

Note: SE is improved from a meta-heuristic to a heuristic even if there is only a slight change in two parameters F and N. This is because the ISE makes use of the information extracted by the PIN from the WFLOP.

```
begin
    for P = P_1 : P_3 do
        /*Constructing wind condition models*/
        Calling wind speed v_0, wind direction θ and its frequency.
        for n = [15, 20, 25] do
            /*Determining the number of wind turbines*/
            for L = L0 : L12 do
                /*Determining the wind farm land model*/
                /*Calling the wake effect model*/
                Calculation of actual wind speed v_i according to Eqs. (3.8)-(3.12).
                /*Constructing the objective function */
                Construct the objective function η using Eqs. (3.13)-(3.17).
                /*Execute ISE*/
                Randomly initialize N = 5 individuals.
                Initialize the scaling factor F = 10.
                for i = 1 : N do
                    Transform the individual X_i into a 2-dimensional matrix using
                     Eqs. (3.2)-(3.7).
                    Based on Eq. (3.17), calculate f(X_i) = η(X_i).
                end
                while Terminal Condition do
                    /*Execute the updating units*/
                    for i = 1 : N do
                        for j = 1 : D do
                            Execute Eq. (5.2).
                        end
                    end
                    Boundary detection.
                    for i = 1 : N do
                        Transform the temporary Individual U_i into a 2-dimensional
                         matrix using Eqs. (3.2)-(3.7).
                        Based on Eq. (3.17), calculate f(U_i) = η(U_i).
                    end
                    /*Execute the selection operation*/
                    for i = 1 : N do
                        Execute Eq. (5.5).
                    end
                end
            end
        end
    end
end
```

Algorithm 2: Pseudocode of ISE

Chapter 6

Experimental results and analysis

6.1 Performance evaluation criteria

The following assessment tools were used to gauge how well MHAs performed:

1) "+", "=", and "−": When ISE performs better than other MHAs, it is denoted as "+". When there is no significant difference between them, it is noted as "=". When ISE performs worse than others, it is denoted as "−". The basis for this assessment comes from the Wilcoxon rank-sum test.

2) Wilcoxon rank-sum test: The Wilcoxon rank-sum test is a non-parametric evaluation of the null hypothesis that two samples originate from the same population in comparison to a competing hypothesis. The Wilcoxon rank-sum test was used to compare the data obtained after 51 times of function optimization in order to determine the differences between ISE on each function and other MHAs, and $W/T/L$ is used to represent these differences.

3) Wilcoxon signed-rank test: In the Wilcoxon signed-rank test, p-value is the probability of observing a test statistic as more extreme than the observed value under the null hypothesis. In this study, when the p-value is less than 0.05, it means that ISE is significantly better than other MHAs, and when the p-value is greater than 0.95, it means that ISE is significantly worse than others.

4) $W/T/L$: W is the number of functions for which ISE is significantly better than other algorithms, T is the number of functions for which ISE is not significantly different from other algorithms, and L is the number of functions for which ISE is significantly worse than other algorithms.

5) Friedman test: Non-parametric tests like the Friedman test are used. The alternative hypothesis in this test is that the medians of two or more algorithms are different, while the null hypothesis is that the medians of the various algorithms are equal. In this study, the larger the value of F_r, the better the algorithm performs on WFLOP.

6) Box-and-whisker diagrams: The line above the box denotes the maximum value, and the line below the box denotes the minimum value. The top and bottom edges of the box, respectively, stand in for the first and third quartiles. The red line represents the median, and the red "+" symbol denotes extreme values. Additionally, the performance of the algorithm is more unstable the greater the difference between the maximum and minimum values.

7) Convergence curve: This graph records the history of the current optimal at each iteration. The function evaluation numbers are represented by the x-axis and y-axis shows the average error value.

6.2 Performance evaluation of spatial information sampling algorithms

In this section, to verify the effectiveness of SIS, we conducted experiments on benchmark functions taken from IEEE CEC2017 [39], real-world problems taken from IEEE CEC2011 [77], and a position optimization problem of wave energy converters.

Table 6.1: CEC2017 and CEC2011's definition.

CEC2017 benchmark functions			CEC 2011 real-world optimization problems	
Name	Property	Optimal value	Name	Property
F01		100	G01	A parameter estimation for Frequency-Modulated Sound Waves
F02	Unimodal functions	200	G02	A Lennard-Jones potential problem
F03		300	G03	A bifunctional catalyst blend control problem
F04		400	G04	A stirred tank reactor control problem
F05		500		
F06		600	G05	
F07	Simple multimodal functions	700		Two Tersoff potential minimization problems
F08		800	G06	
F09		900		
F10		1000	G07	A radar polyphase code design problem
F11		1100	G08	A transmission network expansion problem
F12		1200	G09	A transmission pricing problem
F13		1300	G10	An antenna array design problem
F14		1400		
F15	Hybrid functions	1500	G11.1	
F16		1600		Two dynamic economic dispatch problems
F17		1700	G11.2	
F18		1800	G11.3	
F19		1900	G11.4	
F20		2000	G11.5	Five static economic dispatch problems
F21		2100	G11.6	
F22		2200	G11.7	
F23		2300		
F24		2400	G11.8	
F25		2500	G11.9	Three hydrothermal scheduling problems
F26	Composition functions	2600	G11.10	
F27		2700		
F28		2800	G12	
F29		2900		Two spacecraft trajectory optimization problems
F30		3000	G13	

Table 6.2: Parameter settings on CEC2017 and 2011.

Algorithms	Parameters
SIS	$b \in (0, 0.1]$
SCA	$\alpha = 2$
GWO	$\alpha = 2$
PSO	$c = 2$
GSA	$G_0 = 100$, $\alpha = 20$
DE	$F = 0.5$, $CR = 0.9$
CS	$P_a = 0.25$, $\alpha = 0.01$
CGWO	$\alpha = 2$, $r = 5$
MDBSO	$K = 5$, $\mu = 0.5$
CGSA-M	$G_0 = 100$, $\alpha = 20$, $LP = 50$
GLPSO	$\omega = 0.7298$, $pm = 0.01$, $c = 1.49618$, $sg = 7$
HGSA	$G_0 = 100$, $L = 20$, $w_1(t) = 1 - t^6/T^6$, $w_2(t) = t^6/T^6$
DNLGSA	$G_0 = 100$, $\alpha = 20$, $c_1(t) = 0.5 - 0.5t^{1/6}/T^{1/6}$, $c_2(t) = 1.5t^{1/6}/T^{1/6}$, $k = 10$, $gm = 5$

Table 6.3: Experimental results of CEC2107 on 30 dimensions.

	SIS		DE			CS			GWO			PSO			GSA			DNLGSA		
	mean	std	mean	std		mean	std		mean	std		mean	std		mean	std		mean	std	
F01	1.410E+03	2.346E+03	7.802E-15	7.142E-15	-	3.777E+06	1.119E+06	+	9.886E+08	7.803E+08	+	5.114E+10	4.752E+09	+	2.037E+03	1.169E+03	+	3.001E+07	2.121E+08	+
F03	2.727E+03	1.536E+04	2.980E+01	3.314E+01	+	7.524E+04	8.704E+03	+	2.992E+04	1.054E+04	+	1.073E+05	1.337E+04	+	8.330E+04	5.395E+03	+	1.731E+04	1.567E+04	+
F04	8.332E+01	2.233E+01	3.825E+01	2.821E+01	-	7.442E+01	6.614E+00	-	1.624E+02	4.256E+01	+	1.006E+04	1.706E+03	+	1.351E+02	1.346E+01	+	2.796E+02	1.355E+02	+
F05	8.301E+01	2.056E+01	1.774E+02	8.788E+00	+	2.282E+02	2.370E+01	+	8.673E+01	3.323E+01	=	4.271E+02	2.222E+01	+	2.324E+02	1.613E+01	+	1.486E+02	3.165E+01	+
F06	2.365E+00	2.211E+00	2.514E-08	3.990E-08	-	4.765E+01	3.845E+00	+	4.430E+00	2.722E+00	+	8.495E+01	4.509E+00	+	5.038E+01	3.395E+00	+	4.119E+01	7.302E+00	+
F07	1.280E+02	2.421E+01	2.092E+02	1.020E+01	+	5.163E+02	2.983E+01	+	1.315E+02	3.030E+01	=	1.485E+03	8.328E+01	+	8.725E+01	1.123E+01	-	2.940E+02	7.471E+01	+
F08	8.600E+01	1.639E+01	1.785E+02	1.248E+01	+	2.018E+02	1.779E+01	+	7.649E+01	2.341E+01	-	3.920E+02	2.019E+01	+	1.540E+02	1.377E+01	+	1.195E+02	2.962E+01	+
F09	1.389E+01	1.419E+01	0.000E+00	0.000E+00	-	9.856E+03	1.086E+03	+	4.949E+02	3.886E+02	+	1.370E+04	1.362E+03	+	1.986E+03	3.064E+02	+	3.128E+03	1.347E+03	+
F10	3.403E+03	8.538E+02	7.002E+03	2.617E+02	+	3.498E+03	2.289E+02	=	3.176E+03	9.326E+02	-	7.203E+03	3.303E+02	+	3.918E+03	3.664E+02	+	4.177E+03	6.503E+02	+
F11	1.258E+02	4.284E+01	5.339E+01	2.073E+01	-	1.184E+02	1.797E+01	=	4.117E+02	3.932E+02	+	6.154E+03	1.105E+03	+	3.482E+02	8.194E+01	+	3.888E+02	2.910E+02	+
F12	5.764E+05	4.631E+05	6.797E+03	3.366E+03	-	3.282E+05	1.205E+05	-	3.277E+07	3.582E+07	+	5.959E+09	1.019E+09	+	9.261E+06	2.256E+07	+	1.593E+08	1.906E+08	+
F13	5.538E+04	2.919E+04	8.043E+01	1.040E+01	-	1.248E+04	5.933E+03	-	3.735E+06	1.918E+07	+	2.358E+09	7.882E+08	+	2.781E+04	4.890E+03	-	1.967E+04	1.500E+04	-
F14	2.614E+03	2.374E+03	6.211E+01	6.868E+00	-	1.030E+04	6.903E+03	+	1.379E+05	2.833E+05	+	5.131E+05	2.647E+05	+	4.758E+05	1.116E+05	+	8.620E+04	1.822E+05	+
F15	3.798E+04	2.242E+04	3.766E+01	6.348E+00	-	1.483E+03	1.209E+03	-	1.990E+05	4.712E+05	=	2.063E+08	9.443E+07	+	1.022E+04	1.873E+03	-	1.019E+04	9.933E+03	-
F16	6.740E+02	2.050E+02	1.056E+03	4.836E+02	+	9.942E+02	1.068E+02	+	7.016E+02	2.689E+02	=	2.920E+03	2.263E+02	+	1.610E+03	2.960E+02	+	1.251E+03	3.277E+02	+
F17	1.981E+02	1.135E+02	7.530E+01	9.659E+00	-	3.791E+02	7.891E+01	+	2.534E+02	1.165E+02	+	1.344E+03	1.661E+02	+	1.149E+03	1.885E+02	+	5.910E+02	2.364E+02	+
F18	1.053E+05	5.129E+04	3.734E+01	3.692E+00	-	1.326E+05	4.183E+04	+	5.464E+05	7.051E+05	+	9.248E+06	3.908E+06	+	3.346E+05	1.757E+05	+	2.344E+05	3.939E+05	+
F19	1.636E+05	9.184E+04	1.731E+01	5.913E+00	-	1.586E+03	1.807E+03	-	6.001E+05	6.486E+05	+	3.380E+08	1.272E+08	+	1.187E+04	4.158E+03	-	8.822E+03	1.795E+04	-
F20	3.986E+02	1.292E+02	4.107E+01	2.358E+01	-	5.084E+02	8.198E+01	+	3.470E+02	1.275E+02	-	8.263E+02	7.564E+01	+	1.005E+03	1.579E+02	+	6.114E+02	2.040E+02	+
F21	2.851E+02	1.843E+01	3.720E+02	1.015E+01	+	3.295E+02	1.174E+02	+	2.764E+02	2.019E+01	-	5.872E+02	2.915E+01	+	4.536E+02	1.685E+01	+	3.237E+02	2.992E+01	+
F22	1.000E+02	1.611E-03	1.000E+02	1.168E-13	-	2.104E+03	1.601E+03	+	1.454E+03	1.451E+03	+	5.567E+03	5.420E+02	+	3.922E+03	1.864E+03	+	2.451E+03	2.217E+03	+
F23	4.259E+02	1.791E+01	5.205E+02	1.472E+01	+	6.792E+02	3.280E+01	+	4.376E+02	2.749E+01	+	9.433E+02	4.119E+01	+	1.295E+03	1.224E+02	+	6.849E+02	8.187E+01	+
F24	4.906E+02	1.371E+01	5.883E+02	1.483E+01	+	5.838E+02	2.682E+02	=	5.164E+02	5.088E+01	+	1.047E+03	5.573E+01	+	8.676E+02	4.748E+01	+	7.783E+02	9.283E+01	+
F25	3.867E+02	1.992E+00	3.867E+02	2.373E-02	-	3.939E+02	3.461E+00	+	4.524E+02	2.268E+01	+	3.829E+03	6.900E+02	+	4.335E+02	1.024E+01	+	5.058E+02	4.957E+01	+
F26	1.554E+03	6.748E+02	2.401E+03	2.317E+02	+	8.370E+02	3.315E+02	-	1.821E+03	3.447E+02	=	7.017E+03	4.893E+02	+	4.076E+03	9.225E+02	+	3.475E+03	1.125E+03	+
F27	5.161E+02	1.368E+01	4.791E+02	1.037E+01	-	6.409E+02	1.920E+01	+	5.381E+02	1.807E+01	+	1.104E+03	8.803E+01	+	1.824E+03	2.493E+02	+	7.673E+02	1.462E+02	+
F28	3.384E+02	4.711E+01	3.148E+02	3.754E+01	-	4.350E+02	1.205E+01	+	5.587E+02	5.606E+01	+	3.490E+03	4.161E+02	+	5.312E+02	8.182E+01	+	6.282E+02	1.183E+02	+
F29	7.445E+02	1.148E+02	6.118E+02	1.219E+02	-	1.021E+03	7.809E+01	+	7.819E+02	1.531E+02	=	2.625E+03	1.915E+02	+	1.799E+03	2.336E+02	+	1.355E+03	3.182E+02	+
F30	5.663E+05	4.060E+05	2.130E+03	9.168E+01	-	4.725E+04	1.927E+04	-	5.647E+06	5.048E+06	+	2.856E+08	7.835E+07	+	1.600E+05	1.279E+05	-	2.564E+06	4.197E+06	+
W/T/L	-/-/-		10/0/19			19/3/7			19/6/4			29/0/0			24/0/5			25/1/3		

	SIS		CGWO			HGSA			SCA			CGSA-M			MDBSO			GLPSO		
	mean	std	mean	std		mean	std		mean	std		mean	std		mean	std		mean	std	
F01	1.410E+03	2.346E+03	4.516E+07	5.917E+07	+	2.840E+03	2.568E+03	+	1.234E+10	1.886E+09	+	1.799E+03	9.351E+02	+	5.369E+03	6.222E+03	+	9.855E+04	4.741E+05	+
F03	2.727E+03	1.536E+04	2.322E+03	1.794E+03	+	4.483E+04	3.599E+03	+	3.524E+04	6.480E+03	+	8.280E+04	6.211E+03	+	7.313E+02	1.584E+03	+	2.191E+04	5.145E+03	+
F04	8.332E+01	2.233E+01	1.056E+02	2.064E+01	+	1.191E+02	2.141E+00	+	9.429E+02	2.408E+02	+	1.350E+02	1.605E+01	+	6.736E+01	3.157E+01	-	2.914E+02	9.243E+01	+
F05	8.301E+01	2.056E+01	9.160E+01	3.133E+01	=	1.512E+02	1.364E+01	+	2.781E+02	2.057E+01	+	2.245E+02	1.738E+01	+	1.136E+02	4.026E+01	+	1.761E+02	1.916E+01	+
F06	2.365E+00	2.211E+00	5.261E+00	3.445E+00	+	8.907E+00	5.858E+00	+	4.956E+01	5.783E+00	+	5.005E+01	3.223E+00	+	1.381E+01	9.373E+00	+	5.087E+00	2.062E+00	+
F07	1.280E+02	2.421E+01	1.657E+02	4.104E+01	+	4.026E+01	2.350E+00	-	4.235E+02	3.849E+01	+	8.717E+01	1.107E+01	-	1.942E+02	1.049E+02	+	1.620E+02	5.406E+01	+
F08	8.600E+01	1.639E+01	7.421E+01	2.336E+01	-	1.042E+02	8.549E+00	+	2.501E+02	1.856E+01	+	1.525E+02	1.385E+01	+	1.140E+02	3.879E+01	+	1.535E+02	3.818E+01	+
F09	1.389E+01	1.419E+01	6.224E+02	4.394E+02	+	5.466E-14	5.736E-14	-	4.322E+03	9.179E+02	+	2.009E+03	2.613E+02	+	5.497E+02	5.606E+02	+	1.409E+01	9.247E+00	=
F10	3.403E+03	8.538E+02	2.889E+03	7.519E+02	-	3.183E+03	4.904E+02	=	7.216E+03	2.893E+02	+	3.847E+03	4.265E+02	+	6.765E+03	7.269E+02	+	6.542E+03	3.351E+02	+
F11	1.258E+02	4.284E+01	1.583E+02	4.778E+01	+	9.613E+01	2.965E+01	-	1.034E+03	4.362E+02	+	3.596E+02	1.106E+02	+	1.173E+02	4.357E+01	=	1.322E+02	6.007E+01	=
F12	5.764E+05	4.631E+05	8.726E+06	6.098E+06	+	1.352E+05	7.064E+04	-	1.040E+09	2.393E+08	+	1.127E+07	2.245E+07	+	8.238E+04	2.758E+05	-	7.840E+06	1.328E+07	+
F13	5.538E+04	2.919E+04	1.470E+05	8.013E+04	+	1.246E+04	5.210E+03	-	4.171E+08	1.851E+08	+	2.890E+04	5.595E+03	-	1.512E+04	1.855E+04	-	5.504E+04	2.297E+05	-
F14	2.614E+03	2.374E+03	3.574E+03	6.921E+03	-	7.247E+03	5.010E+03	+	1.374E+05	7.293E+04	+	4.750E+05	1.282E+05	+	6.883E+03	5.061E+03	+	3.526E+04	8.101E+04	+
F15	3.798E+04	2.242E+04	3.150E+04	2.357E+04	-	7.404E+02	5.749E+02	-	1.202E+07	9.820E+06	+	1.015E+04	2.031E+03	-	8.540E+03	8.042E+03	-	8.491E+03	8.313E+03	-
F16	6.740E+02	2.050E+02	7.497E+02	2.292E+02	=	1.153E+03	1.836E+02	+	2.001E+03	2.166E+02	+	1.548E+03	2.987E+02	+	7.769E+02	4.505E+02	=	1.359E+03	2.055E+02	+
F17	1.981E+02	1.135E+02	2.355E+02	1.380E+02	=	1.044E+03	1.898E+02	+	6.989E+02	1.654E+02	+	1.165E+03	2.041E+02	+	2.276E+02	1.467E+02	=	2.777E+02	1.646E+02	+
F18	1.053E+05	5.129E+04	7.682E+04	5.416E+04	-	6.117E+04	1.930E+04	-	3.332E+06	1.539E+06	+	2.864E+05	1.538E+05	+	1.227E+05	1.035E+05	=	6.947E+05	7.499E+05	+
F19	1.636E+05	9.184E+04	8.541E+04	9.097E+04	-	2.867E+03	1.167E+03	-	2.467E+07	1.334E+07	+	1.053E+04	3.279E+03	-	1.186E+04	1.298E+04	-	9.548E+03	1.393E+04	-
F20	3.986E+02	1.292E+02	3.394E+02	1.250E+02	-	9.078E+02	1.905E+02	+	6.324E+02	1.278E+02	+	9.756E+02	1.946E+02	+	2.511E+02	1.768E+02	-	2.793E+02	1.377E+02	-
F21	2.851E+02	1.843E+01	2.796E+02	2.623E+01	-	3.209E+02	3.538E+01	+	4.563E+02	1.681E+01	+	4.579E+02	2.081E+01	+	3.025E+02	4.534E+01	+	3.743E+02	2.345E+01	+
F22	1.000E+02	1.611E-03	1.405E+03	1.592E+03	+	1.911E+02	6.439E+02	+	5.876E+03	2.511E+03	+	4.172E+03	1.521E+03	+	3.067E+03	3.220E+03	+	1.021E+02	2.319E+00	+
F23	4.259E+02	1.791E+01	4.531E+02	3.613E+01	+	4.731E+02	1.275E+02	+	6.845E+02	2.393E+01	+	1.313E+03	1.302E+02	+	4.326E+02	2.846E+01	=	5.930E+02	2.099E+01	+
F24	4.906E+02	1.371E+01	5.362E+02	4.334E+01	+	5.182E+02	3.901E+01	+	7.641E+02	2.414E+01	+	8.843E+02	5.830E+01	+	5.379E+02	5.002E+01	+	6.565E+02	2.180E+01	+
F25	3.867E+02	1.992E+00	4.129E+02	1.688E+01	+	3.917E+02	8.595E+00	+	7.053E+02	7.408E+01	+	4.338E+02	8.944E+00	+	4.040E+02	2.155E+01	+	4.330E+02	2.126E+01	+
F26	1.554E+03	6.748E+02	1.930E+03	4.342E+02	+	2.529E+02	4.991E+01	-	4.333E+03	3.172E+02	+	4.080E+03	7.605E+02	+	2.080E+03	9.125E+02	+	2.945E+03	9.361E+02	+
F27	5.161E+02	1.368E+01	5.298E+02	1.301E+01	+	5.552E+02	2.274E+01	+	7.051E+02	4.123E+01	+	1.841E+03	3.309E+02	+	5.383E+02	1.570E+01	+	6.666E+02	2.153E+01	+
F28	3.384E+02	4.711E+01	4.697E+02	3.509E+01	+	3.097E+02	2.678E+01	-	1.019E+03	1.150E+02	+	5.236E+02	5.699E+01	+	3.874E+02	5.651E+01	+	5.465E+02	7.722E+01	+
F29	7.445E+02	1.148E+02	8.067E+02	1.341E+02	+	1.197E+03	2.116E+02	+	1.753E+03	2.522E+02	+	1.831E+03	2.235E+02	+	8.406E+02	1.861E+02	+	8.682E+02	1.783E+02	+
F30	5.663E+05	4.060E+05	1.195E+06	8.347E+05	+	7.428E+03	1.707E+03	-	6.672E+07	2.421E+07	+	1.449E+05	9.645E+04	-	6.913E+03	3.245E+03	-	9.170E+04	1.539E+05	-
W/T/L	-/-/-		18/3/8			17/1/11			29/0/0			24/0/5			17/5/7			22/2/5		

Table 6.4: Experimental results of CEC2107 on 50 dimensions.

	SIS		DE			CS			GWO			PSO			GSA			DNLGSA		
	mean	std	mean	std		mean	std		mean	std		mean	std		mean	std		mean	std	
F01	3.640E+03	5.141E+03	5.450E+01	1.916E+02	-	1.300E+06	4.953E+05	+	4.992E+09	2.605E+09	+	1.356E+11	1.138E+10	+	8.815E+02	1.162E+03	-	8.091E+07	5.524E+08	+
F03	1.127E+03	7.311E+03	1.033E+05	1.543E+04	+	1.874E+05	1.289E+04	+	7.185E+04	1.583E+04	+	2.269E+05	2.398E+04	+	1.682E+05	1.057E+04	+	6.851E+04	6.385E+04	+
F04	1.310E+02	5.632E+01	6.281E+01	4.486E+01	-	9.008E+01	1.236E+01	-	4.574E+02	1.831E+02	+	3.335E+04	4.357E+03	+	2.194E+02	7.399E+01	+	7.394E+02	4.451E+02	+
F05	1.943E+02	3.068E+01	3.579E+02	1.458E+01	+	4.473E+02	2.863E+01	+	1.904E+02	3.748E+01	=	8.387E+02	2.663E+01	+	3.259E+02	1.921E+01	+	2.836E+02	4.408E+01	+
F06	1.582E+01	6.356E+00	1.314E-07	8.519E-07	-	5.875E+01	3.329E+00	+	1.065E+01	3.009E+00	-	1.040E+02	4.435E+00	+	5.680E+01	2.968E+00	+	5.010E+01	6.743E+00	+
F07	2.621E+02	4.316E+01	4.030E+02	1.337E+01	+	9.191E+02	4.218E+01	+	3.007E+02	6.105E+01	+	3.400E+03	1.411E+02	+	2.225E+02	2.667E+01	-	7.394E+02	1.136E+02	+
F08	1.952E+02	3.821E+01	3.560E+02	1.529E+01	+	4.355E+02	2.901E+01	+	1.988E+02	4.678E+01	=	8.394E+02	3.128E+01	+	3.497E+02	2.121E+01	+	2.838E+02	4.137E+01	+
F09	9.819E+02	9.865E+02	1.957E-02	8.959E-02	-	3.625E+04	3.423E+03	+	4.193E+03	1.873E+03	+	4.812E+04	3.765E+03	+	8.331E+03	6.923E+02	+	1.006E+04	2.338E+03	+
F10	5.584E+03	1.244E+03	1.311E+04	3.671E+02	+	6.401E+03	2.372E+02	+	5.787E+03	8.454E+02	+	1.345E+04	3.803E+02	+	6.823E+03	5.875E+02	+	6.698E+03	1.075E+03	+
F11	2.091E+02	4.514E+01	1.378E+02	2.825E+01	-	2.713E+02	2.370E+01	+	1.786E+03	1.152E+03	+	2.119E+04	3.022E+03	+	1.238E+03	2.332E+02	+	1.101E+03	9.637E+02	+
F12	4.322E+06	2.421E+06	5.037E+04	3.042E+04	-	2.047E+06	3.370E+05	-	3.851E+08	5.978E+08	+	4.403E+10	4.606E+09	+	1.998E+06	5.520E+05	-	4.557E+08	5.050E+08	+
F13	7.763E+04	4.050E+04	3.317E+02	2.207E+02	-	4.842E+03	2.951E+03	-	9.062E+07	1.305E+08	+	1.502E+10	3.029E+09	+	2.673E+04	3.587E+03	-	4.077E+07	2.646E+08	-
F14	1.720E+04	1.687E+04	1.281E+02	8.807E+00	-	5.317E+04	2.779E+04	+	4.245E+05	4.261E+05	+	8.693E+06	3.867E+06	+	3.366E+05	2.260E+05	+	1.100E+06	2.160E+06	+
F15	3.201E+04	1.403E+04	1.132E+02	6.729E+00	-	6.247E+03	3.539E+03	-	6.728E+06	1.313E+07	+	3.526E+09	8.297E+08	+	1.525E+04	3.252E+03	-	1.819E+06	1.225E+07	-
F16	1.098E+03	3.005E+02	2.784E+03	4.167E+02	+	1.713E+03	1.283E+02	+	1.332E+03	4.159E+02	+	5.563E+03	3.809E+02	+	2.014E+03	3.121E+02	+	2.149E+03	5.607E+02	+
F17	8.931E+02	2.122E+02	1.408E+03	4.412E+02	+	1.227E+03	1.206E+02	+	9.150E+02	1.906E+02	=	5.190E+03	5.005E+02	+	1.840E+03	3.268E+02	+	1.658E+03	3.466E+02	+
F18	1.631E+05	6.431E+04	6.881E+02	4.981E+02	-	4.681E+05	1.852E+05	+	2.185E+06	2.222E+06	+	4.888E+07	1.760E+07	+	1.386E+06	9.503E+05	+	4.797E+06	6.146E+06	+
F19	2.694E+05	1.251E+05	5.902E+01	1.023E+01	-	1.345E+04	5.252E+03	-	1.988E+06	4.523E+06	+	1.489E+09	3.936E+08	+	2.491E+04	5.392E+03	-	7.869E+04	2.622E+05	-
F20	8.396E+02	2.113E+02	1.086E+03	4.589E+02	+	1.177E+03	1.143E+02	+	7.306E+02	2.541E+02	-	2.002E+03	1.349E+02	+	1.557E+03	2.900E+02	+	1.383E+03	3.597E+02	+
F21	3.848E+02	2.825E+01	5.579E+02	1.487E+01	+	6.425E+02	2.954E+01	+	3.857E+02	2.996E+01	=	1.032E+03	3.820E+01	+	6.362E+02	3.206E+01	+	5.096E+02	7.151E+01	+
F22	1.751E+03	2.748E+03	5.061E+03	6.506E+03	=	7.144E+03	2.799E+02	+	5.691E+03	1.527E+03	+	1.398E+04	3.712E+02	+	9.190E+03	5.647E+02	+	7.702E+03	9.062E+02	+
F23	6.162E+02	3.828E+01	7.705E+02	1.773E+01	+	1.112E+03	4.825E+01	+	6.273E+02	5.956E+01	=	1.738E+03	6.628E+01	+	2.049E+03	1.428E+02	+	1.290E+03	1.561E+02	+
F24	6.625E+02	3.059E+01	8.300E+02	3.883E+01	+	1.362E+03	1.115E+02	+	7.133E+02	1.004E+02	+	1.879E+03	8.471E+01	+	1.353E+03	6.518E+01	+	1.424E+03	1.544E+02	+
F25	5.136E+02	2.765E+01	5.048E+02	3.201E+01	-	5.537E+02	1.208E+01	+	8.797E+02	1.880E+02	+	2.103E+04	2.457E+03	+	7.376E+02	8.176E+01	+	1.111E+03	3.039E+02	+
F26	3.144E+03	3.572E+02	3.913E+03	7.609E+02	+	3.129E+03	1.986E+03	-	3.299E+03	4.956E+02	=	1.529E+04	6.295E+02	+	3.045E+03	2.129E+03	-	7.943E+03	1.078E+03	+
F27	6.275E+02	4.645E+01	5.070E+02	8.300E+00	-	1.236E+03	7.311E+01	+	8.064E+02	1.348E+02	+	2.771E+03	1.984E+02	+	3.611E+03	4.303E+02	+	1.987E+03	4.986E+02	+
F28	4.748E+02	2.007E+01	4.684E+02	1.959E+01	-	5.498E+02	1.624E+01	+	1.095E+03	2.839E+02	+	1.008E+04	7.686E+02	+	6.846E+02	9.777E+01	+	1.368E+03	4.442E+02	+
F29	1.150E+03	2.932E+02	7.996E+02	4.757E+02	-	1.601E+03	1.279E+02	+	1.274E+03	2.173E+02	+	8.698E+03	1.295E+03	+	2.651E+03	3.459E+02	+	3.620E+03	1.046E+03	+
F30	1.961E+07	3.848E+06	6.250E+05	3.047E+04	-	2.375E+06	3.798E+05	-	6.512E+07	2.208E+07	+	2.742E+09	5.645E+08	+	4.118E+07	5.548E+06	+	2.016E+08	8.909E+07	+
W/T/L	-/-/-		12/1/16			22/0/7			21/6/2			29/0/0			22/0/7			26/0/3		

	SIS		CGWO			HGSA			SCA			CGSA-M			MDBSO			GLPSO		
	mean	std	mean	std		mean	std		mean	std		mean	std		mean	std		mean	std	
F01	3.640E+03	5.141E+03	3.160E+08	4.577E+08	+	7.945E+02	1.115E+03	-	3.844E+10	5.663E+09	+	5.386E+02	9.972E+02	-	7.715E+03	8.426E+03	+	6.138E+06	4.045E+07	=
F03	1.127E+03	7.311E+03	1.464E+04	6.042E+03	+	1.180E+05	9.514E+03	+	1.006E+05	1.573E+04	+	1.701E+05	9.531E+03	+	2.118E+04	1.197E+04	+	7.827E+04	1.101E+04	+
F04	1.310E+02	5.632E+01	2.071E+02	3.884E+01	+	1.958E+02	3.970E+01	+	5.661E+03	1.354E+03	+	2.049E+02	7.095E+01	+	1.064E+02	4.568E+01	-	8.643E+02	2.489E+02	+
F05	1.943E+02	3.068E+01	2.149E+02	7.492E+01	=	2.676E+02	2.065E+01	+	5.511E+02	2.920E+01	+	3.311E+02	2.037E+01	+	2.397E+02	5.788E+01	+	3.566E+02	4.186E+01	+
F06	1.582E+01	6.356E+00	1.082E+01	3.475E+00	-	2.362E+01	4.394E+00	+	6.866E+01	4.962E+00	+	5.611E+01	2.452E+00	+	2.771E+01	9.306E+00	+	1.472E+01	2.961E+00	=
F07	2.621E+02	4.316E+01	3.673E+02	9.125E+01	+	7.097E+01	4.037E+00	-	9.066E+02	6.448E+01	+	2.218E+02	2.451E+01	-	4.983E+02	1.855E+02	+	3.677E+02	8.170E+01	+
F08	1.952E+02	3.821E+01	1.990E+02	5.195E+01	=	2.918E+02	1.582E+01	+	5.512E+02	3.043E+01	+	3.528E+02	2.332E+01	+	2.461E+02	7.146E+01	+	3.620E+02	3.855E+01	+
F09	9.819E+02	9.865E+02	4.734E+03	1.509E+03	+	1.133E+01	8.013E+01	-	2.079E+04	3.709E+03	+	8.288E+03	5.758E+02	+	3.143E+03	2.397E+03	+	1.488E+03	1.104E+03	+
F10	5.584E+03	1.244E+03	5.808E+03	1.115E+03	=	5.747E+03	5.356E+02	+	1.334E+04	4.102E+02	+	6.873E+03	5.905E+02	+	1.311E+04	6.143E+02	+	1.231E+04	4.412E+02	+
F11	2.091E+02	4.514E+01	3.340E+02	6.979E+01	+	1.262E+02	1.352E+01	-	4.802E+03	1.210E+03	+	1.246E+03	2.816E+02	+	2.065E+02	6.014E+01	=	7.270E+02	6.007E+02	+
F12	4.322E+06	2.421E+06	5.998E+07	3.686E+07	+	8.335E+05	3.748E+05	-	1.149E+10	2.630E+09	+	1.884E+06	4.695E+05	-	5.520E+05	3.586E+05	-	1.251E+08	3.145E+08	+
F13	7.763E+04	4.050E+04	9.347E+05	8.648E+05	+	5.693E+02	6.358E+02	-	2.661E+09	8.451E+08	+	2.551E+04	3.866E+03	-	6.112E+03	6.980E+03	-	2.880E+06	1.276E+07	-
F14	1.720E+04	1.687E+04	3.625E+04	4.158E+04	+	2.290E+04	1.282E+04	+	1.936E+06	9.174E+05	+	2.819E+05	9.584E+04	+	4.264E+04	3.476E+04	+	2.809E+05	4.382E+05	+
F15	3.201E+04	1.403E+04	7.803E+04	4.879E+04	+	7.845E+03	1.791E+03	-	3.400E+08	1.462E+08	+	1.578E+04	4.073E+03	-	8.745E+03	6.322E+03	-	6.184E+03	6.436E+03	-
F16	1.098E+03	3.005E+02	1.268E+03	3.842E+02	+	1.828E+03	3.048E+02	+	3.789E+03	3.437E+02	+	1.980E+03	3.725E+02	+	1.902E+03	7.314E+02	+	2.785E+03	4.031E+02	+
F17	8.931E+02	2.122E+02	1.049E+03	2.582E+02	+	1.670E+03	3.095E+02	+	2.575E+03	2.438E+02	+	1.896E+03	2.437E+02	+	1.333E+03	5.173E+02	+	1.505E+03	2.726E+02	+
F18	1.631E+05	6.431E+04	3.429E+05	2.340E+05	+	1.815E+05	6.779E+04	=	1.422E+07	6.718E+06	+	1.316E+06	7.176E+05	+	1.176E+05	9.653E+04	-	3.868E+06	4.309E+06	+
F19	2.694E+05	1.251E+05	5.848E+05	3.852E+05	+	1.423E+04	3.336E+03	-	2.199E+08	1.058E+08	+	2.439E+04	7.368E+03	-	1.656E+04	1.209E+04	-	6.479E+04	3.813E+05	-
F20	8.396E+02	2.113E+02	8.078E+02	2.529E+02	=	1.315E+03	3.107E+02	+	1.773E+03	1.885E+02	+	1.608E+03	2.763E+02	+	1.275E+03	4.787E+02	+	1.313E+03	3.192E+02	+
F21	3.848E+02	2.825E+01	4.038E+02	5.846E+01	=	4.561E+02	2.659E+01	+	7.620E+02	3.225E+01	+	6.303E+02	2.795E+01	+	4.475E+02	7.559E+01	+	5.756E+02	2.577E+01	+
F22	1.751E+03	2.748E+03	5.717E+03	2.260E+03	+	7.902E+03	5.189E+02	+	1.366E+04	3.714E+02	+	9.167E+03	5.935E+02	+	1.339E+04	3.412E+02	+	1.122E+04	3.842E+03	+
F23	6.162E+02	3.828E+01	6.597E+02	9.400E+01	+	1.071E+03	1.964E+02	+	1.208E+03	5.621E+01	+	2.039E+03	1.427E+02	+	6.243E+02	6.456E+01	=	9.861E+02	4.881E+01	+
F24	6.625E+02	3.059E+01	7.534E+02	9.083E+01	+	8.866E+02	4.895E+01	+	1.263E+03	5.272E+01	+	1.353E+03	5.719E+01	+	7.673E+02	1.088E+02	+	1.055E+03	4.607E+01	+
F25	5.136E+02	2.765E+01	6.221E+02	6.734E+01	+	5.813E+02	1.493E+01	+	3.426E+03	5.342E+02	+	7.208E+02	8.416E+01	+	5.505E+02	3.860E+01	+	9.207E+02	1.121E+02	+
F26	3.144E+03	3.572E+02	3.786E+03	8.880E+02	+	3.000E+02	7.596E-13	-	9.058E+03	6.189E+02	+	4.065E+03	2.455E+03	=	4.387E+03	1.253E+03	+	5.958E+03	6.938E+02	+
F27	6.275E+02	4.645E+01	7.235E+02	7.996E+01	+	1.401E+03	2.788E+02	+	1.672E+03	1.656E+02	+	3.704E+03	4.835E+02	+	8.172E+02	9.579E+01	+	1.419E+03	1.126E+02	+
F28	4.748E+02	2.007E+01	6.224E+02	8.236E+01	+	5.023E+02	2.110E+01	+	3.533E+03	4.530E+02	+	7.228E+02	1.121E+02	+	4.996E+02	2.713E+01	+	1.207E+03	2.199E+02	+
F29	1.150E+03	2.932E+02	1.328E+03	3.623E+02	+	1.706E+03	2.706E+02	+	4.261E+03	5.919E+02	+	2.511E+03	2.747E+02	+	1.314E+03	3.198E+02	+	2.037E+03	4.919E+02	+
F30	1.961E+07	3.848E+06	2.327E+07	7.349E+06	+	1.340E+06	9.608E+04	-	5.830E+08	1.837E+08	+	4.323E+07	5.363E+06	+	9.699E+05	2.086E+05	-	1.236E+07	6.858E+06	-
W/T/L	-/-/-		23/5/1			18/1/10			29/0/0			22/1/6			20/2/7			23/2/4		

Table 6.5: Experimental results of CEC2107 on 100 dimensions.

	SIS		DE			CS			GWO			PSO			GSA			DNLGSA		
	mean	std	mean	std		mean	std		mean	std		mean	std		mean	std		mean	std	
F01	5.380E+03	6.810E+03	4.860E+03	4.900E+03	=	1.066E+05	4.298E+04	+	3.048E+10	7.660E+09	+	3.987E+11	2.166E+10	+	3.702E+03	2.589E+03	=	4.878E+06	5.201E+06	+
F03	7.035E+04	3.467E+04	3.909E+05	2.819E+04	+	5.062E+05	2.536E+04	+	2.058E+05	1.967E+04	+	5.932E+05	2.967E+04	+	3.409E+05	1.108E+04	+	2.954E+05	1.535E+05	+
F04	2.678E+02	3.603E+01	2.121E+02	4.113E+01	-	2.314E+02	2.572E+01	-	2.588E+03	8.323E+02	+	1.213E+05	1.094E+04	+	1.024E+03	6.354E+02	+	3.246E+03	2.087E+03	+
F05	5.174E+02	6.553E+01	8.290E+02	2.055E+01	+	1.148E+03	4.273E+01	+	5.425E+02	6.074E+01	+	2.000E+03	4.479E+01	+	8.039E+02	3.103E+01	+	7.076E+02	8.308E+01	+
F06	3.902E+01	5.783E+00	3.356E-03	1.272E-02	-	7.436E+01	2.235E+00	+	2.760E+01	4.045E+00	-	1.263E+02	2.694E+00	+	5.723E+01	1.642E+00	+	5.663E+01	4.380E+00	+
F07	7.432E+02	7.748E+01	9.280E+02	2.174E+01	+	2.185E+03	5.984E+01	+	1.044E+03	9.365E+01	+	9.096E+03	3.464E+02	+	9.156E+02	7.493E+01	+	2.479E+03	3.329E+02	+
F08	5.359E+02	7.256E+01	8.292E+02	2.191E+01	+	1.183E+03	4.342E+01	+	5.691E+02	6.522E+01	+	2.092E+03	5.180E+01	+	9.555E+02	4.313E+01	+	7.925E+02	1.034E+02	+
F09	1.627E+04	4.198E+03	8.540E+00	1.287E+01	-	1.114E+05	5.673E+03	+	2.098E+04	1.031E+04	=	1.364E+05	6.598E+03	+	1.911E+04	6.847E+02	+	2.203E+04	2.867E+03	+
F10	1.217E+04	1.005E+03	2.983E+04	4.877E+02	+	1.636E+04	3.713E+02	+	1.417E+04	2.724E+03	+	3.035E+04	4.622E+02	+	1.455E+04	9.180E+02	+	1.491E+04	1.697E+03	+
F11	1.245E+03	1.716E+02	6.415E+02	9.389E+01	-	5.244E+03	6.240E+02	+	3.781E+04	9.647E+03	+	2.270E+05	1.962E+04	+	3.742E+04	9.452E+03	+	2.883E+04	3.436E+04	+
F12	1.444E+07	6.232E+06	2.269E+05	7.832E+04	-	9.080E+06	1.225E+06	-	4.682E+09	3.086E+09	+	1.720E+11	1.353E+10	+	1.541E+07	4.111E+07	-	5.871E+09	3.899E+09	+
F13	4.862E+04	1.772E+04	2.365E+03	1.763E+03	-	5.511E+03	2.320E+03	-	5.167E+08	5.070E+08	+	3.492E+10	4.016E+09	+	2.021E+04	2.757E+03	-	4.238E+05	1.958E+06	-
F14	1.309E+05	6.164E+04	7.453E+03	1.039E+04	-	5.758E+05	1.464E+05	+	4.314E+06	3.532E+06	+	7.196E+07	1.391E+07	+	5.617E+05	9.870E+04	+	1.244E+06	1.365E+06	+
F15	4.228E+04	1.436E+04	1.146E+03	1.172E+03	-	1.177E+03	5.553E+02	-	6.864E+07	1.237E+08	+	1.310E+10	1.918E+09	+	6.743E+03	1.245E+03	-	1.096E+05	4.433E+05	-
F16	2.949E+03	5.257E+02	7.885E+03	2.641E+02	+	4.384E+03	2.304E+02	+	3.853E+03	5.258E+02	+	1.681E+04	1.025E+03	+	5.292E+03	5.537E+02	+	6.137E+03	1.428E+03	+
F17	2.278E+03	3.959E+02	4.783E+03	5.613E+02	+	2.990E+03	1.657E+02	+	2.769E+03	5.245E+02	+	3.585E+05	2.107E+05	+	3.376E+03	4.835E+02	+	4.184E+03	6.176E+02	+
F18	2.645E+05	7.945E+04	1.257E+05	6.171E+04	-	1.386E+06	2.498E+05	+	3.910E+06	2.600E+06	+	1.323E+08	2.652E+07	+	4.823E+05	7.493E+04	+	2.033E+06	4.981E+06	+
F19	5.822E+05	1.867E+05	1.385E+03	1.583E+03	-	1.130E+03	1.081E+03	-	7.035E+07	1.047E+08	+	1.350E+10	1.513E+09	+	4.843E+03	1.245E+03	-	5.476E+06	1.458E+07	=
F20	2.486E+03	4.024E+02	4.849E+03	3.608E+02	+	3.243E+03	2.068E+02	+	2.399E+03	6.840E+02	=	5.422E+03	3.106E+02	+	4.255E+03	4.756E+02	+	3.569E+03	5.554E+02	+
F21	7.550E+02	6.684E+01	1.052E+03	2.502E+01	+	1.369E+03	4.086E+01	+	7.633E+02	5.937E+01	=	2.453E+03	5.933E+01	+	1.384E+03	7.623E+01	+	1.374E+03	1.787E+02	+
F22	1.293E+04	3.969E+03	3.082E+04	4.870E+02	+	1.820E+04	4.323E+02	+	1.634E+04	2.994E+03	+	3.148E+04	4.665E+02	+	1.859E+04	9.135E+02	+	1.757E+04	3.045E+03	+
F23	1.168E+03	7.657E+01	6.276E+02	1.166E+02	-	1.486E+03	3.607E+01	+	1.171E+03	3.876E+02	-	3.591E+03	1.475E+02	+	4.326E+03	2.674E+02	+	2.995E+03	4.969E+02	+
F24	1.483E+03	9.689E+01	9.959E+02	1.854E+02	-	2.099E+03	4.194E+01	+	1.643E+03	8.413E+02	+	6.626E+03	3.459E+02	+	2.767E+03	1.742E+02	+	4.405E+03	4.388E+02	+
F25	7.698E+02	6.799E+01	7.491E+02	5.188E+01	-	7.842E+02	2.500E+01	=	2.701E+03	5.214E+02	+	6.299E+04	4.055E+03	+	1.675E+03	1.919E+02	+	3.243E+03	9.815E+02	+
F26	8.676E+03	1.358E+03	4.055E+03	1.651E+03	-	1.626E+04	2.236E+03	+	1.018E+04	1.042E+03	+	5.006E+04	2.649E+03	+	1.694E+04	4.268E+03	+	2.728E+04	2.683E+03	+
F27	8.178E+02	6.838E+01	6.223E+02	1.758E+01	-	1.258E+03	4.950E+01	+	1.142E+03	1.041E+02	+	7.098E+03	4.051E+02	+	6.765E+03	9.450E+02	+	3.908E+03	8.926E+02	+
F28	6.171E+02	4.270E+01	5.596E+02	2.879E+01	-	6.546E+02	1.270E+01	+	3.862E+03	1.103E+03	+	4.074E+04	1.744E+03	+	1.508E+03	3.635E+02	+	5.522E+03	2.365E+03	+
F29	3.612E+03	4.268E+02	4.620E+03	1.061E+03	+	4.540E+03	1.513E+02	+	4.496E+03	5.955E+02	+	1.080E+05	4.204E+04	+	5.749E+03	4.401E+02	+	8.749E+03	2.706E+03	+
F30	4.078E+06	1.456E+06	3.488E+03	1.063E+03	-	1.671E+05	1.821E+05	-	3.400E+08	2.804E+08	+	2.207E+10	2.999E+09	+	3.513E+06	1.555E+07	-	4.928E+08	3.824E+08	+
W/T/L	-/-/-		11/1/17			22/1/6			24/3/2			29/0/0			23/1/5			26/1/2		

	SIS		CGWO			HGSA			SCA			CGSA-M			MDBSO			GLPSO		
	mean	std	mean	std		mean	std		mean	std		mean	std		mean	std		mean	std	
F01	5.380E+03	6.810E+03	5.434E+09	2.935E+09	+	3.707E+03	3.211E+03	=	1.531E+11	9.584E+09	+	3.747E+03	2.599E+03	=	1.272E+04	1.864E+04	=	9.755E+04	1.848E+05	+
F03	7.035E+04	3.467E+04	8.823E+04	1.509E+04	+	2.744E+05	1.552E+04	+	2.861E+05	1.995E+04	+	3.428E+05	1.233E+04	+	2.025E+05	4.349E+04	+	1.492E+05	4.428E+04	+
F04	2.678E+02	3.603E+01	7.370E+02	1.677E+02	+	2.736E+02	3.846E+01	=	2.588E+04	3.423E+03	+	8.699E+02	2.918E+02	+	2.560E+02	3.787E+01	-	3.081E+02	5.051E+01	+
F05	5.174E+02	6.553E+01	5.768E+02	1.513E+02	+	7.287E+02	3.137E+01	+	1.351E+03	5.763E+01	+	8.115E+02	2.977E+01	+	6.618E+02	1.253E+02	+	3.946E+02	6.658E+01	-
F06	3.902E+01	5.783E+00	2.779E+01	5.125E+00	-	3.113E+01	2.947E+00	-	8.885E+01	3.950E+00	+	5.762E+01	1.560E+00	+	4.641E+01	7.685E+00	+	1.438E-01	3.827E-02	-
F07	7.432E+02	7.748E+01	1.097E+03	2.232E+02	+	1.518E+02	8.209E+00	-	2.687E+03	1.203E+02	+	8.917E+02	7.581E+01	+	1.881E+03	5.922E+02	+	7.417E+02	8.550E+01	=
F08	5.359E+02	7.256E+01	5.983E+02	1.661E+02	=	7.954E+02	3.085E+01	+	1.405E+03	5.557E+01	+	9.492E+02	3.998E+01	+	6.933E+02	1.313E+02	+	3.766E+02	5.894E+01	-
F09	1.627E+04	4.198E+03	2.966E+04	6.730E+03	+	2.081E+03	7.172E+02	-	6.669E+04	6.906E+03	+	1.910E+04	8.600E+02	+	3.265E+04	1.273E+04	+	8.940E+03	3.517E+03	-
F10	1.217E+04	1.005E+03	1.492E+04	3.510E+03	+	1.225E+04	8.714E+02	=	3.023E+04	4.870E+02	+	1.435E+04	7.362E+02	+	2.973E+04	2.588E+03	+	1.119E+04	1.167E+03	-
F11	1.245E+03	1.716E+02	4.138E+03	1.439E+03	+	4.394E+03	1.405E+03	+	6.980E+04	1.102E+04	+	3.815E+04	5.249E+03	+	1.083E+03	2.284E+02	-	3.231E+04	1.353E+04	+
F12	1.444E+07	6.232E+06	4.606E+08	2.662E+08	+	1.329E+06	4.346E+05	-	5.331E+10	7.136E+09	+	1.896E+07	5.244E+07	-	1.986E+06	1.510E+06	-	3.595E+07	1.746E+07	+
F13	4.862E+04	1.772E+04	9.415E+06	1.885E+07	+	3.031E+03	2.063E+03	-	8.224E+09	1.303E+09	+	2.038E+04	2.772E+03	-	8.442E+03	6.918E+03	-	2.420E+04	1.928E+04	-
F14	1.309E+05	6.164E+04	5.213E+05	2.602E+05	+	2.037E+05	3.621E+04	+	1.801E+07	6.980E+06	+	5.519E+05	8.836E+04	+	1.317E+05	8.142E+04	=	3.769E+06	3.642E+06	+
F15	4.228E+04	1.436E+04	1.383E+06	1.819E+06	+	8.601E+02	6.547E+02	-	2.566E+09	6.868E+08	+	6.905E+03	1.461E+03	-	3.500E+03	3.895E+03	-	5.793E+03	4.997E+03	-
F16	2.949E+03	5.257E+02	4.003E+03	1.051E+03	+	4.904E+03	5.010E+02	+	1.081E+04	6.022E+02	+	5.379E+03	5.745E+02	+	3.877E+03	1.418E+03	+	4.085E+03	7.461E+02	+
F17	2.278E+03	3.959E+02	2.871E+03	6.458E+02	+	3.203E+03	3.943E+02	+	9.135E+03	1.205E+03	+	3.471E+03	4.910E+02	+	3.799E+03	1.253E+03	+	3.391E+03	4.840E+02	+
F18	2.645E+05	7.945E+04	9.186E+05	5.088E+05	+	2.813E+05	5.077E+04	=	3.340E+07	1.146E+07	+	4.871E+05	1.006E+05	+	3.136E+05	1.284E+05	=	4.552E+06	4.224E+06	+
F19	5.822E+05	1.867E+05	4.656E+06	2.132E+06	+	1.226E+03	9.443E+02	-	2.111E+09	6.412E+08	+	5.270E+03	1.419E+03	-	3.548E+03	4.532E+03	-	5.520E+03	5.474E+03	-
F20	2.486E+03	4.024E+02	2.920E+03	7.263E+02	+	3.891E+03	3.827E+02	+	5.116E+03	2.624E+02	+	4.246E+03	4.954E+02	+	4.748E+03	5.706E+02	+	2.877E+03	5.376E+02	+
F21	7.550E+02	6.684E+01	8.243E+02	1.843E+02	=	9.193E+02	4.243E+01	+	1.778E+03	6.635E+01	+	1.381E+03	7.776E+01	+	8.663E+02	1.304E+02	+	6.539E+02	5.677E+01	-
F22	1.293E+04	3.969E+03	1.764E+04	4.462E+03	+	1.694E+04	8.212E+02	+	3.130E+04	6.217E+02	+	1.849E+04	9.369E+02	+	3.079E+04	5.412E+02	+	1.252E+04	1.109E+03	-
F23	1.168E+03	7.657E+01	1.097E+03	1.011E+02	-	3.091E+03	2.906E+02	+	2.468E+03	8.346E+01	+	4.375E+03	2.859E+02	+	1.136E+03	1.112E+02	-	8.129E+02	4.525E+01	-
F24	1.483E+03	9.689E+01	1.615E+03	2.087E+02	+	1.264E+03	7.487E+01	-	3.899E+03	1.741E+02	+	2.812E+03	2.652E+02	+	1.523E+03	1.433E+02	=	1.375E+03	6.757E+01	-
F25	7.698E+02	6.799E+01	1.407E+03	1.603E+02	+	8.390E+02	5.914E+01	+	1.145E+04	1.529E+03	+	1.629E+03	1.896E+02	+	8.053E+02	5.498E+01	+	8.454E+02	5.749E+01	+
F26	8.676E+03	1.358E+03	1.033E+04	1.706E+03	+	5.524E+02	1.803E+03	-	2.920E+04	1.471E+03	+	1.610E+04	4.916E+03	+	1.240E+04	2.515E+03	+	8.555E+03	5.981E+02	-
F27	8.178E+02	6.838E+01	1.011E+03	9.130E+01	+	1.453E+03	2.107E+02	+	4.022E+03	3.771E+02	+	7.145E+03	7.720E+02	+	1.054E+03	8.866E+01	+	8.547E+02	5.908E+01	+
F28	6.171E+02	4.270E+01	1.222E+03	2.296E+02	+	6.247E+02	2.500E+01	=	1.547E+04	1.586E+03	+	1.428E+03	3.439E+02	+	5.984E+02	4.641E+01	-	6.658E+02	4.056E+01	+
F29	3.612E+03	4.268E+02	4.405E+03	6.151E+02	+	4.462E+03	3.878E+02	+	1.258E+04	1.250E+03	+	5.777E+03	4.239E+02	+	3.826E+03	6.621E+02	+	3.396E+03	5.700E+02	-
F30	4.078E+06	1.456E+06	5.318E+07	2.898E+07	+	9.267E+03	2.152E+03	-	5.490E+09	1.001E+09	+	2.624E+06	9.390E+06	-	1.018E+04	6.802E+03	-	1.318E+05	9.161E+04	-
W/T/L	-/-/-		25/2/2			14/5/10			29/0/0			23/1/5			16/4/9			13/1/15		

Table 6.6: Experimental results on CEC2011.

	SIS		DE			CS			GWO			PSO			GSA			DNLGSA		
	mean	std	mean	std		mean	std		mean	std		mean	std		mean	std		mean	std	
G01	1.871E+01	4.091E+00	1.410E+00	3.747E+00	-	1.896E+01	2.418E+00	=	1.648E+01	6.179E+00	=	2.374E+01	1.746E+00	+	2.583E+01	1.556E+00	+	2.170E+01	3.769E+00	+
G02	-1.723E+01	4.022E+00	-9.802E+00	7.620E-01	+	-1.242E+01	1.049E+00	+	-2.506E+01	1.599E+00	-	-4.386E+00	4.846E-01	+	-1.855E+01	3.930E+00	-	-2.152E+01	4.190E+00	-
G03	1.151E-05	1.082E-15	1.151E-05	2.336E-19	-	1.152E-05	7.602E-09	+	1.151E-05	6.719E-13	+	1.151E-05	1.847E-12	+	1.151E-05	4.123E-19	-	1.151E-05	3.398E-19	-
G04	2.007E+01	2.891E+00	1.786E+01	3.288E+00	-	1.722E+01	2.558E+00	-	1.429E+01	1.913E-01	-	1.556E+01	1.510E+00	-	1.953E+01	2.156E+00	-	1.696E+01	3.318E+00	-
G05	-3.344E+01	1.735E+00	-2.143E+01	1.168E+00	+	-3.449E+01	5.344E-01	-	-3.257E+01	3.440E+00	=	-1.953E+01	1.336E+00	+	-3.028E+01	3.806E+00	+	-3.124E+01	3.553E+00	+
G06	-1.395E+01	1.732E+00	-1.607E+01	9.587E-01	-	-2.816E+01	8.266E-01	-	-2.500E+01	3.558E+00	-	-1.352E+01	1.293E+00	=	-1.845E+01	2.951E+00	-	-1.803E+01	3.560E+00	-
G07	1.068E+00	3.944E-01	1.719E+00	1.181E-01	+	1.180E+00	6.933E-02	+	9.248E-01	4.044E-01	-	1.723E+00	1.181E-01	+	9.193E-01	2.275E-01	=	1.101E+00	2.434E-01	+
G08	2.274E+02	8.832E+00	2.200E+02	0.000E+00	-	2.274E+02	1.144E+01	=	2.229E+02	7.781E+00	-	2.335E+02	1.076E+01	+	2.830E+02	7.052E+01	+	3.260E+02	1.676E+02	+
G09	1.800E+05	5.627E+04	3.960E+03	7.271E+02	-	4.643E+03	6.965E+02	-	5.942E+03	2.945E+03	-	2.449E+06	6.657E+04	+	1.362E+03	1.825E+02	-	6.310E+05	7.735E+04	+
G10	-1.582E+01	5.469E+00	-2.172E+01	9.663E-02	-	-1.276E+01	1.052E+00	+	-1.754E+01	3.758E+00	-	-8.441E+00	9.112E-01	+	-1.126E+01	5.182E-01	+	-1.325E+01	2.219E+00	+
G11.1	5.236E+04	6.467E+02	6.655E+04	3.336E+03	+	5.751E+04	4.865E+02	+	7.124E+04	3.524E+04	+	1.876E+08	1.000E+07	+	5.218E+04	3.627E+02	=	1.736E+06	5.082E+05	+
G11.2	2.285E+07	4.598E+05	1.742E+07	5.123E+04	-	1.760E+07	1.619E+04	-	2.008E+07	2.830E+05	-	5.201E+07	6.485E+05	+	3.224E+07	1.040E+06	+	4.134E+07	1.386E+06	+
G11.3	1.547E+04	1.370E+01	1.544E+04	6.094E-06	-	1.546E+04	8.227E+00	-	1.547E+04	2.328E+01	=	1.584E+04	3.431E+02	+	1.203E+05	5.726E+04	+	1.549E+04	2.575E+01	+
G11.4	1.937E+04	2.756E+02	1.840E+04	1.535E+02	-	1.896E+04	8.505E+01	-	1.926E+04	1.981E+02	-	1.960E+04	3.202E+02	+	1.920E+04	1.150E+02	-	1.936E+04	2.119E+02	=
G11.5	3.311E+04	5.608E+01	3.279E+04	1.835E+01	-	3.308E+04	3.552E+01	-	3.599E+04	2.045E+04	=	1.539E+05	4.449E+04	+	3.324E+05	3.840E+04	+	8.251E+04	5.508E+04	+
G11.6	1.390E+05	3.269E+03	1.359E+05	1.909E+03	-	1.356E+05	1.340E+03	-	8.484E+05	5.047E+06	+	2.258E+06	1.629E+06	+	1.464E+05	2.182E+03	+	1.456E+05	5.680E+03	+
G11.7	1.975E+06	8.170E+04	2.090E+06	1.081E+05	+	1.934E+06	1.043E+04	-	2.313E+08	1.635E+09	+	5.175E+09	7.772E+08	+	2.720E+06	6.020E+05	+	5.522E+08	1.086E+09	+
G11.8	9.455E+05	3.504E+03	1.302E+06	1.139E+05	+	9.788E+05	1.002E+04	+	9.512E+05	3.534E+03	+	8.007E+07	6.636E+06	+	9.420E+05	1.257E+03	-	2.012E+07	5.763E+06	+
G11.9	1.136E+06	8.939E+04	1.918E+06	1.600E+05	+	1.474E+06	7.252E+04	+	1.199E+06	1.094E+05	+	7.947E+07	6.531E+06	+	9.907E+05	4.785E+04	-	1.986E+07	5.290E+06	+
G11.10	9.454E+05	3.410E+03	1.303E+06	1.284E+05	+	9.782E+05	1.028E+04	+	9.517E+05	3.548E+03	+	8.063E+07	5.422E+06	+	9.421E+05	1.353E+03	-	1.934E+07	5.967E+06	+
G12	1.686E+01	3.797E+00	1.617E+01	2.923E+00	-	2.230E+01	1.657E+00	+	1.910E+01	3.945E+00	+	3.946E+01	3.315E+00	+	4.164E+01	8.120E+00	+	2.388E+01	4.756E+00	+
G13	2.182E+01	2.098E+00	1.799E+01	3.255E+00	-	2.564E+01	2.137E+00	+	2.293E+01	2.796E+00	+	3.896E+01	2.838E+00	+	5.341E+01	6.618E+00	+	2.969E+01	6.533E+00	+
W/T/L	-/-/-		8/0/14			10/2/10			9/4/9			20/1/1			11/2/9			17/1/4		

	SIS		CGWO			HGSA			SCA			CGSA-M			MDBSO			GLPSO		
	mean	std	mean	std		mean	std		mean	std		mean	std		mean	std		mean	std	
G01	1.871E+01	4.091E+00	1.739E+01	6.880E+00	=	1.417E+01	6.503E+00	-	1.617E+01	4.751E+00	-	2.525E+01	1.323E+00	+	1.038E+01	6.264E+00	-	1.234E+01	5.582E+00	-
G02	-1.723E+01	4.022E+00	-2.567E+01	1.087E+00	-	-2.456E+01	2.283E+00	-	-1.192E+01	9.773E-01	+	-1.838E+01	3.772E+00	-	-2.310E+01	5.954E+00	-	-1.645E+01	4.390E+00	=
G03	1.151E-05	1.082E-15	1.151E-05	1.249E-12	+	1.151E-05	1.927E-12	+	1.151E-05	2.336E-12	+	1.151E-05	4.293E-19	-	1.151E-05	1.244E-18	-	1.151E-05	7.394E-18	-
G04	2.007E+01	2.891E+00	1.430E+01	2.600E-01	-	1.552E+01	1.377E+00	-	1.521E+01	1.122E+00	-	1.804E+01	2.811E+00	-	1.832E+01	3.106E+00	-	1.550E+01	2.079E+00	-
G05	-3.344E+01	1.735E+00	-3.206E+01	4.569E+00	=	-3.301E+01	2.108E+00	=	-2.084E+01	1.067E+00	+	-2.995E+01	3.382E+00	+	-2.019E+01	9.431E-01	+	-2.517E+01	2.629E+00	+
G06	-1.395E+01	1.732E+00	-2.424E+01	3.521E+00	-	-2.190E+01	2.297E+00	-	-1.545E+01	1.346E+00	-	-1.846E+01	2.765E+00	-	-1.262E+01	4.016E+00	+	-2.074E+01	3.021E+00	-
G07	1.068E+00	3.944E-01	9.119E-01	3.136E-01	-	7.128E-01	1.318E-01	-	1.693E+00	1.157E-01	+	9.808E-01	1.814E-01	=	1.541E+00	2.401E-01	+	1.705E+00	1.194E-01	+
G08	2.274E+02	8.832E+00	2.511E+02	1.145E+02	-	2.204E+02	2.135E+00	-	2.355E+02	1.288E+01	+	2.772E+02	4.405E+01	+	2.208E+02	4.534E+00	-	2.200E+02	0.000E+00	-
G09	1.800E+05	5.627E+04	9.237E+03	3.012E+03	-	2.101E+05	3.875E+04	+	8.236E+05	9.021E+04	+	1.331E+03	2.190E+02	-	2.978E+04	1.848E+04	-	1.331E+06	7.222E+04	+
G10	-1.582E+01	5.469E+00	-1.839E+01	3.415E+00	-	-1.286E+01	6.137E-01	+	-1.242E+01	1.259E+00	+	-1.129E+01	4.344E-01	+	-1.031E+01	6.521E-02	+	-1.839E+01	1.952E+00	=
G11.1	5.236E+04	6.467E+02	6.748E+04	1.583E+03	+	5.120E+04	4.833E+02	-	8.095E+07	8.596E+06	+	5.216E+04	4.054E+02	=	5.690E+06	2.864E-09	+	3.949E+05	2.065E+05	+
G11.2	2.285E+07	4.598E+05	2.046E+07	4.057E+05	-	2.050E+07	1.768E+05	-	4.843E+07	7.004E+05	+	3.231E+07	1.064E+06	+	2.526E+07	3.048E+05	+	3.577E+07	7.933E+05	+
G11.3	1.547E+04	1.370E+01	1.547E+04	1.822E+01	=	4.673E+04	3.697E+04	+	1.602E+04	4.527E+02	+	9.092E+04	4.944E+04	+	1.548E+04	1.950E+01	+	1.547E+04	1.610E+01	=
G11.4	1.937E+04	2.756E+02	1.913E+04	1.583E+02	-	1.914E+04	1.348E+02	-	1.959E+04	2.928E+02	+	1.917E+04	1.049E+02	-	1.936E+04	1.746E+02	=	1.921E+04	1.747E+02	-
G11.5	3.311E+04	5.608E+01	3.313E+04	1.090E+02	=	3.325E+04	2.413E+01	+	1.617E+05	4.172E+04	+	3.265E+05	4.379E+04	+	4.553E+06	3.286E+06	+	3.312E+04	9.556E+01	=
G11.6	1.390E+05	3.269E+03	1.450E+06	6.652E+06	=	1.430E+05	2.014E+03	+	3.789E+06	3.442E+06	+	1.458E+05	1.936E+03	+	7.018E+07	1.693E+07	+	1.383E+05	2.295E+03	=
G11.7	1.975E+06	8.170E+04	4.665E+08	2.321E+09	+	1.941E+06	6.685E+03	-	5.777E+09	8.298E+08	+	2.743E+06	5.348E+05	+	1.843E+10	3.423E+09	+	2.028E+06	8.295E+04	+
G11.8	9.455E+05	3.504E+03	1.260E+06	6.853E+05	+	9.430E+05	1.688E+03	-	7.628E+07	5.044E+06	+	9.421E+05	1.628E+03	-	2.694E+07	4.659E+06	+	1.395E+07	3.240E+06	+
G11.9	1.136E+06	8.939E+04	1.561E+06	7.016E+05	+	1.189E+06	1.018E+05	+	7.665E+07	7.221E+06	+	9.899E+05	5.383E+04	-	2.609E+07	6.056E+05	+	1.570E+07	3.952E+06	+
G11.10	9.454E+05	3.410E+03	1.259E+06	5.828E+05	+	9.433E+05	1.906E+03	-	7.618E+07	5.910E+06	+	9.418E+05	1.250E+03	-	2.608E+07	2.970E+05	+	1.441E+07	3.586E+06	+
G12	1.686E+01	3.797E+00	1.918E+01	3.623E+00	+	2.650E+01	5.342E+00	+	3.598E+01	3.877E+00	+	4.029E+01	6.913E+00	+	#DIV/0!	#DIV/0!	+	1.919E+01	3.866E+00	+
G13	2.182E+01	2.098E+00	2.293E+01	2.706E+00	+	3.740E+01	5.824E+00	+	3.492E+01	2.653E+00	+	5.251E+01	7.455E+00	+	#DIV/0!	#DIV/0!	+	2.380E+01	2.991E+00	+
W/T/L	-/-/-		8/5/9			9/1/12			19/0/3			11/2/9			15/1/6			11/5/6		

Table 6.7: Friedman test.

CEC2017									CEC2011			DNM		
D=30			D=50			D=100								
Algorithm	Score	Ranking	Algorithm	Score	Ranking	Algorithm	Score	Ranking	Algorithm	Score	Ranking	Algorithm	Score	Ranking
DE	3.2241	1	**SIS**	3.2069	1	**SIS**	3.5517	1	HGSA	4.9545	1	**SIS**	2.1	1
SIS	3.7241	2	DE	3.7586	2	HGSA	4.2414	2	CS	5	2			
HGSA	4.3966	3	HGSA	4.5862	3	GLPSO	4.3793	3	DE	5.0227	3			
MDBSO	4.6897	4	MDBSO	4.8276	4	DE	4.4828	4	GWO	5.1364	4	IMODE	2.2	2
CGWO	5.1379	5	CGWO	5.1379	5	MDBSO	5.2759	5	CGWO	5.4091	5			
CS	6.3448	6	GWO	5.9655	6	CGWO	6.1034	6	**SIS**	5.7273	6			
GWO	6.4138	7	CS	6.5517	7	GWO	6.8276	7	GLPSO	6.4773	7	SCJADE	3.25	3
GLPSO	6.7931	8	GLPSO	7.7931	8	CS	6.8966	8	CGSA-M	7.1818	8			
DNLGSA	8.3103	9	CGSA-M	7.8966	9	GSA	7.7586	9	GSA	7.5909	9			
CGSA-M	9	10	GSA	7.9655	10	CGSA-M	7.9655	10	DNLGSA	8.5455	10	SEDE	3.4	4
GSA	9.2069	11	DNLGSA	9.0345	11	DNLGSA	9.069	11	MDBSO	8.5909	11			
SCA	11.069	12	SCA	11.4138	12	SCA	11.5517	12	SCA	10.0455	12			
PSO	12.6897	13	PSO	12.8621	13	PSO	12.8966	13	PSO	11.3182	13	CJADE	4.05	5

6.2.1 Experimental data and comparison results of spatial information sampling algorithms on CEC2017 and CEC2011

To analyze SIS's performance, we made a comparison of CEC2017 and CEC2011, and they are shown in Table 6.1. It should be mentioned that the $F2$ function in CEC2017 was omitted due to its unstable performance, particularly at high dimensions [39]. In this section, we compared the following algorithms with SIS: DE, CS, GWO, PSO, GSA, DNLGSA, CGWO, HGSA, SCA, CGSA-M, MDBSO, and GLPSO. The common parameters were set as follows: The function's evaluation number E is set to $10^4 * D$, where D is the number of the dimension. In order to obtain statistical data, each algorithm was executed 51 times for each function. The unique parameters of each algorithm are shown in Table 6.2. It should be noted that we have dynamically adjusted the parameters of SIS, and its formula is $b = 0.1 \cdot (E_c/E)$, where E_c is the current number of evaluation times. And when E_c equals $E/2$, $\delta x^t = \delta x^1$.

For all compared algorithms, Tables 6.3, 6.4, 6.5 and 6.6 summarized the classification results in terms of the mean test error and its standard deviation (std). At CEC2017, we tested and compared various algorithms when the dimensions were 30, 50, and 100, respectively, to analyze the performance change of SIS from medium dimension to large dimension. According to $W/T/L$, the winning number of SIS in Table 6.3 is 10, 19, 19, 29, 24, 25, 18, 17, 29, 24, 17, and 22 in comparison to DE, CS, GWO, PSO, GSA, DNLGSA, CGWO, HGSA, SCA, CGSA-M, MDBSO, and GLPSO. Meanwhile, the Friedman test in Table 6.7 shows that among the thirteen algorithms, SIS ranks second, which is stronger than its peers except DE. It demonstrates SIS's ability to perform well on functions with medium dimensions. The results of $W/T/L$ in Table 6.4 show that SIS is remarkably superior to twelve algorithms 12, 22, 21, 29, 22, 26, 23, 18, 29, 22, 20 and 23 functions, respectively. Meanwhile, the Friedman test shows that among the thirteen algorithms, SIS ranks first. The result shows that

on functions with high dimensions, SIS keeps predominant performance. In Table 6.5, the results of $W/T/L$ indicates that SIS significantly outperforms the others on 11, 22, 24, 29, 23, 26, 25, 14, 29, 23, 16 and 13 functions, respectively. Meanwhile, the Friedman test also shows that among the thirteen algorithms, SIS ranks first. It should be emphasized that in the Friedman test data of 30, 50, and 100 dimensions, the ranking of SIS not only changes from the second in 30 dimensions to the first in 50 dimensions, but also widens the score gap between SIS and the second ranking algorithm in 50 and 100 dimensions, which shows the excellent performance of SIS in large dimensions.

Fig. 6.1 shows box-and-whisker diagrams of optimal solutions obtained by thirteen algorithms on F5, F16, and F22 with 30 dimensions, F3, F10, and F24 with 50 dimensions, and F8, F17, and F20 with 100 dimensions. From Fig. 6.1, in comparison to other twelve algorithms with different dimensions, SIS has almost the smallest distribution and the least error of optimal solutions, indicating its superior performance and stability. Fig. 6.2 shows the convergence graphs of average optimal solutions obtained by thirteen algorithms on F5, F16, and F22 with 30 dimensions, F3, F10, and F24 with 50 dimensions, and F8, F17, and F20 with 100 dimensions. The convergence curve of SIS is quite different from that of other algorithms. Other algorithms basically converge rapidly in the early stages of iteration, while SIS converges steadily in the middle stages of iteration, which fully proves that SIS has strong solution space adaptability. As shown in Fig. 6.2, SIS is able to continually find better solutions and alleviate premature convergence.

In Table 6.3, according to $W/T/L$, the winning number of SIS in comparison with the other twelve algorithms is 8, 10, 9, 20, 11, 17, 8, 9, 19, 11, 15, and 11, respectively. Meanwhile, the Friedman test in Table 6.7 shows that among the thirteen algorithms, SIS ranks sixth, which shows that SIS is capable of optimizing functions in real-world

problems of CEC2011.

Through the above comparison, it can be seen that SIS is on par with DE in CEC2017 and 2011. It should be emphasized that DE can be said to be one of the most powerful random real parameter optimization algorithms [78]. When compared with DE, some studies choose parameters that weaken DE. However, in this paper, we choose the optimal parameter scheme of DE in CEC2017 and 2011. In section 6.2.2, we compare SIS with the improved algorithms based on DE to further verify the performance of SIS.

6.2.2 Position optimization of wave energy converters

In this section, we attempt to use SIS to optimize the placement of oscillating buoy-type WECs, and we compare SIS with an improved differential evolution algorithm (IDE) [79] modified specifically for this problem under four real wave regimes (Perth, Adelaide, Tasmania, and Sydney). To ensure the fairness of comparison, in this paper, the calculation formula and related parameters of energy obtained through WECs are consistent with IDE.

In the experiment, both SIS and IDE were run 10 times, with 300 iterations each. b is set to a random number between 0 and 0.1 in SIS. The results of the 4-buoy layout problem in the four real wave scenarios are summarized in Table 6.8. In each wave scenario, the output with the best performance is highlighted in bold. It can be found that the maximum value of SIS in the four wave scenarios is significantly higher than that of IDE, and the mean and minimum values are also obviously dominant, except for the Sydney scenario. This shows that even in the face of the IDE, which has been specially modified for specific optimization problems, SIS still occupies an absolute advantage.

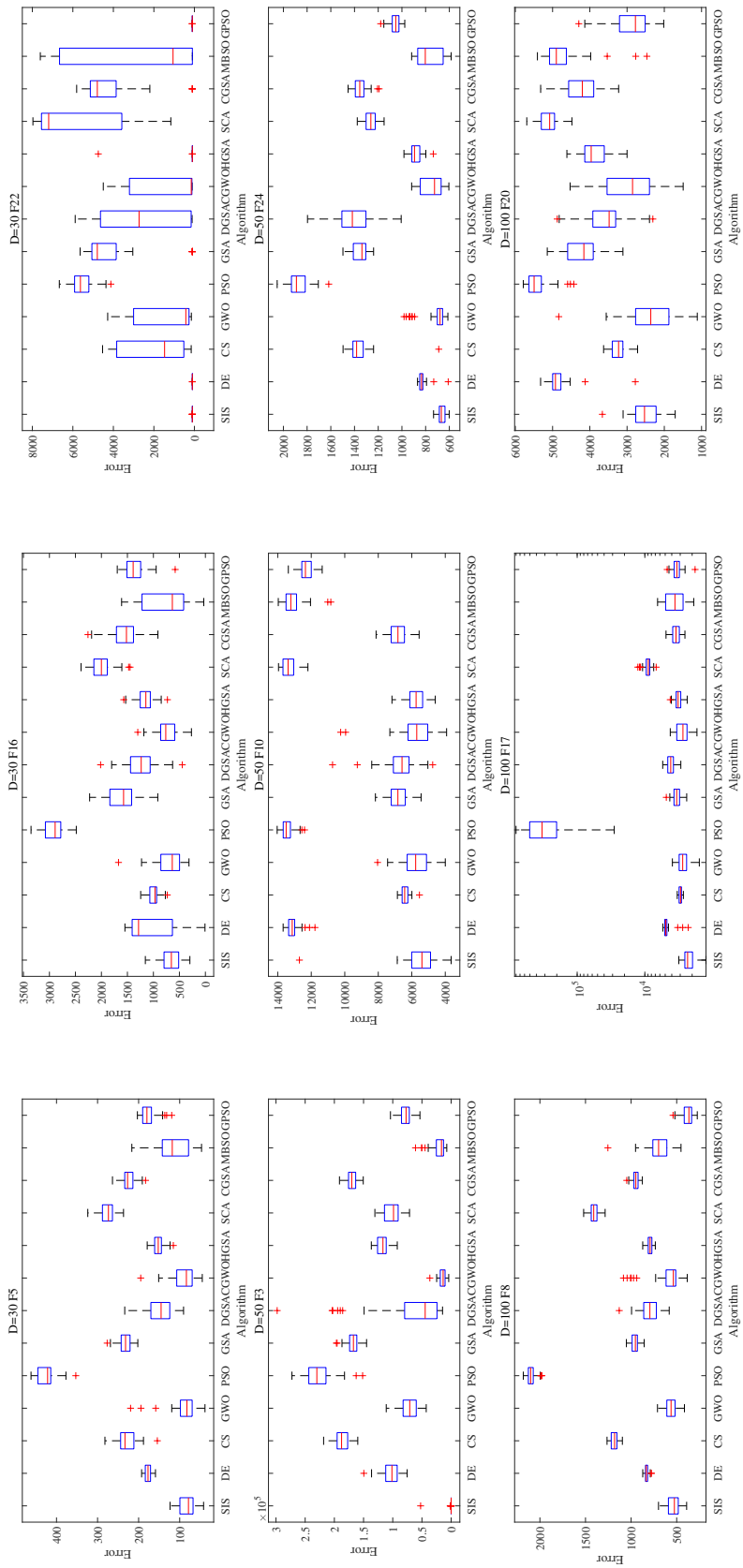

Figure 6.1: Box-and-whisker diagrams comparison on CEC2017.

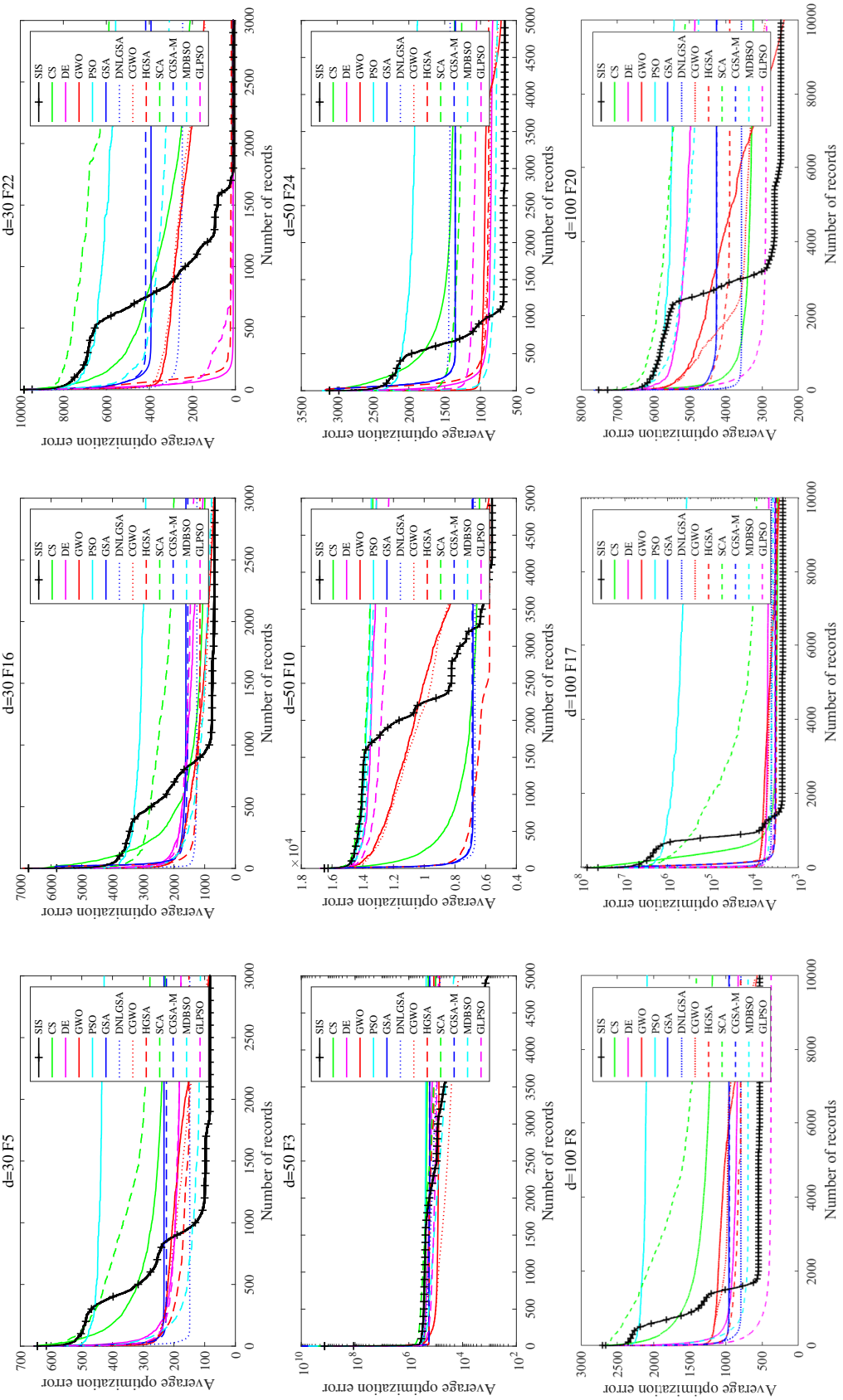

Figure 6.2: Convergence graphs comparison on CEC2017.

Table 6.8: Record of the best 4-buoy layouts per experiment (Power(Watt)).

	Tasmania		Adelaide		Perth		Sydney	
	SIS	IDE	SIS	IDE	SIS	IDE	SIS	IDE
max	**1.341E+06**	1.095E+06	**8.349E+05**	4.023E+05	**7.985E+05**	3.996E+05	**4.232E+05**	4.127E+05
min	**1.273E+06**	1.095E+06	**7.536E+05**	4.023E+05	**7.277E+05**	3.996E+05	4.100E+05	4.127E+05
mean	**1.311E+06**	1.095E+06	**8.055E+05**	4.023E+05	**7.656E+05**	3.996E+05	4.120E+05	4.127E+05
1	1.277E+06	1.095E+06	8.287E+05	4.023E+05	7.729E+05	3.996E+05	4.123E+05	4.127E+05
2	1.341E+06	1.095E+06	8.287E+05	4.023E+05	7.738E+05	3.996E+05	4.110E+05	4.127E+05
3	1.273E+06	1.095E+06	7.779E+05	4.023E+05	7.457E+05	3.996E+05	4.105E+05	4.127E+05
4	1.300E+06	1.095E+06	7.536E+05	4.023E+05	7.985E+05	3.996E+05	4.103E+05	4.127E+05
5	1.336E+06	1.095E+06	7.611E+05	4.023E+05	7.277E+05	3.996E+05	4.232E+05	4.127E+05
6	1.316E+06	1.095E+06	8.349E+05	4.023E+05	7.561E+05	3.996E+05	4.100E+05	4.127E+05
7	1.336E+06	1.095E+06	7.924E+05	4.023E+05	7.694E+05	3.996E+05	4.107E+05	4.127E+05
8	1.295E+06	1.095E+06	8.265E+05	4.023E+05	7.661E+05	3.996E+05	4.108E+05	4.127E+05
9	1.341E+06	1.095E+06	8.259E+05	4.023E+05	7.565E+05	3.996E+05	4.109E+05	4.127E+05
10	1.300E+06	1.095E+06	8.250E+05	4.023E+05	7.891E+05	3.996E+05	4.105E+05	4.127E+05

6.3 Performance evaluation of the improved spherical evolutionary algorithm

In this section, ISE, SE, DE, CJADE, SCJADE [80], SUGGA [71], and LSHADE [81] are tested. Among them, SE creatively adopts a hypersphere search model, which opened a new path for the design of meta-heuristics, and its improved version has an excellent performance in photovoltaic optimization research [82]. DE is proven to be one of the best algorithms in the field of meta-heuristics [78]. CJADE and SCJADE are two well-known improved algorithms based on DE, and SCJADE is an improved version of CJADE. LSHADE ranked first in the IEEE CEC 2014 competition. In addition, the genetic algorithm is the origin of almost all algorithms and has a high visibility [83]. SUGGA is the latest improved version of the genetic algorithm for wind farm layout optimization. The parameters of each algorithm are set as shown in Table 6.9.

Seven algorithms are tested on 13 designed wind farms with various numbers of wind turbines using the wind distributions P_1, P_2, and P_3. Fig. 6.3 shows the 12 different wind farm lands with constraints from landowners. There are 120 available cells in Group 1's wind farms $L1$–$L6$, and 132 cells available cells in Group 2's wind farms $L7$–$L12$, while $L0$, the baseline when all farm owners participate unanimously, has 144 cells available. Each land has a total area of $3415104m^2$ and a cell width of $154m$. Each algorithm needs to be run 51 times on different wind farm lands in each wind direction and had the same number of evaluation times (20,000).

6.3.1 Biased exploitation algorithms vs. biased exploration algorithms

In this section, we first tested ISE, SE, DE, CJADE, and SCJADE. These five algorithms are highly representative. The degree distribution of the PINs of SE and DE has the characteristics of Poisson distribution, which makes the algorithm more explo-

Table 6.9: Parameter settings of algorithms.

Algorithms	Parameters
ISE	$N = 5$, $F = 10$, $D_c = 1/3 \cdot D$
SE	$N = 100$, $F \in (0, 1]$, $D_c = 1/3 \cdot D$
DE	$N = 100$, $F = 0.9$, $CR = 1/3$
CJADE	$N = 100$, $F \in (0, 1]$, $CR \in (0, 1]$, $p = 0.05$
SCJADE	$N = 100$, $F \in (0, 1]$, $CR \in (0, 1]$, $p = 0.05$
LSHADE	$N = 18 \cdot D$, $F \in (0, 1]$, $CR \in (0, 1]$, $p = 0.11$, $H = 5$
SUGGA	$N = 120$, $p_e = 0.2$, $p_c = 0.6$, $p_m = 0.1$, $p_r = 0.5$

(a) Wind farm land L1

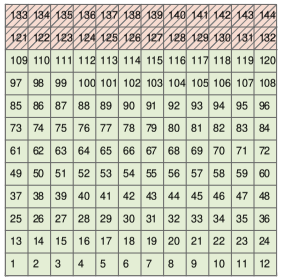

(b) Wind farm land L2

(c) Wind farm land L3

(d) Wind farm land L4

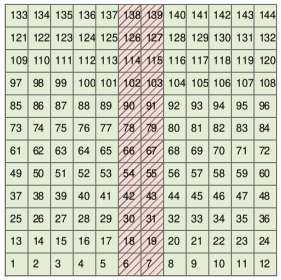

(e) Wind farm land L5

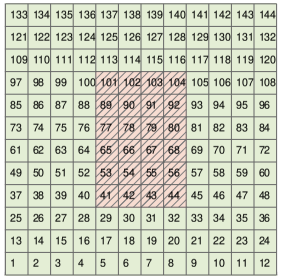

(f) Wind farm land L6

(g) Wind farm land L7

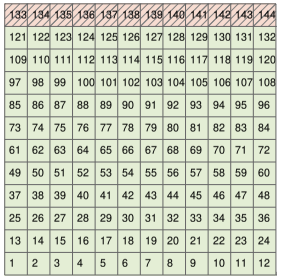

(h) Wind farm land L8

(i) Wind farm land L9

(j) Wind farm land L10

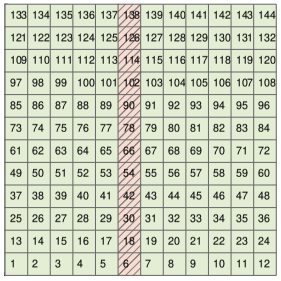

(k) Wind farm land L11

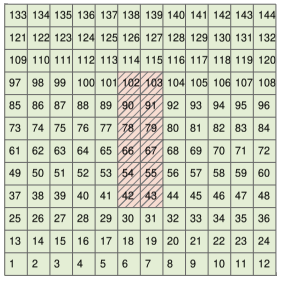

(l) Wind farm land L12

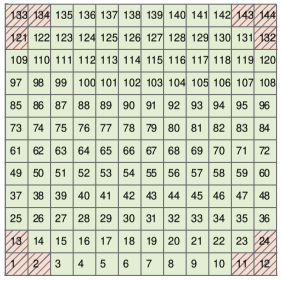

Figure 6.3: Different wind farm locations that are subject to restrictions from landowners.

Table 6.10: Comparison of efficiency performance for wind profile P_1.

	ISE		SE			DE			CJADE			SCJADE		
$P_1(15)$	mean	std	mean	std		mean	std		mean	std		mean	std	
L0	9.788E-01	4.199E-04	9.759E-01	1.194E-03	+	9.727E-01	1.988E-03	+	9.686E-01	2.971E-03	+	9.700E-01	3.188E-03	+
L1	9.696E-01	1.121E-16	9.664E-01	1.440E-03	+	9.634E-01	2.382E-03	+	9.584E-01	3.619E-03	+	9.603E-01	3.431E-03	+
L2	9.789E-01	1.958E-04	9.771E-01	9.454E-04	+	9.753E-01	1.270E-03	+	9.748E-01	2.265E-03	+	9.747E-01	1.921E-03	+
L3	9.641E-01	1.022E-03	9.528E-01	2.732E-03	+	9.488E-01	3.427E-03	+	9.456E-01	4.377E-03	+	9.462E-01	4.595E-03	+
L4	9.642E-01	9.380E-04	9.522E-01	2.324E-03	+	9.474E-01	3.329E-03	+	9.444E-01	4.437E-03	+	9.443E-01	4.932E-03	+
L5	9.789E-01	1.958E-04	9.774E-01	8.578E-04	+	9.766E-01	1.435E-03	+	9.757E-01	1.441E-03	+	9.759E-01	1.685E-03	+
L6	9.788E-01	3.322E-04	9.739E-01	1.611E-03	+	9.671E-01	3.077E-03	+	9.618E-01	5.131E-03	+	9.608E-01	4.633E-03	+
L7	9.747E-01	2.376E-04	9.716E-01	1.486E-03	+	9.679E-01	2.621E-03	+	9.650E-01	3.473E-03	+	9.639E-01	3.536E-03	+
L8	9.789E-01	2.371E-16	9.766E-01	1.219E-03	+	9.747E-01	1.850E-03	+	9.723E-01	2.819E-03	+	9.730E-01	2.082E-03	+
L9	9.716E-01	6.066E-04	9.649E-01	1.996E-03	+	9.610E-01	2.516E-03	+	9.584E-01	3.698E-03	+	9.573E-01	3.834E-03	+
L10	9.715E-01	6.759E-04	9.651E-01	1.850E-03	+	9.617E-01	2.747E-03	+	9.574E-01	4.263E-03	+	9.582E-01	5.165E-03	+
L11	9.789E-01	1.360E-16	9.768E-01	1.159E-03	+	9.752E-01	1.547E-03	+	9.733E-01	2.303E-03	+	9.736E-01	2.426E-03	+
L12	9.788E-01	5.045E-04	9.735E-01	1.394E-03	+	9.689E-01	2.843E-03	+	9.645E-01	3.563E-03	+	9.636E-01	3.789E-03	+
W/T/L	-/-/-		13/0/0			13/0/0			13/0/0			13/0/0		
$P_1(20)$	mean	std	mean	std		mean	std		mean	std		mean	std	
L0	9.521E-01	2.395E-03	9.234E-01	4.147E-03	+	9.149E-01	7.277E-03	+	9.049E-01	6.574E-03	+	9.077E-01	7.738E-03	+
L1	9.337E-01	2.333E-03	9.028E-01	3.912E-03	+	8.945E-01	8.087E-03	+	8.835E-01	7.138E-03	+	8.870E-01	7.662E-03	+
L2	9.541E-01	1.761E-03	9.353E-01	2.825E-03	+	9.331E-01	4.854E-03	+	9.271E-01	6.502E-03	+	9.290E-01	6.141E-03	+
L3	9.339E-01	3.630E-03	8.875E-01	6.461E-03	+	8.722E-01	6.360E-03	+	8.702E-01	8.547E-03	+	8.705E-01	8.882E-03	+
L4	9.332E-01	3.828E-03	8.859E-01	4.553E-03	+	8.732E-01	5.820E-03	+	8.687E-01	6.231E-03	+	8.666E-01	6.853E-03	+
L5	9.546E-01	1.345E-03	9.392E-01	2.720E-03	+	9.339E-01	5.351E-03	+	9.332E-01	6.057E-03	+	9.337E-01	5.254E-03	+
L6	9.471E-01	4.004E-03	9.066E-01	5.100E-03	+	8.883E-01	7.499E-03	+	8.800E-01	8.042E-03	+	8.808E-01	7.655E-03	+
L7	9.442E-01	2.252E-03	9.140E-01	5.009E-03	+	9.050E-01	5.735E-03	+	8.954E-01	7.696E-03	+	8.969E-01	9.288E-03	+
L8	9.531E-01	2.157E-03	9.304E-01	3.385E-03	+	9.254E-01	5.623E-03	+	9.194E-01	7.039E-03	+	9.208E-01	5.633E-03	+
L9	9.440E-01	3.209E-03	9.069E-01	4.481E-03	+	8.957E-01	6.191E-03	+	8.915E-01	9.645E-03	+	8.906E-01	8.874E-03	+
L10	9.433E-01	3.343E-03	9.082E-01	4.666E-03	+	8.969E-01	6.282E-03	+	8.899E-01	6.712E-03	+	8.892E-01	7.694E-03	+
L11	9.531E-01	2.225E-03	9.318E-01	2.661E-03	+	9.271E-01	7.303E-03	+	9.215E-01	7.595E-03	+	9.238E-01	5.838E-03	+
L12	9.476E-01	2.713E-03	9.139E-01	4.407E-03	+	9.003E-01	7.071E-03	+	8.897E-01	6.516E-03	+	8.918E-01	8.425E-03	+
W/T/L	-/-/-		13/0/0			13/0/0			13/0/0			13/0/0		
$P_1(25)$	mean	std	mean	std		mean	std		mean	std		mean	std	
L0	9.105E-01	3.525E-03	8.595E-01	5.847E-03	+	8.425E-01	6.167E-03	+	8.368E-01	9.387E-03	+	8.385E-01	9.031E-03	+
L1	8.849E-01	3.788E-03	8.302E-01	5.371E-03	+	8.158E-01	5.540E-03	+	8.076E-01	7.590E-03	+	8.100E-01	7.251E-03	+
L2	9.133E-01	3.101E-03	8.782E-01	5.208E-03	+	8.616E-01	6.128E-03	+	8.586E-01	9.307E-03	+	8.603E-01	8.528E-03	+
L3	8.422E-01	2.859E-03	8.046E-01	5.472E-03	+	7.918E-01	5.685E-03	+	7.852E-01	5.459E-03	+	7.883E-01	7.275E-03	+
L4	8.428E-01	2.958E-03	8.034E-01	5.622E-03	+	7.910E-01	5.834E-03	+	7.836E-01	7.671E-03	+	7.844E-01	8.058E-03	+
L5	9.152E-01	2.983E-03	8.823E-01	6.255E-03	+	8.660E-01	6.934E-03	+	8.637E-01	7.619E-03	+	8.623E-01	9.137E-03	+
L6	8.727E-01	4.348E-03	8.298E-01	3.947E-03	+	8.085E-01	5.941E-03	+	8.048E-01	8.059E-03	+	8.047E-01	8.506E-03	+
L7	8.972E-01	4.704E-03	8.457E-01	5.667E-03	+	8.315E-01	6.452E-03	+	8.234E-01	9.112E-03	+	8.249E-01	7.906E-03	+
L8	9.114E-01	4.164E-03	8.702E-01	5.889E-03	+	8.540E-01	5.672E-03	+	8.464E-01	7.762E-03	+	8.531E-01	9.477E-03	+
L9	8.782E-01	3.511E-03	8.357E-01	4.879E-03	+	8.193E-01	7.161E-03	+	8.127E-01	6.842E-03	+	8.156E-01	7.271E-03	+
L10	8.792E-01	3.449E-03	8.352E-01	5.870E-03	+	8.189E-01	5.732E-03	+	8.129E-01	6.494E-03	+	8.146E-01	8.651E-03	+
L11	9.130E-01	3.509E-03	8.714E-01	5.481E-03	+	8.562E-01	6.481E-03	+	8.533E-01	8.731E-03	+	8.530E-01	7.693E-03	+
L12	8.963E-01	4.436E-03	8.433E-01	5.437E-03	+	8.260E-01	5.720E-03	+	8.163E-01	7.666E-03	+	8.191E-01	7.893E-03	+
W/T/L	-/-/-		13/0/0			13/0/0			13/0/0			13/0/0		

Table 6.11: Comparison of efficiency performance for wind profile P_2.

	ISE		SE			DE			CJADE			SCJADE		
$P_2(15)$	mean	std	mean	std		mean	std		mean	std		mean	std	
L0	9.717E-01	2.330E-03	9.651E-01	2.553E-03	+	9.524E-01	4.926E-03	+	9.572E-01	4.600E-03	+	9.570E-01	4.982E-03	+
L1	9.496E-01	1.872E-03	9.433E-01	3.087E-03	+	9.282E-01	5.648E-03	+	9.344E-01	5.006E-03	+	9.352E-01	4.255E-03	+
L2	9.567E-01	1.656E-03	9.508E-01	2.833E-03	+	9.381E-01	4.047E-03	+	9.415E-01	3.759E-03	+	9.424E-01	4.532E-03	+
L3	9.504E-01	2.478E-03	9.439E-01	2.989E-03	+	9.286E-01	5.034E-03	+	9.305E-01	5.001E-03	+	9.309E-01	6.545E-03	+
L4	9.561E-01	1.961E-03	9.491E-01	2.575E-03	+	9.360E-01	4.703E-03	+	9.352E-01	3.933E-03	+	9.364E-01	5.179E-03	+
L5	9.669E-01	2.403E-03	9.580E-01	3.240E-03	+	9.427E-01	3.432E-03	+	9.434E-01	5.100E-03	+	9.449E-01	5.025E-03	+
L6	9.678E-01	1.286E-03	9.629E-01	2.938E-03	+	9.454E-01	6.216E-03	+	9.470E-01	5.424E-03	+	9.467E-01	5.450E-03	+
L7	9.616E-01	2.121E-03	9.561E-01	3.231E-03	+	9.413E-01	4.822E-03	+	9.463E-01	4.057E-03	+	9.472E-01	4.530E-03	+
L8	9.646E-01	1.958E-03	9.597E-01	3.374E-03	+	9.457E-01	5.134E-03	+	9.498E-01	4.801E-03	+	9.512E-01	3.365E-03	+
L9	9.620E-01	2.041E-03	9.560E-01	2.977E-03	+	9.402E-01	4.554E-03	+	9.442E-01	4.806E-03	+	9.451E-01	4.596E-03	+
L10	9.648E-01	2.269E-03	9.584E-01	2.390E-03	+	9.452E-01	4.553E-03	+	9.461E-01	4.897E-03	+	9.469E-01	5.521E-03	+
L11	9.705E-01	2.482E-03	9.639E-01	3.545E-03	+	9.496E-01	4.763E-03	+	9.522E-01	4.835E-03	+	9.513E-01	4.952E-03	+
L12	9.685E-01	1.636E-03	9.637E-01	2.566E-03	+	9.492E-01	4.266E-03	+	9.525E-01	4.986E-03	+	9.527E-01	3.844E-03	+
W/T/L	-/-/-		13/0/0			13/0/0			13/0/0			13/0/0		
$P_2(20)$	mean	std	mean	std		mean	std		mean	std		mean	std	
L0	9.115E-01	2.973E-03	8.991E-01	3.272E-03	+	8.773E-01	5.082E-03	+	8.847E-01	5.433E-03	+	8.859E-01	4.598E-03	+
L1	8.747E-01	2.595E-03	8.621E-01	3.066E-03	+	8.444E-01	4.896E-03	+	8.506E-01	5.395E-03	+	8.517E-01	4.880E-03	+
L2	8.923E-01	2.357E-03	8.822E-01	3.478E-03	+	8.623E-01	5.137E-03	+	8.656E-01	6.333E-03	+	8.657E-01	5.209E-03	+
L3	8.732E-01	2.516E-03	8.622E-01	3.963E-03	+	8.422E-01	6.285E-03	+	8.440E-01	5.280E-03	+	8.472E-01	7.606E-03	+
L4	8.925E-01	2.237E-03	8.805E-01	3.400E-03	+	8.591E-01	4.908E-03	+	8.605E-01	5.171E-03	+	8.616E-01	4.824E-03	+
L5	8.972E-01	2.285E-03	8.871E-01	2.672E-03	+	8.679E-01	4.912E-03	+	8.694E-01	4.641E-03	+	8.691E-01	4.981E-03	+
L6	8.984E-01	2.624E-03	8.833E-01	4.536E-03	+	8.611E-01	5.294E-03	+	8.624E-01	5.219E-03	+	8.648E-01	7.828E-03	+
L7	8.949E-01	3.131E-03	8.829E-01	4.296E-03	+	8.609E-01	5.372E-03	+	8.687E-01	5.226E-03	+	8.702E-01	4.929E-03	+
L8	9.037E-01	2.533E-03	8.923E-01	3.787E-03	+	8.701E-01	6.467E-03	+	8.763E-01	5.091E-03	+	8.771E-01	5.637E-03	+
L9	8.955E-01	3.419E-03	8.814E-01	3.958E-03	+	8.602E-01	4.663E-03	+	8.660E-01	5.465E-03	+	8.656E-01	5.238E-03	+
L10	9.026E-01	2.575E-03	8.910E-01	3.974E-03	+	8.704E-01	6.097E-03	+	8.730E-01	4.515E-03	+	8.755E-01	6.146E-03	+
L11	9.065E-01	2.808E-03	8.954E-01	4.250E-03	+	8.747E-01	5.238E-03	+	8.783E-01	5.115E-03	+	8.797E-01	4.911E-03	+
L12	9.069E-01	3.604E-03	8.906E-01	3.705E-03	+	8.704E-01	4.948E-03	+	8.740E-01	5.322E-03	+	8.763E-01	5.672E-03	+
W/T/L	-/-/-		13/0/0			13/0/0			13/0/0			13/0/0		
$P_2(25)$	mean	std	mean	std		mean	std		mean	std		mean	std	
L0	8.431E-01	2.321E-03	8.263E-01	3.440E-03	+	8.047E-01	4.257E-03	+	8.133E-01	4.788E-03	+	8.152E-01	5.025E-03	+
L1	7.955E-01	2.480E-03	7.812E-01	3.134E-03	+	7.618E-01	4.864E-03	+	7.699E-01	5.279E-03	+	7.696E-01	4.715E-03	+
L2	8.201E-01	2.520E-03	8.046E-01	3.618E-03	+	7.836E-01	4.922E-03	+	7.884E-01	5.766E-03	+	7.893E-01	4.607E-03	+
L3	7.956E-01	2.702E-03	7.801E-01	3.197E-03	+	7.618E-01	4.554E-03	+	7.624E-01	4.248E-03	+	7.663E-01	4.278E-03	+
L4	8.213E-01	2.168E-03	8.054E-01	3.763E-03	+	7.831E-01	4.973E-03	+	7.851E-01	5.396E-03	+	7.875E-01	4.336E-03	+
L5	8.336E-01	2.762E-03	8.183E-01	3.751E-03	+	7.949E-01	3.603E-03	+	7.977E-01	5.738E-03	+	7.997E-01	5.484E-03	+
L6	8.271E-01	3.012E-03	8.073E-01	4.861E-03	+	7.836E-01	5.766E-03	+	7.838E-01	4.750E-03	+	7.850E-01	5.368E-03	+
L7	8.207E-01	2.988E-03	8.052E-01	3.821E-03	+	7.851E-01	5.401E-03	+	7.928E-01	5.010E-03	+	7.949E-01	5.290E-03	+
L8	8.333E-01	2.682E-03	8.171E-01	3.836E-03	+	7.958E-01	5.620E-03	+	8.012E-01	4.698E-03	+	8.024E-01	5.883E-03	+
L9	8.205E-01	2.911E-03	8.051E-01	2.993E-03	+	7.828E-01	5.489E-03	+	7.899E-01	5.665E-03	+	7.901E-01	5.109E-03	+
L10	8.328E-01	2.823E-03	8.169E-01	3.630E-03	+	7.954E-01	4.918E-03	+	8.013E-01	5.654E-03	+	8.022E-01	5.680E-03	+
L11	8.417E-01	2.814E-03	8.260E-01	3.716E-03	+	8.038E-01	5.720E-03	+	8.079E-01	4.748E-03	+	8.097E-01	5.655E-03	+
L12	8.381E-01	2.568E-03	8.187E-01	3.905E-03	+	7.962E-01	6.163E-03	+	7.994E-01	5.090E-03	+	8.009E-01	4.777E-03	+
W/T/L	-/-/-		13/0/0			13/0/0			13/0/0			13/0/0		

Table 6.12: Comparison of efficiency performance for wind profile P_3.

	ISE		SE			DE			CJADE			SCJADE		
$P_3(15)$	mean	std	mean	std		mean	std		mean	std		mean	std	
L0	9.933E-01	4.355E-04	9.838E-01	2.791E-03	+	9.771E-01	3.448E-03	+	9.717E-01	5.189E-03	+	9.721E-01	4.187E-03	+
L1	9.904E-01	6.608E-04	9.763E-01	3.007E-03	+	9.717E-01	3.852E-03	+	9.649E-01	5.240E-03	+	9.651E-01	4.976E-03	+
L2	9.933E-01	4.105E-04	9.878E-01	2.263E-03	+	9.829E-01	3.453E-03	+	9.785E-01	4.088E-03	+	9.794E-01	4.585E-03	+
L3	9.886E-01	7.289E-04	9.773E-01	2.854E-03	+	9.694E-01	4.579E-03	+	9.660E-01	4.672E-03	+	9.646E-01	5.413E-03	+
L4	9.886E-01	7.501E-04	9.780E-01	2.417E-03	+	9.707E-01	3.307E-03	+	9.658E-01	3.946E-03	+	9.668E-01	5.326E-03	+
L5	9.934E-01	3.848E-04	9.876E-01	2.350E-03	+	9.835E-01	2.525E-03	+	9.817E-01	3.277E-03	+	9.809E-01	3.748E-03	+
L6	9.917E-01	1.030E-03	9.790E-01	3.194E-03	+	9.678E-01	4.341E-03	+	9.603E-01	5.378E-03	+	9.619E-01	4.549E-03	+
L7	9.920E-01	5.126E-04	9.809E-01	2.690E-03	+	9.740E-01	3.909E-03	+	9.688E-01	4.833E-03	+	9.698E-01	4.589E-03	+
L8	9.933E-01	5.274E-04	9.863E-01	2.092E-03	+	9.805E-01	4.228E-03	+	9.751E-01	4.380E-03	+	9.773E-01	4.768E-03	+
L9	9.911E-01	5.036E-04	9.811E-01	2.538E-03	+	9.738E-01	2.787E-03	+	9.685E-01	4.258E-03	+	9.709E-01	4.809E-03	+
L10	9.910E-01	5.917E-04	9.807E-01	2.898E-03	+	9.741E-01	3.429E-03	+	9.687E-01	4.595E-03	+	9.689E-01	4.199E-03	+
L11	9.934E-01	3.898E-04	9.859E-01	1.932E-03	+	9.816E-01	3.828E-03	+	9.783E-01	3.887E-03	+	9.779E-01	4.284E-03	+
L12	9.919E-01	1.021E-03	9.804E-01	2.730E-03	+	9.711E-01	4.475E-03	+	9.631E-01	4.561E-03	+	9.642E-01	4.419E-03	+
W/T/L	-/-/-		13/0/0			13/0/0			13/0/0			13/0/0		
$P_3(20)$	mean	std	mean	std		mean	std		mean	std		mean	std	
L0	9.815E-01	2.674E-03	9.492E-01	3.707E-03	+	9.386E-01	4.388E-03	+	9.335E-01	5.000E-03	+	9.342E-01	5.790E-03	+
L1	9.767E-01	2.828E-03	9.355E-01	3.922E-03	+	9.271E-01	5.273E-03	+	9.206E-01	6.295E-03	+	9.213E-01	6.072E-03	+
L2	9.820E-01	2.519E-03	9.564E-01	3.259E-03	+	9.462E-01	3.421E-03	+	9.402E-01	3.689E-03	+	9.423E-01	5.359E-03	+
L3	9.708E-01	3.870E-03	9.375E-01	3.867E-03	+	9.261E-01	4.698E-03	+	9.233E-01	5.218E-03	+	9.228E-01	5.691E-03	+
L4	9.717E-01	3.268E-03	9.415E-01	3.874E-03	+	9.294E-01	3.492E-03	+	9.259E-01	4.655E-03	+	9.269E-01	4.340E-03	+
L5	9.825E-01	2.529E-03	9.564E-01	3.924E-03	+	9.473E-01	4.363E-03	+	9.454E-01	5.268E-03	+	9.455E-01	4.788E-03	+
L6	9.682E-01	3.803E-03	9.387E-01	4.930E-03	+	9.223E-01	4.535E-03	+	9.149E-01	5.538E-03	+	9.165E-01	6.024E-03	+
L7	9.786E-01	3.401E-03	9.419E-01	3.759E-03	+	9.338E-01	5.026E-03	+	9.279E-01	6.762E-03	+	9.273E-01	6.386E-03	+
L8	9.820E-01	2.562E-03	9.540E-01	4.411E-03	+	9.442E-01	5.062E-03	+	9.383E-01	5.092E-03	+	9.376E-01	5.255E-03	+
L9	9.771E-01	4.140E-03	9.441E-01	3.885E-03	+	9.336E-01	5.283E-03	+	9.279E-01	5.014E-03	+	9.303E-01	8.407E-03	+
L10	9.777E-01	3.321E-03	9.460E-01	4.320E-03	+	9.348E-01	3.976E-03	+	9.281E-01	4.816E-03	+	9.295E-01	6.226E-03	+
L11	9.823E-01	2.777E-03	9.547E-01	3.593E-03	+	9.453E-01	4.670E-03	+	9.415E-01	6.139E-03	+	9.433E-01	5.559E-03	+
L12	9.709E-01	3.757E-03	9.410E-01	3.944E-03	+	9.271E-01	4.347E-03	+	9.171E-01	4.058E-03	+	9.201E-01	6.469E-03	+
W/T/L	-/-/-		13/0/0			13/0/0			13/0/0			13/0/0		
$P_3(25)$	mean	std	mean	std		mean	std		mean	std		mean	std	
L0	9.563E-01	5.593E-03	9.101E-01	4.200E-03	+	9.003E-01	5.053E-03	+	8.928E-01	5.794E-03	+	8.941E-01	4.831E-03	+
L1	9.457E-01	4.554E-03	8.928E-01	3.669E-03	+	8.833E-01	4.902E-03	+	8.777E-01	4.958E-03	+	8.801E-01	6.320E-03	+
L2	9.559E-01	5.087E-03	9.190E-01	4.796E-03	+	9.073E-01	3.828E-03	+	9.005E-01	5.602E-03	+	9.024E-01	4.917E-03	+
L3	9.367E-01	5.259E-03	8.933E-01	4.113E-03	+	8.829E-01	4.921E-03	+	8.796E-01	5.817E-03	+	8.807E-01	5.624E-03	+
L4	9.377E-01	3.943E-03	9.027E-01	4.450E-03	+	8.897E-01	3.922E-03	+	8.851E-01	5.444E-03	+	8.865E-01	5.059E-03	+
L5	9.570E-01	5.269E-03	9.180E-01	4.598E-03	+	9.092E-01	5.023E-03	+	9.052E-01	5.627E-03	+	9.074E-01	5.757E-03	+
L6	9.343E-01	4.777E-03	8.958E-01	4.148E-03	+	8.783E-01	5.183E-03	+	8.729E-01	5.542E-03	+	8.743E-01	5.404E-03	+
L7	9.506E-01	6.830E-03	9.025E-01	4.546E-03	+	8.920E-01	3.951E-03	+	8.848E-01	5.377E-03	+	8.868E-01	6.709E-03	+
L8	9.559E-01	4.040E-03	9.157E-01	4.138E-03	+	9.042E-01	5.091E-03	+	8.991E-01	4.980E-03	+	8.999E-01	6.134E-03	+
L9	9.478E-01	4.796E-03	9.034E-01	4.021E-03	+	8.927E-01	4.791E-03	+	8.880E-01	5.840E-03	+	8.901E-01	6.356E-03	+
L10	9.482E-01	4.923E-03	9.066E-01	4.217E-03	+	8.949E-01	4.736E-03	+	8.880E-01	4.289E-03	+	8.905E-01	5.480E-03	+
L11	9.559E-01	5.695E-03	9.149E-01	3.361E-03	+	9.065E-01	4.185E-03	+	9.016E-01	4.853E-03	+	9.029E-01	5.803E-03	+
L12	9.359E-01	3.364E-03	8.978E-01	3.356E-03	+	8.823E-01	4.532E-03	+	8.763E-01	5.887E-03	+	8.746E-01	4.640E-03	+
W/T/L	-/-/-		13/0/0			13/0/0			13/0/0			13/0/0		

Table 6.13: Friedman test of five algorithms on WFLOP.

	ISE	SE	DE	SCJADE	CJADE
Score	5	4	2.3419	2.1197	1.5385
Rank	1	2	3	4	5

ration oriented. In contrast, the degree distribution of PINs of CJADE and SCJADE has the characteristics of a power-law distribution, which makes the algorithm more biased towards exploitation [38]. The results of the wind farm efficiency tests on wind distribution P_1, P_2, and P_3 are compiled in Tables 6.10, 6.11, and 6.12. As can be seen from the table, the ISE far outperforms the other algorithms for all conditions for wind farms $L1$-$L12$ and for the three wind turbine numbers (15, 20, 25). The values of $W/T/L$ are all 13/0/0, indicating that the ISE significantly outperforms the other algorithms in either condition, and there is not even a single tie, which is quite rare in the field of optimization algorithms.

Fig. 6.14 shows the box-and-whisker diagrams of the conversion efficiency of each algorithm in Group 1 and Group 2. As can be seen from Fig. 6.14, the performance of each algorithm in the cases of P_1 and P_3 of the wind distribution perfectly validates the conclusion that the exploration-biased algorithm is superior to the exploitation-biased algorithm on WFLOP. The ISE has the strongest exploration and therefore the best performance. SE belongs to the exploration-biased Poisson distribution, and its mechanism is more exploration-biased compared to DE, so it performs better than DE, which is also a Poisson distribution. Also, since CJADE and SCJADE belong to the power-law distribution of biased exploitation, their performance on WFLOP is weaker than that of DE. SCJADE is an improvement of CJADE, whose main operation is to improve the local search of CJADE on the optimal individual from a random search to a difference between two individuals.

In P_2 of Fig. 6.14, a different situation emerges from that of P_1 and P_3, with DE being the worst-performing algorithm. There may be three unrelated reasons:

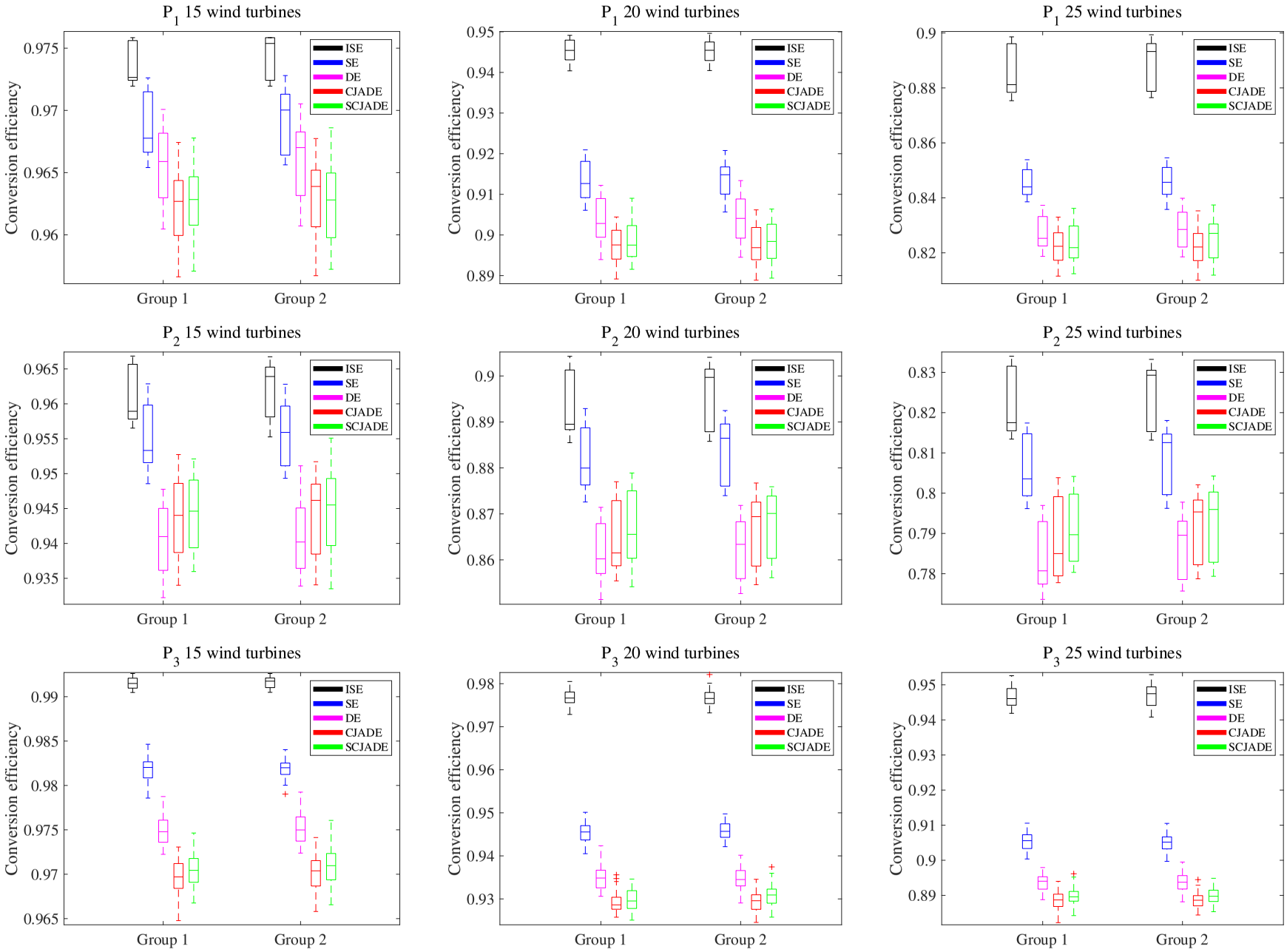

Table 6.14: Conversion efficiency on wind distribution P_1, P_2, and P_3.

1) ***Reason 1***: The different mechanisms of the different algorithms lead to unexpected results. For example, in CJADE and SCJADE, chaotic maps are introduced to control the search radius of the local search. Due to the ergodicity [27] and pseudo-randomness [28] of chaotic maps, the local search range of CJADE and SCJADE may suddenly increase, thus allowing the algorithms to enhance exploration while maintaining a power-law distribution.

2) ***Reason 2***: Since P_2 is an equal incoming wind in all four directions, the result is a large search space in each direction, and there may be some local optimal region in the solution space in each direction, thus leaving the algorithm some room for improvement in both biased exploitation and biased exploration. In other words, both the biased exploitation algorithm and the biased exploration algorithm will outperform the DE in this wind condition.

3) ***Reason 3***: This can be verified by the fact that the optimization results of the algorithms in P_2 are less robust than those of P_1 and P_3 in Fig. 6.14. It is also possible to combine the performance of SE and DE as well as CJADE and SCJADE for analysis. It can be seen that while CJADE outperforms DE, SCJADE is far inferior to SE, suggesting that the exploration-biased algorithm has a higher potential for improvement on P_2.

We will also conduct an in-depth analysis of the two speculations mentioned above in our next work.

Table 6.13 shows the Friedman test results obtained by subjecting the data obtained after optimizing P_1, P_2, and P_3 by the five algorithms. The test results show that ISE with the strongest exploration has the best performance, SE ranks second, DE with Poisson distribution ranks third, and CJADE and SCJADE have the worst performance due to biased exploitation. The above results show that the exploration-biased algorithm outperforms the exploitation-biased algorithm on this WFLOP. It

also proves that our improvement to enhance the SE exploration capability is correct.

6.3.2 ISE vs. SUGGA and LSHADE

In this section, we compare the ISE with the SUGGA and LSHADE. In the SUGGA algorithm, a new step called "support vector regression guided relocation of the worst turbine" is used in the GA. This gives SUGGA powerful optimization capabilities. LSHADE is a successful history-based adaptive DE variant with linear population size reduction that has been considered among the most efficient evolutionary algorithms. Since techniques beyond meta-heuristics are used in SUGGA and population adaptive methods are used in LSHADE, it is difficult to precisely define the exploitation or exploration of the two algorithms.

Since these two algorithms are highly comparable as state-of-the-art algorithms, we compare ISE with them in this section. As can be seen in Tables 6.15, 6.16, and 6.17, the ISE outperforms the SUGGA and LSHADE on all wind distributions P_1, P_2, and P_3. In addition, we perform the Wilcoxon signed-rank test, and the p-values obtained were recorded in the table. The results based on p-values show that the ISE has a value of 6/3/0 and 9/0/0 for $W/T/L$ compared to SUGGA and LSHADE. This shows that ISE has significant advantages and no significant disadvantages compared to SUGGA. When compared to LSHADE, ISE has a definite advantage.

Table 6.15: Comparison between ISE, SUGGA, and LSHADE under wind profile P_1.

	ISE		SUGGA			LSHADE		
$P_1(15)$	mean	std	mean	std		mean	std	
L0	9.788E-01	4.199E-04	9.775E-01	1.110E-15	+	9.782E-01	9.005E-04	+
L1	9.696E-01	1.121E-16	9.730E-01	1.221E-15	-	9.693E-01	8.710E-04	+
L2	9.789E-01	1.958E-04	9.775E-01	1.110E-15	+	9.789E-01	5.571E-16	=
L3	9.641E-01	1.022E-03	9.719E-01	6.661E-16	-	9.595E-01	1.771E-03	+
L4	9.642E-01	9.380E-04	9.789E-01	5.551E-16	-	9.599E-01	2.091E-03	+
L5	9.789E-01	1.958E-04	9.789E-01	5.551E-16	=	9.788E-01	2.741E-04	=
L6	9.788E-01	3.322E-04	9.775E-01	1.110E-15	+	9.762E-01	1.731E-03	+
L7	9.747E-01	2.376E-04	9.761E-01	8.882E-16	-	9.740E-01	9.703E-04	+
L8	9.789E-01	2.371E-16	9.789E-01	5.551E-16	=	9.787E-01	4.859E-04	+
L9	9.716E-01	6.066E-04	9.691E-01	1.110E-15	+	9.697E-01	1.133E-03	+
L10	9.715E-01	6.759E-04	9.775E-01	1.110E-15	-	9.688E-01	2.672E-03	+
L11	9.789E-01	1.360E-16	9.789E-01	5.551E-16	+	9.788E-01	4.199E-04	+
L12	9.788E-01	5.045E-04	9.775E-01	1.110E-15	+	9.764E-01	1.007E-03	+
W/T/L	-/-/-		6/2/5			11/2/0		
p-value	-		8.529E-01			1.328E-03		
$P_1(20)$	mean	std	mean	std		mean	std	
L0	9.521E-01	2.395E-03	9.474E-01	9.992E-16	+	9.362E-01	4.477E-03	+
L1	9.337E-01	2.333E-03	9.279E-01	0.000E+00	+	9.169E-01	5.616E-03	+
L2	9.541E-01	1.761E-03	9.495E-01	8.882E-16	+	9.478E-01	2.695E-03	+
L3	9.339E-01	3.630E-03	9.439E-01	8.882E-16	-	9.038E-01	6.053E-03	+
L4	9.332E-01	3.828E-03	9.381E-01	1.110E-15	-	9.055E-01	6.483E-03	+
L5	9.546E-01	1.345E-03	9.440E-01	0.000E+00	+	9.487E-01	3.237E-03	+
L6	9.471E-01	4.004E-03	9.307E-01	0.000E+00	+	9.188E-01	4.969E-03	+
L7	9.442E-01	2.252E-03	9.324E-01	0.000E+00	+	9.287E-01	4.410E-03	+
L8	9.531E-01	2.157E-03	9.472E-01	0.000E+00	+	9.434E-01	5.643E-03	+
L9	9.440E-01	3.209E-03	9.378E-01	7.772E-16	+	9.241E-01	4.673E-03	+
L10	9.433E-01	3.343E-03	9.412E-01	6.661E-16	+	9.245E-01	4.030E-03	+
L11	9.531E-01	2.225E-03	9.417E-01	0.000E+00	+	9.451E-01	2.300E-03	+
L12	9.476E-01	2.713E-03	9.398E-01	5.551E-16	+	9.258E-01	4.768E-03	+
W/T/L	-/-/-		10/0/2			13/0/0		
p-value	-		1.266E-02			8.308E-04		
$P_1(25)$	mean	std	mean	std		mean	std	
L0	9.105E-01	3.525E-03	8.925E-01	0.000E+00	+	8.775E-01	7.431E-03	+
L1	8.849E-01	3.788E-03	8.714E-01	0.000E+00	+	8.485E-01	7.553E-03	+
L2	9.133E-01	3.101E-03	8.917E-01	0.000E+00	+	8.967E-01	6.628E-03	+
L3	8.422E-01	2.859E-03	8.679E-01	0.000E+00	-	8.202E-01	5.215E-03	+
L4	8.428E-01	2.958E-03	8.541E-01	0.000E+00	-	8.196E-01	6.714E-03	+
L5	9.152E-01	2.983E-03	8.973E-01	9.992E-16	+	8.964E-01	1.097E-02	+
L6	8.727E-01	4.348E-03	8.627E-01	5.551E-16	+	8.464E-01	6.551E-03	+
L7	8.972E-01	4.704E-03	8.790E-01	6.661E-16	+	8.645E-01	9.067E-03	+
L8	9.114E-01	4.164E-03	8.942E-01	0.000E+00	+	8.891E-01	7.318E-03	+
L9	8.782E-01	3.511E-03	8.645E-01	0.000E+00	+	8.521E-01	5.392E-03	+
L10	8.792E-01	3.449E-03	8.855E-01	6.661E-16	-	8.511E-01	5.959E-03	+
L11	9.130E-01	3.509E-03	9.013E-01	0.000E+00	+	8.919E-01	6.354E-03	+
L12	8.963E-01	4.436E-03	8.681E-01	7.772E-16	+	8.605E-01	5.709E-03	+
W/T/L	-/-/-		10/0/3			13/0/0		
p-value	-		2.135E-02			8.308E-04		

Table 6.16: Comparison between ISE, SUGGA, and LSHADE under wind profile P_2.

	ISE		SUGGA			LSHADE		
$P_2(15)$	mean	std	mean	std		mean	std	
L0	9.717E-01	2.330E-03	9.615E-01	1.221E-15	+	9.661E-01	4.618E-03	+
L1	9.496E-01	1.872E-03	9.591E-01	0.000E+00	-	9.445E-01	3.833E-03	+
L2	9.567E-01	1.656E-03	9.494E-01	0.000E+00	+	9.523E-01	3.378E-03	+
L3	9.504E-01	2.478E-03	9.489E-01	0.000E+00	+	9.447E-01	4.651E-03	+
L4	9.561E-01	1.961E-03	9.570E-01	0.000E+00	-	9.513E-01	3.380E-03	+
L5	9.669E-01	2.403E-03	9.591E-01	0.000E+00	+	9.599E-01	3.113E-03	+
L6	9.678E-01	1.286E-03	9.612E-01	5.551E-16	+	9.637E-01	2.648E-03	+
L7	9.616E-01	2.121E-03	9.617E-01	0.000E+00	=	9.564E-01	4.287E-03	+
L8	9.646E-01	1.958E-03	9.631E-01	0.000E+00	+	9.596E-01	3.539E-03	+
L9	9.620E-01	2.041E-03	9.555E-01	0.000E+00	+	9.560E-01	4.706E-03	+
L10	9.648E-01	2.269E-03	9.634E-01	0.000E+00	+	9.593E-01	3.385E-03	+
L11	9.705E-01	2.482E-03	9.637E-01	6.661E-16	+	9.644E-01	4.455E-03	+
L12	9.685E-01	1.636E-03	9.630E-01	1.221E-15	+	9.632E-01	3.842E-03	+
W/T/L	-/-/-		10/1/2			13/0/0		
p-value	-		1.802E-02			8.308E-04		
$P_2(20)$	mean	std	mean	std		mean	std	
L0	9.115E-01	2.973E-03	9.002E-01	6.661E-16	+	8.977E-01	6.081E-03	+
L1	8.747E-01	2.595E-03	8.969E-01	0.000E+00	-	8.612E-01	6.298E-03	+
L2	8.923E-01	2.357E-03	8.970E-01	8.882E-16	-	8.840E-01	5.019E-03	+
L3	8.732E-01	2.516E-03	9.020E-01	8.882E-16	-	8.624E-01	7.637E-03	+
L4	8.925E-01	2.237E-03	8.950E-01	5.551E-16	-	8.832E-01	5.052E-03	+
L5	8.972E-01	2.285E-03	8.882E-01	6.661E-16	+	8.874E-01	6.401E-03	+
L6	8.984E-01	2.624E-03	8.986E-01	0.000E+00	=	8.863E-01	7.444E-03	+
L7	8.949E-01	3.131E-03	8.774E-01	0.000E+00	+	8.821E-01	6.848E-03	+
L8	9.037E-01	2.533E-03	9.014E-01	7.772E-16	+	8.915E-01	7.643E-03	+
L9	8.955E-01	3.419E-03	8.864E-01	0.000E+00	+	8.814E-01	7.598E-03	+
L10	9.026E-01	2.575E-03	9.042E-01	0.000E+00	-	8.915E-01	7.786E-03	+
L11	9.065E-01	2.808E-03	9.066E-01	6.661E-16	=	8.959E-01	6.615E-03	+
L12	9.069E-01	3.604E-03	9.003E-01	0.000E+00	+	8.915E-01	7.676E-03	+
W/T/L	-/-/-		6/2/5			13/0/0		
p-value	-		4.170E-01			8.308E-04		
$P_2(25)$	mean	std	mean	std		mean	std	
L0	8.431E-01	2.321E-03	8.333E-01	0.000E+00	+	8.260E-01	5.456E-03	+
L1	7.955E-01	2.480E-03	8.185E-01	0.000E+00	-	7.819E-01	5.904E-03	+
L2	8.201E-01	2.520E-03	8.333E-01	0.000E+00	-	8.086E-01	7.008E-03	+
L3	7.956E-01	2.702E-03	8.265E-01	0.000E+00	-	7.806E-01	8.221E-03	+
L4	8.213E-01	2.168E-03	8.235E-01	0.000E+00	-	8.083E-01	5.164E-03	+
L5	8.336E-01	2.762E-03	8.233E-01	0.000E+00	+	8.214E-01	4.329E-03	+
L6	8.271E-01	3.012E-03	8.294E-01	0.000E+00	-	8.114E-01	6.172E-03	+
L7	8.207E-01	2.988E-03	8.296E-01	5.551E-16	-	8.051E-01	5.646E-03	+
L8	8.333E-01	2.682E-03	8.298E-01	1.110E-15	+	8.179E-01	8.515E-03	+
L9	8.205E-01	2.911E-03	8.184E-01	0.000E+00	+	8.025E-01	8.439E-03	+
L10	8.328E-01	2.823E-03	8.281E-01	5.551E-16	+	8.192E-01	7.579E-03	+
L11	8.417E-01	2.814E-03	8.293E-01	0.000E+00	+	8.284E-01	7.124E-03	+
L12	8.381E-01	2.568E-03	8.337E-01	0.000E+00	+	8.194E-01	1.008E-02	+
W/T/L	-/-/-		7/0/6			13/0/0		
p-value	-		5.830E-01			8.308E-04		

Table 6.17: Comparison between ISE, SUGGA, and LSHADE under wind profile P_3.

	ISE		SUGGA			LSHADE		
$P_3(15)$	mean	std	mean	std		mean	std	
L0	9.933E-01	4.355E-04	9.902E-01	1.221E-15	+	9.891E-01	2.963E-03	+
L1	9.904E-01	6.608E-04	9.858E-01	1.221E-15	+	9.852E-01	2.761E-03	+
L2	9.933E-01	4.105E-04	9.913E-01	7.772E-16	+	9.914E-01	2.316E-03	+
L3	9.886E-01	7.289E-04	9.867E-01	6.661E-16	+	9.833E-01	2.292E-03	+
L4	9.886E-01	7.501E-04	9.838E-01	7.772E-16	+	9.835E-01	2.291E-03	+
L5	9.934E-01	3.848E-04	9.903E-01	7.772E-16	+	9.914E-01	1.910E-03	+
L6	9.917E-01	1.030E-03	9.878E-01	7.772E-16	+	9.837E-01	2.964E-03	+
L7	9.920E-01	5.126E-04	9.868E-01	0.000E+00	+	9.871E-01	2.339E-03	+
L8	9.933E-01	5.274E-04	9.909E-01	7.772E-16	+	9.904E-01	2.295E-03	+
L9	9.911E-01	5.036E-04	9.907E-01	1.110E-15	+	9.866E-01	2.691E-03	+
L10	9.910E-01	5.917E-04	9.870E-01	9.992E-16	+	9.860E-01	3.273E-03	+
L11	9.934E-01	3.898E-04	9.902E-01	7.772E-16	+	9.909E-01	2.028E-03	+
L12	9.919E-01	1.021E-03	9.846E-01	1.110E-15	+	9.849E-01	3.435E-03	+
W/T/L	-/-/-		13/0/0			13/0/0		
p-value	-		8.308E-04			8.308E-04		
$P_3(20)$	mean	std	mean	std		mean	std	
L0	9.815E-01	2.674E-03	9.670E-01	9.992E-16	+	9.591E-01	5.656E-03	+
L1	9.767E-01	2.828E-03	9.660E-01	6.661E-16	+	9.502E-01	5.999E-03	+
L2	9.820E-01	2.519E-03	9.758E-01	5.551E-16	+	9.666E-01	3.817E-03	+
L3	9.708E-01	3.870E-03	9.678E-01	0.000E+00	+	9.477E-01	6.553E-03	+
L4	9.717E-01	3.268E-03	9.699E-01	5.551E-16	+	9.502E-01	5.984E-03	+
L5	9.825E-01	2.529E-03	9.721E-01	5.551E-16	+	9.665E-01	5.394E-03	+
L6	9.682E-01	3.803E-03	9.651E-01	0.000E+00	+	9.449E-01	4.928E-03	+
L7	9.786E-01	3.401E-03	9.655E-01	7.772E-16	+	9.551E-01	6.216E-03	+
L8	9.820E-01	2.562E-03	9.712E-01	9.992E-16	+	9.642E-01	5.373E-03	+
L9	9.771E-01	4.140E-03	9.769E-01	6.661E-16	=	9.550E-01	4.354E-03	+
L10	9.777E-01	3.321E-03	9.682E-01	5.551E-16	+	9.543E-01	5.503E-03	+
L11	9.823E-01	2.777E-03	9.776E-01	1.332E-15	+	9.637E-01	5.745E-03	+
L12	9.709E-01	3.757E-03	9.572E-01	6.661E-16	+	9.486E-01	4.253E-03	+
W/T/L	-/-/-		12/1/0			13/0/0		
p-value	-		8.308E-04			8.308E-04		
$P_3(25)$	mean	std	mean	std		mean	std	
L0	9.563E-01	5.593E-03	9.488E-01	5.551E-16	+	9.240E-01	5.844E-03	+
L1	9.457E-01	4.554E-03	9.327E-01	1.110E-15	+	9.063E-01	7.352E-03	+
L2	9.559E-01	5.087E-03	9.439E-01	0.000E+00	+	9.290E-01	7.121E-03	+
L3	9.367E-01	5.259E-03	9.353E-01	0.000E+00	+	9.061E-01	5.577E-03	+
L4	9.377E-01	3.943E-03	9.394E-01	0.000E+00	-	9.118E-01	4.646E-03	+
L5	9.570E-01	5.269E-03	9.454E-01	8.882E-16	+	9.290E-01	8.546E-03	+
L6	9.343E-01	4.777E-03	9.284E-01	1.110E-15	+	9.033E-01	5.214E-03	+
L7	9.506E-01	6.830E-03	9.418E-01	0.000E+00	+	9.145E-01	7.358E-03	+
L8	9.559E-01	4.040E-03	9.472E-01	0.000E+00	+	9.277E-01	5.014E-03	+
L9	9.478E-01	4.796E-03	9.456E-01	8.882E-16	+	9.159E-01	5.727E-03	+
L10	9.482E-01	4.923E-03	9.439E-01	5.551E-16	+	9.186E-01	4.651E-03	+
L11	9.559E-01	5.695E-03	9.543E-01	0.000E+00	+	9.289E-01	6.396E-03	+
L12	9.359E-01	3.364E-03	9.177E-01	5.551E-16	+	9.081E-01	5.093E-03	+
W/T/L	-/-/-		12/0/1			13/0/0		
p-value	-		1.667E-03			8.308E-04		

Chapter 7

Discussions

7.1 Discussions on spatial information sampling algorithm

To further analyze the characteristics of SIS and prove the effectiveness of the intelligent scheme, we discussed the parameters, individual search trajectory, population diversity, and time complexity of SIS.

7.1.1 Discussion of parameters and mechanisms

To further validate the effectiveness of the intelligent scheme, we captured two parts of the SIS for discussion. First, the most important thing to verify is whether the intelligent scheme works as expected, so we designed a set of controlled trials. We proposed the SIS algorithm with a randomized deflation mechanism, whose data are detailed in column "Random" in Table 7.1. The difference between the randomized

Table 7.1: A discussion of the parameters and mechanisms of SIS on CEC 2017 D=30.

	β=0.1		β=0.05			β=0.075			β=0.125			β=0.15			Random		
	mean	std	mean	std		mean	std		mean	std		mean	std		mean	std	
F1	1.410E+03	2.346E+03	4.349E+03	5.027E+03	+	4.540E+03	5.083E+03	+	5.797E+03	5.629E+03	+	4.035E+03	4.767E+03	+	4.916E+09	1.346E+10	+
F3	2.727E+03	1.536E+04	2.308E+04	4.289E+04	+	1.266E+04	3.508E+04	+	2.233E+03	1.402E+04	-	2.254E+03	1.610E+04	-	4.125E+04	3.884E+04	+
F4	8.332E+01	2.233E+01	7.936E+01	3.594E+01	-	8.448E+01	2.903E+01	+	9.150E+01	3.184E+01	+	8.465E+01	3.586E+01	+	1.103E+03	2.447E+03	+
F5	8.301E+01	2.056E+01	9.267E+01	2.309E+01	+	9.509E+01	2.693E+01	+	1.004E+02	2.704E+01	+	9.832E+01	2.801E+01	+	1.536E+02	9.069E+01	+
F6	2.365E+00	2.211E+00	1.076E+00	1.290E+00	-	2.291E+00	2.135E+00	-	3.088E+00	3.228E+00	+	4.019E+00	6.249E+00	+	2.172E+01	2.180E+01	+
F7	1.280E+02	2.421E+01	1.371E+02	3.199E+01	+	1.367E+02	2.386E+01	+	1.410E+02	3.213E+01	+	1.375E+02	2.786E+01	+	3.079E+02	3.025E+02	+
F8	8.600E+01	1.639E+01	9.889E+01	2.743E+01	+	9.469E+01	2.433E+01	+	9.575E+01	2.250E+01	+	9.921E+01	2.174E+01	+	1.493E+02	8.679E+01	+
F9	1.389E+01	1.419E+01	1.092E+01	1.383E+01	-	1.997E+01	2.624E+01	+	2.102E+01	2.220E+01	+	2.412E+01	3.336E+01	+	1.926E+03	3.105E+03	+
F10	3.403E+03	8.538E+02	4.421E+03	1.964E+03	+	3.641E+03	9.946E+02	+	3.520E+03	7.726E+02	+	3.534E+03	6.980E+02	+	4.654E+03	1.856E+03	+
F11	1.258E+02	4.284E+01	1.301E+02	5.504E+01	+	1.478E+02	4.912E+01	+	1.434E+02	4.742E+01	+	1.409E+02	4.590E+01	+	1.068E+03	1.969E+03	+
F12	5.764E+05	4.631E+05	6.679E+05	7.337E+05	+	5.871E+05	5.274E+05	+	8.761E+05	8.519E+05	+	7.201E+05	6.329E+05	+	2.830E+08	1.151E+09	+
F13	5.538E+04	2.919E+04	7.928E+04	5.807E+04	+	8.058E+04	3.881E+04	+	9.276E+04	6.551E+04	+	7.772E+04	3.584E+04	+	1.834E+08	5.393E+08	+
F14	2.614E+03	2.374E+03	2.653E+03	3.290E+03	+	3.368E+03	2.777E+03	+	3.243E+03	3.246E+03	+	3.481E+03	4.610E+03	+	9.606E+04	1.857E+05	+
F15	3.798E+04	2.242E+04	6.186E+04	3.984E+04	+	5.649E+04	2.958E+04	+	4.924E+04	2.593E+04	+	6.020E+04	4.571E+04	+	3.074E+07	7.290E+07	+
F16	6.740E+02	2.050E+02	7.046E+02	2.237E+02	+	7.073E+02	2.319E+02	+	7.029E+02	2.582E+02	+	7.321E+02	2.604E+02	+	1.271E+03	6.472E+02	+
F17	1.981E+02	1.135E+02	2.608E+02	1.322E+02	+	2.596E+02	1.627E+02	+	2.593E+02	1.495E+02	+	2.902E+02	1.557E+02	+	4.819E+02	3.569E+02	+
F18	1.053E+05	5.129E+04	1.418E+05	7.727E+04	+	1.398E+05	8.530E+04	+	1.682E+05	1.351E+05	+	1.380E+05	9.719E+04	+	1.003E+06	2.002E+06	+
F19	1.636E+05	9.184E+04	1.214E+05	7.624E+04	-	1.364E+05	7.089E+04	-	1.297E+05	6.357E+04	-	1.200E+05	6.092E+04	-	4.350E+07	1.231E+08	+
F20	3.986E+02	1.292E+02	4.480E+02	1.727E+02	+	4.136E+02	1.564E+02	+	4.302E+02	1.454E+02	+	4.469E+02	1.742E+02	+	5.252E+02	1.971E+02	+
F21	2.851E+02	1.843E+01	2.892E+02	1.923E+01	+	2.914E+02	2.163E+01	+	2.969E+02	2.025E+01	+	2.940E+02	2.133E+01	+	3.582E+02	7.757E+01	+
F22	1.000E+02	1.611E-03	2.191E+02	8.296E+02	+	1.003E+02	8.027E-01	+	1.001E+02	5.840E-01	+	1.003E+02	8.940E-01	+	7.208E+02	1.436E+03	+
F23	4.259E+02	1.791E+01	4.345E+02	2.417E+01	+	4.404E+02	3.115E+01	+	4.449E+02	3.128E+01	+	4.475E+02	3.264E+01	+	5.258E+02	1.239E+02	+
F24	4.906E+02	1.371E+01	4.970E+02	1.966E+01	+	4.966E+02	2.547E+01	+	5.053E+02	1.946E+01	+	4.981E+02	2.527E+01	+	6.081E+02	1.649E+02	+
F25	3.867E+02	1.992E+00	3.867E+02	1.663E+00	-	3.875E+02	3.332E+00	+	3.879E+02	4.822E+00	+	3.866E+02	1.410E+00	-	4.105E+02	1.020E+02	+
F26	1.554E+03	6.748E+02	1.737E+03	5.498E+02	+	1.903E+03	4.911E+02	+	1.665E+03	6.495E+02	+	1.813E+03	5.795E+02	+	2.056E+03	8.251E+02	+
F27	5.161E+02	1.368E+01	5.133E+02	1.080E+01	-	5.157E+02	1.218E+01	-	5.188E+02	1.278E+01	+	5.237E+02	1.333E+01	+	5.854E+02	1.490E+02	+
F28	3.384E+02	4.711E+01	3.485E+02	5.564E+01	+	3.400E+02	5.556E+01	+	3.560E+02	5.384E+01	+	3.529E+02	5.516E+01	+	5.389E+02	5.145E+02	+
F29	7.445E+02	1.148E+02	7.468E+02	1.487E+02	+	7.964E+02	1.776E+02	+	7.730E+02	1.225E+02	+	8.283E+02	1.475E+02	+	1.080E+03	4.317E+02	+
F30	5.663E+05	4.060E+05	5.059E+05	3.584E+05	-	4.939E+05	3.832E+05	-	4.960E+05	2.914E+05	-	5.301E+05	4.285E+05	-	2.276E+07	6.653E+07	+
$W/T/L$	-/-/-		22/0/7			25/0/4			26/0/3			25/0/4			29/0/0		

deflation mechanism and the intelligent scheme is shown in equation Eq. (7.1).

$$(c)\begin{cases}(a)\begin{cases}\delta x^{t+1} = (1+b)\cdot\delta x^{t} \\ o^{t+1} = L_m\end{cases} & \text{if } R > 0.5 \\ (b)\begin{cases}\delta x^{t+1} = (1-b)\cdot\delta x^{t} \\ o^{t+1} = R_m\end{cases} & \text{if } R < 0.5\end{cases} \tag{7.1}$$

where R is a random number with a value range between 0 and 1. A comparison of the data in the table shows that the intelligent scheme crushes the randomized deflation mechanism in terms of performance. Moreover, in the Wilcoxon rank-sum test, the $W/T/L$ obtained by SIS compared with Random is 29/0/0. The above results fully demonstrate that SIS with an intelligent scheme has a significant advantage over SIS with a random deflation mechanism. Thus, the effectiveness of the intelligent scheme used by SIS is proven.

The second part is a discussion of the hyper-parameter b. Since b directly controls the expansion and contraction magnitude of the SIS population, the adjustment of b directly leads to changes in the performance of the algorithm. Therefore, we discuss β in b in order to demonstrate that the intelligent scheme plays a role in the operation of the algorithm on the one hand and to find the optimal β value on the other hand. From Table 7.1, it can be found that the mean value of SIS at β=0.1 has a great advantage relative to other values. In addition, the results of the Wilcoxon rank-sum test showed that the $W/T/L$ at β=0.1 is 12/13/4, 11/17/1, 13/13/3, and 13/13/3 compared to β=0.05, β=0.075, β=0.125, and β=0.15, respectively. The discussion for the β demonstrated the effect of the magnitude of population expansion and contraction on the performance of the algorithm. This is further proof of the important role played

by the intelligent scheme.

7.1.2 Search trajectory

Fig. 7.1 depicts SIS's landscape search trajectory in two dimensions in CEC2017 on F3, F4, and F10. The lines in the figure are contour lines of fitness value, and the redder the line color, the greater the fitness value. In F3, we recorded images at 2, 100, and 200 iterations, respectively. It can be found that the population keeps the trend of narrowing the search scope on F3, and the population eventually converges to a minimum range. The search trajectory on F3 highlights the exploitation ability of SIS. In F4, we recorded images at 102, 105, and 200 iterations, respectively. It can be found that the search range of the population is expanding from the 102th iteration to the 105th iteration, but after 200 iterations, the population is still reduced to a minimum range. F4 shows that exploration ability is emphasized in the middle of iteration and exploitation ability is emphasized in the latter stage of iteration. In F10, we recorded images at 99, 102, and 200 iterations, respectively. It can be found that the search range of the SIS population is expanded from the 99th iteration to the 102th iteration, and even to the 200th iteration, its population still maintains a certain search range. The above results show that exploration ability is emphasized in F10. The search trajectories of SIS on F3, F4, and F10 fully show that SIS can switch exploitation and exploration independently according to different solution space environments, which proves the effectiveness of the intelligent scheme.

7.1.3 Population diversity of spatial information sampling algorithm

Population diversity is one of the important ways to judge the exploitation and exploration of algorithms. Generally speaking, the greater the diversity value, the more the algorithm is inclined to exploration, otherwise, the algorithm is inclined to ex-

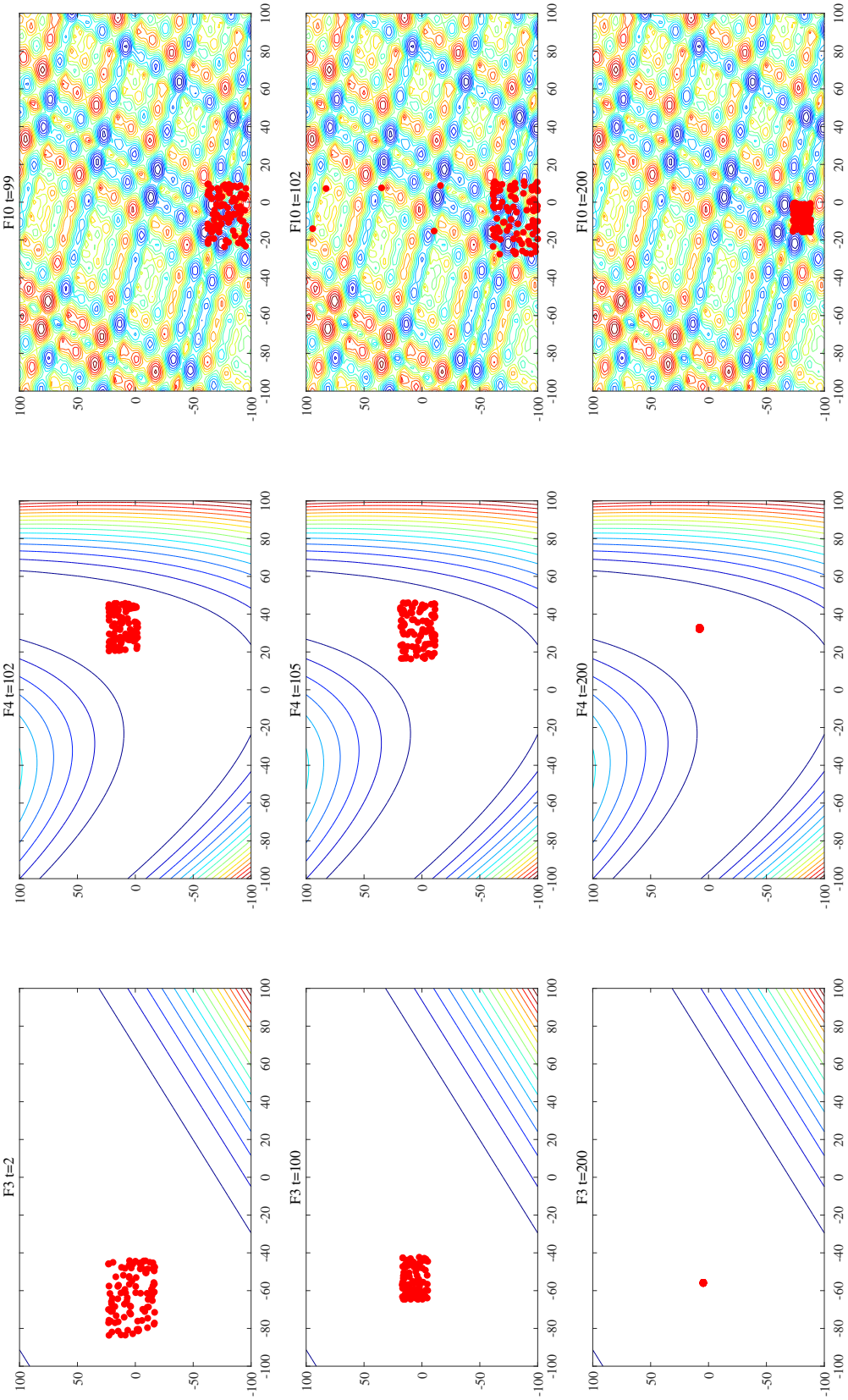

Figure 7.1: Search history of individuals of SIS in 2 dimensions in CEC2017.

ploitation. The formula for population diversity based on distance is as follows:

$$u = \frac{1}{N}\sqrt{\sum_{i=1}^{N}\left(\|x_i - x_{mean}\|\right)^2} \tag{7.2}$$

where u is the population diversity. N is population size, and x_i is the ith individual. x_{mean}, which is calculated as $x_{mean} = \frac{1}{N}\sum_{i=1}^{N} x_i$ is the average of the population.

Fig. 7.2 depicts the diversity of SIS, DE, and HGSA in 30 dimensions in CEC2017 on F3, F16, and F24. The above three algorithms are all outstanding algorithms, and their diversity is representative. It can be seen that although the diversity of DE and HGSA is different, there is a trend of decreasing diversity more or less. However, the diversity of SIS remains unchanged because of its special population construction mechanism. This characteristic makes SIS maintain the balance of exploitation and exploration at the later stages of iteration. In other words, due to the intelligent scheme, SIS can maintain a good balance between exploitation and exploration at any time of iteration.

7.1.4 Computational complexity of spatial information sampling algorithm

The preceding experiments demonstrated that SIS is effective. The following is an examination of the time complexity of SIS:

(1) Population initialization needs $O(N)$, where N is the population size;

(2) Evaluating fitness of each individual's needs $O(N)$;

(3) Sorting points require $O(N)$;

(4) New individual generated needs $O(N)$;

(5) Boundary detection needs $O(N)$.

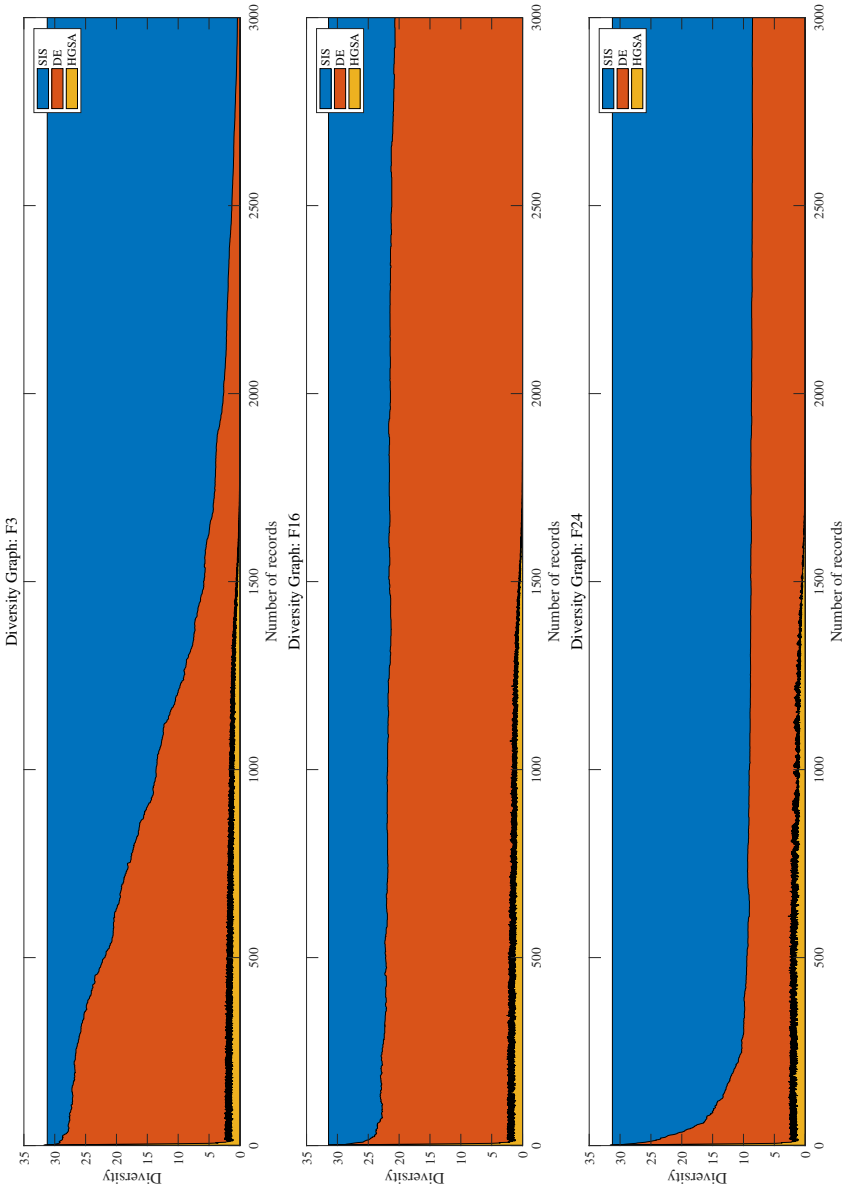

Figure 7.2: Diversity of SIS, DE and HGSA in 30 dimensions in CEC2017.

The total time complexity of SIS after T iterations is:

$$\begin{aligned} & O(N) + T \cdot [O(N) + O(N) + O(N) + O(N)] \\ & = O(N) + 4 \cdot T \cdot O(N) \\ & = (4T + 1) \cdot O(N) \end{aligned} \tag{7.3}$$

As a result, SIS's time complexity is $O(N)$.

7.2 Discussions on improved spherical evolution

This section demonstrates that SE has a strong exploration capability from both PIN and diversity perspectives. All statistics were performed at IEEE CEC2017 [39], a set of standard functions widely used to test algorithm performance.

7.2.1 Validation of population interaction network for spherical evolution

Table 7.2: Fitting results of SE.

	Poisson		Power law	
	SSE	R^2	*SSE*	R^2
mean	**7.085E-02**	**9.835E-01**	8.323E-02	8.386E-01
std	1.856E-02	3.431E-03	3.639E-02	9.818E-02

The fitting results of SE on the IEEE CEC2017 F3 function are shown in Fig. 7.3. The degrees of the nodes are shown on the horizontal axis. The degree is the sum of the connected edges of each individual with other individuals. The statistics and fitting of the degree distribution are consistent with the literature [38]. The vertical axis displays the nodes' cumulative distribution function. From Fig. 7.3, we can see that the cumulative distribution function of the PIN fits the Poisson model relatively well compared to the power-law model. To more accurately assess which model best fits the cumulative distribution function, we compute the difference in fitting between the original data and various models using *SSE* and R^2. To obtain the original data,

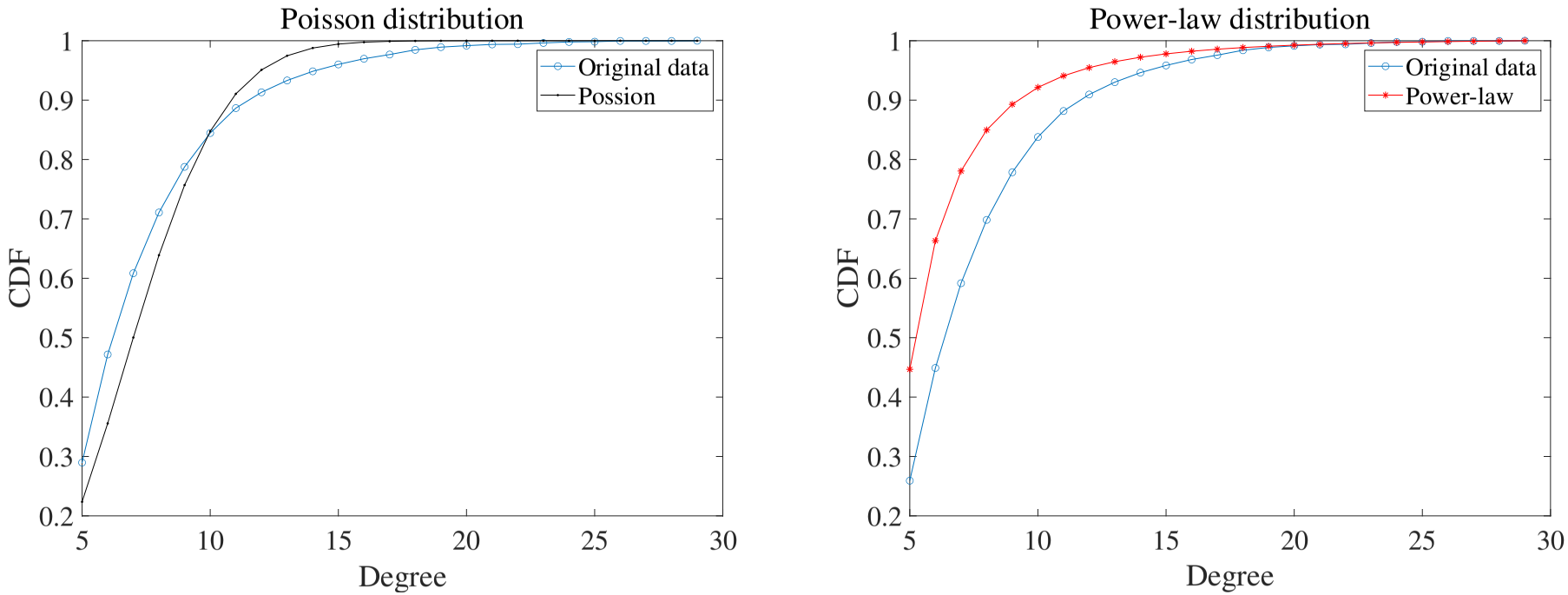

Figure 7.3: Two fitting models' cumulative distribution functions for SE.

SE is independently repeated 30 times on IEEE CEC2017 with 3000 iterations per run and a population size $N = 100$. *SSE* is the sum of squared errors between the original data and the fitted data. A smaller *SSE* indicates that the fitted data is more consistent with the original data. *SSE* works with the following formula:

$$SSE = \sum_{i=1}^{n} (y_i - \hat{y}_i)^2 \tag{7.4}$$

where n indicates the maximum degrees of nodes.y_i and $\hat{y}_i$ are the original data and fitted data, respectively.

R^2 is used to determine whether the fitted data accurately represents the original data. The fitted data can more accurately describe the original data when the value of R^2 is close to 1. R^2 works with the following formula:

$$R^2 = 1 - \frac{\sum_{i=1}^{n} (\hat{y}_i - y_i)^2}{\sum_{i=1}^{n} (y_i - \bar{y})^2} \tag{7.5}$$

where $\bar{y}$ is the mean of original data.

We compute the means of the SE results obtained for each function using these two statistical techniques, and we list the means of each algorithm in Table 7.2. From Table 7.2, we can find that the cumulative distribution function of PIN in SE fits the Poisson model more better.

7.2.2 Diversity in SE and DE

One of the crucial metrics for evaluating algorithmic exploitation and exploration is population diversity. Generally speaking, the algorithm is more inclined to explore the higher the diversity value is; otherwise, the algorithm is more inclined to exploitation.

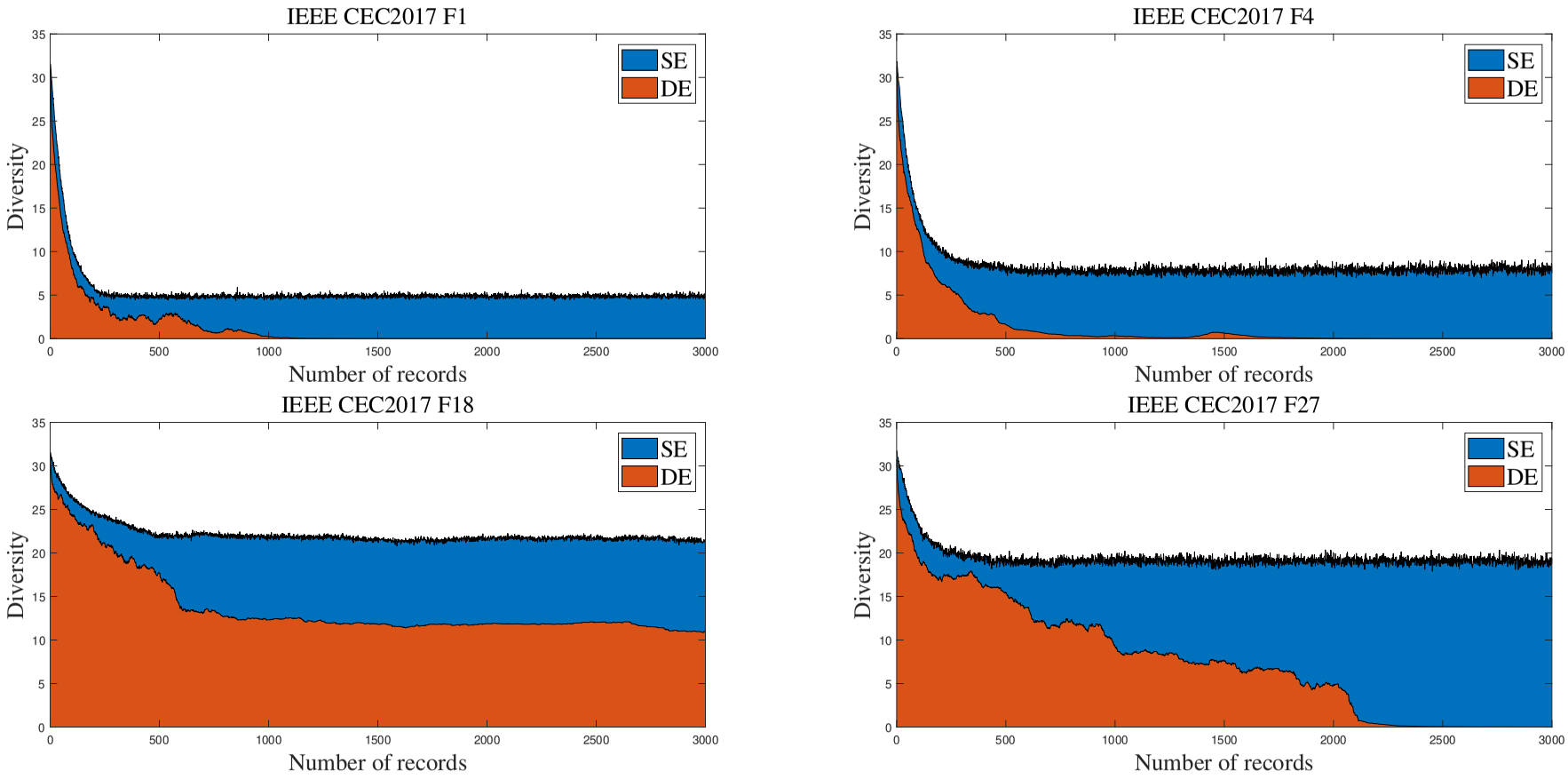

Figure 7.4: Diversity in SE and DE.

The formula for population diversity based on distance is as follows:

$$u = \frac{1}{N}\sqrt{\sum_{i=1}^{N}\left(\|X_i - X_{mean}\|\right)^2} \tag{7.6}$$

where u is the population diversity. N is population size, and X_i is the ith individual. X_{mean}, which is calculated as $X_{mean} = \frac{1}{N}\sum_{i=1}^{N} X_i$ is the average of the population.

Fig. 7.4 depicts the diversity of SE and DE in 30 dimensions in IEEE CEC2017 on F1, F4, F18, and F27. IEEE CEC2017 contains unimodal functions (F1-F3), simple multimodal functions (F4-F10), hybrid functions (F11-F20), and composition functions (F21-F30). It can be found that the population diversity of SE is much higher than that of DE from the beginning to the end of the iteration in the four categories of functions. This suggests that the SE is more oriented towards exploration than the DE.

7.2.3 Computational complexity of improved spherical evolution

The preceding experiments demonstrated that ISE is effective. The following is an examination of the time complexity of ISE:

(1) Population initialization needs $O(N)$, where N is the population size;

(2) Evaluating fitness of each individual's needs $O(N)$;

(3) Sorting points require $O(N)$;

(4) New individual generated needs $O(N)$;

(5) Boundary detection needs $O(N)$.

(6) Population update operation needs $O(N)$. The total time complexity of ISE after T iterations is:

$$
\begin{aligned}
& O(N) + T \cdot [O(N) + O(N) + O(N) + O(N) + O(N)] \\
& = O(N) + 5 \cdot T \cdot O(N) \\
& = (5T + 1) \cdot O(N)
\end{aligned}
\tag{7.7}
$$

As a result, ISE's time complexity is $O(N)$.

Chapter 8

Conclusion

In this paper, to enhance the efficiency of renewable energy conversion, we propose a spatial information sampling algorithm and an improved spherical evolution based on exploitation and exploration theory and population interaction network theory, respectively. By using the special law of the chaotic map in space, we construct the population of SIS, which is divided into two parts to respond to peripheral stimuli and internal stimuli, respectively. Through the above mechanism, the information in the solution space is obtained and analyzed, which gives SIS the ability to explore the solution space independently. The research described in this paper not only simplifies the construction of the algorithm but also promotes its further intelligence. The experimental results on the position optimization problem of wave energy converters prove the preeminent performance of SIS. Based on the population interaction network, we provide a new perspective on the design of heuristic algorithms for the wind farm layout optimization problems. Under three wind directions, three numbers of wind turbines, and 13 land constraints, the SE filtered and improved by the above scheme proved to be superior to the state-of-the-art algorithms.

Some research worthy of noting for future work includes: 1) Further improvement of SIS. 2) The intelligent scheme will be applied to more meta-heuristics to improve their performance. 3) The theoretical analysis or proof for intelligent schemes needs to be studied. 4) Other applications such as protein structure prediction [84] and

neural architecture design [85] will be attempted by SIS. 5) More meta-heuristics will be analyzed and categorized based on PIN theory. 6) Further improvement of the PIN scheme. 7) Population interaction network will be applied to more engineering optimization issues to guide the selection and improvement of meta-heuristics, such as neural architecture design [86], feature selection [87], constrained engineering problems [88], and protein structure prediction [84] will be attempted.

Bibliography

[1] M. Chumburidze, I. Basheleishvili, and A. Khetsuriani, "Dynamic programming and greedy algorithm strategy for solving several classes of graph optimization problems," *BRAIN. Broad Research in Artificial Intelligence and Neuroscience*, vol. 10, no. 1, pp. 101–107, 2019.

[2] I. Grossmann, R. Apap, B. Calfa, P. Garcia-Herreros, and Q. Zhang, "Mathematical programming techniques for optimization under uncertainty and their application in process systems engineering." *Theoretical Foundations of Chemical Engineering*, vol. 51, no. 6, pp. 893–909, 2017.

[3] G. Lan, *First-order and Stochastic Optimization Methods for Machine Learning*. Springer Nature, Switzerland, 2020.

[4] D. S. Hochba, "Approximation algorithms for np-hard problems," *ACM Sigact News*, vol. 28, no. 2, pp. 40–52, 1997.

[5] J. Pearl, *Heuristics: intelligent search strategies for computer problem solving*. Addison-Wesley Pub. Co., Inc., Reading, MA, United States, 1984.

[6] K. Hussain, M. N. M. Salleh, S. Cheng, and Y. Shi, "Metaheuristic research: a comprehensive survey," *Artificial Intelligence Review*, vol. 52, no. 4, pp. 2191–2233, 2019.

[7] K. Sörensen, "Metaheuristics—the metaphor exposed," *International Transactions in Operational Research*, vol. 22, no. 1, pp. 3–18, 2015.

[8] C. L. Camacho Villalón, T. Stützle, and M. Dorigo, "Grey wolf, firefly and bat algorithms: Three widespread algorithms that do not contain any novelty," in *International conference on swarm intelligence*. Springer, 2020, pp. 121–133.

[9] M. Hutson, "Has artificial intelligence become alchemy?" *Science*, vol. 360, no. 6388, pp. 478–478, 2018.

[10] M. Črepinšek, S.-H. Liu, and M. Mernik, "Exploration and exploitation in evolutionary algorithms: A survey," *ACM Computing Surveys (CSUR)*, vol. 45, no. 3, pp. 1–33, 2013.

[11] B. Morales-Castañeda, D. Zaldivar, E. Cuevas, F. Fausto, and A. Rodríguez, "A better balance in metaheuristic algorithms: Does it exist?" *Swarm and Evolutionary Computation*, vol. 54, p. 100671, 2020.

[12] R. Storn and K. Price, "Differential evolution–a simple and efficient heuristic for global optimization over continuous spaces," *Journal of global optimization*, vol. 11, no. 4, pp. 341–359, 1997.

[13] X.-S. Yang and S. Deb, "Cuckoo search via lévy flights," in *2009 World Congress on Nature Biologically Inspired Computing (NaBIC)*, 2009, pp. 210–214.

[14] J. Kennedy and R. Eberhart, "Particle swarm optimization," in *Proceedings of ICNN'95-international conference on neural networks*, vol. 4. IEEE, 1995, pp. 1942–1948.

[15] S. Mirjalili, S. M. Mirjalili, and A. Lewis, "Grey wolf optimizer," *Advances in Engineering Software*, vol. 69, pp. 46–61, 2014.

[16] E. Rashedi, H. Nezamabadi-Pour, and S. Saryazdi, "Gsa: a gravitational search algorithm," *Information Sciences*, vol. 179, no. 13, pp. 2232–2248, 2009.

[17] A. Zhang, G. Sun, J. Ren, X. Li, Z. Wang, and X. Jia, "A dynamic neighborhood learning-based gravitational search algorithm," *IEEE Transactions on Cybernetics*, vol. 48, no. 1, pp. 436–447, 2018.

[18] Z. Xu, H. Yang, J. Li, X. Zhang, B. Lu, and S. Gao, "Comparative study on single and multiple chaotic maps incorporated grey wolf optimization algorithms," *IEEE Access*, vol. 9, pp. 77 416–77 437, 2021.

[19] J. Xu and L. Xu, "Optimal stochastic process optimizer: A new metaheuristic algorithm with adaptive exploration-exploitation property," *IEEE Access*, vol. 9, pp. 108 640–108 664, 2021.

[20] Y. Wang, Y. Yu, S. Gao, H. Pan, and G. Yang, "A hierarchical gravitational search algorithm with an effective gravitational constant," *Swarm and Evolutionary Computation*, vol. 46, pp. 118–139, 2019.

[21] S. Mirjalili, "SCA: a sine cosine algorithm for solving optimization problems," *Knowledge-Based Systems*, vol. 96, pp. 120–133, 2016.

[22] Z. Song, S. Gao, Y. Yu, J. Sun, and Y. Todo, "Multiple chaos embedded gravitational search algorithm," *IEICE Transactions on Information and Systems*, vol. 100, no. 4, pp. 888–900, 2017.

[23] Y. Yu, S. Gao, Y. Wang, Z. Lei, J. Cheng, and Y. Todo, "A multiple diversity-driven brain storm optimization algorithm with adaptive parameters," *IEEE Access*, vol. 7, pp. 126 871–126 888, 2019.

[24] S. Gao, Y. Yu, Y. Wang, J. Wang, J. Cheng, and M. Zhou, "Chaotic local search-based differential evolution algorithms for optimization," *IEEE Transactions on Systems, Man, and Cybernetics: Systems*, vol. 51, no. 6, pp. 3954–3967, 2021.

[25] Y.-J. Gong, J.-J. Li, Y. Zhou, Y. Li, H. S.-H. Chung, Y.-H. Shi, and J. Zhang, "Genetic learning particle swarm optimization," *IEEE Transactions on Cybernetics*, vol. 46, no. 10, pp. 2277–2290, 2016.

[26] H. R. R. Zaman and F. S. Gharehchopogh, "An improved particle swarm optimization with backtracking search optimization algorithm for solving continuous optimization problems," *Engineering with Computers*, pp. 1–35, 2021.

[27] Z. Hua and Y. Zhou, "Image encryption using 2D logistic-adjusted-sine map," *Information Sciences*, vol. 339, pp. 237–253, 2016.

[28] H. Liu and X. Wang, "Color image encryption using spatial bit-level permutation and high-dimension chaotic system," *Optics Communications*, vol. 284, no. 16-17, pp. 3895–3903, 2011.

[29] S. Thurner, R. Hanel, and P. Klimek, *Introduction to the theory of complex systems*. Oxford University Press, United Kingdom, 2018.

[30] I. Sohn, "Small-world and scale-free network models for iot systems," *Mobile Information Systems*, vol. 2017 (2017), Article ID 6752048, 2017.

[31] P. Holme, "Rare and everywhere: Perspectives on scale-free networks," *Nature Communications*, vol. 10, no. 1, pp. 1–3, 2019.

[32] J. Liu, H. A. Abbass, and K. C. Tan, *Evolutionary Computation and Complex Networks*. Springer International Publishing, 2019.

[33] G. Palla, I. Derényi, I. Farkas, and T. Vicsek, "Uncovering the overlapping community structure of complex networks in nature and society," *Nature*, vol. 435, no. 7043, pp. 814–818, 2005.

[34] J. Cheng, M. Ju, M. Zhou, C. Liu, S. Gao, A. Abusorrah, and C. Jiang, "A dynamic evolution method for autonomous vehicle groups in a highway scene," *IEEE Internet of Things Journal*, vol. 9, no. 2, pp. 1445–1457, 2022.

[35] N. Koroniotis, N. Moustafa, and E. Sitnikova, "A new network forensic framework based on deep learning for internet of things networks: A particle deep framework," *Future Generation Computer Systems*, vol. 110, pp. 91–106, 2020.

[36] P. Chunaev, "Community detection in node-attributed social networks: a survey," *Computer Science Review*, vol. 37, p. 100286, 2020.

[37] H. Yang, Y. Yu, J. Cheng, Z. Lei, Z. Cai, Z. Zhang, and S. Gao, "An intelligent metaphor-free spatial information sampling algorithm for balancing exploitation and exploration," *Knowledge-Based Systems*, p. 109081, 2022.

[38] X. Li, J. Li, H. Yang, Y. Wang, and S. Gao, "Population interaction network in representative differential evolution algorithms: Power-law outperforms poisson distribution," *Physica A: Statistical Mechanics and its Applications*, p. 127764, 2022.

[39] N. Awad, M. Ali, J. Liang, B. Qu, and P. Suganthan, "Problem definitions and evaluation criteria for the CEC 2017 special session and competition on single objective real-parameter numerical optimization," *Technical Report, Nanyang Technological University,*, vol. Singapore, 2016.

[40] R. Shakoor, M. Y. Hassan, A. Raheem, and Y.-K. Wu, "Wake effect modeling: A review of wind farm layout optimization using jensen's model," *Renewable and Sustainable Energy Reviews*, vol. 58, pp. 1048–1059, 2016.

[41] D. Tang, "Spherical evolution for solving continuous optimization problems," *Applied Soft Computing*, vol. 81, p. 105499, 2019.

[42] A. Clauset, C. R. Shalizi, and M. E. Newman, "Power-law distributions in empirical data," *SIAM Review*, vol. 51, no. 4, pp. 661–703, 2009.

[43] B. Drew, A. R. Plummer, and M. N. Sahinkaya, "A review of wave energy converter technology," *Proceedings of the Institution of Mechanical Engineers, Part A: Journal of Power and Energy*, vol. 223, no. 8, pp. 887–902, 2009.

[44] N. Y. Sergiienko, B. S. Cazzolato, B. Ding, and M. Arjomandi, "Three-tether axisymmetric wave energy converter: estimation of energy delivery," in *Proc. 3rd Asian Wave and Tidal Energy Conference (AWTEC), Singapore*, 2016, pp. 23–25.

[45] M. Neshat, B. Alexander, N. Y. Sergiienko, and M. Wagner, "New insights into position optimisation of wave energy converters using hybrid local search," *Swarm and Evolutionary Computation*, vol. 59, p. 100744, 2020.

[46] V. Nelson, *Wind energy: Renewable energy and the environment*. CRC Press, Boca Raton, 2009.

[47] S. R. Reddy, "Wind farm layout optimization (windflo): An advanced framework for fast wind farm analysis and optimization," *Applied Energy*, vol. 269, p. 115090, 2020.

[48] G. Gualtieri, "Comparative analysis and improvement of grid-based wind farm layout optimization," *Energy Conversion and Management*, vol. 208, p. 112593, 2020.

[49] L. Wang, A. C. Tan, and Y. Gu, "Comparative study on optimizing the wind farm layout using different design methods and cost models," *Journal of Wind Engineering and Industrial Aerodynamics*, vol. 146, pp. 1–10, 2015.

[50] Z. Liu, J. Peng, X. Hua, and Z. Zhu, "Wind farm optimization considering non-uniformly distributed turbulence intensity," *Sustainable Energy Technologies and Assessments*, vol. 43, p. 100970, 2021.

[51] G. Mosetti, C. Poloni, and B. Diviacco, "Optimization of wind turbine positioning in large windfarms by means of a genetic algorithm," *Journal of Wind Engineering and Industrial Aerodynamics*, vol. 51, no. 1, pp. 105–116, 1994.

[52] S. Grady, M. Hussaini, and M. M. Abdullah, "Placement of wind turbines using genetic algorithms," *Renewable Energy*, vol. 30, no. 2, pp. 259–270, 2005.

[53] X. Gao, H. Yang, L. Lin, and P. Koo, "Wind turbine layout optimization using multi-population genetic algorithm and a case study in hong kong offshore," *Journal of Wind Engineering and Industrial Aerodynamics*, vol. 139, pp. 89–99, 2015.

[54] A. M. Abdelsalam and M. El-Shorbagy, "Optimization of wind turbines siting in a wind farm using genetic algorithm based local search," *Renewable Energy*, vol. 123, pp. 748–755, 2018.

[55] C. Wan, J. Wang, G. Yang, and X. Zhang, "Optimal micro-siting of wind farms by particle swarm optimization," in *International Conference in Swarm Intelligence*. Springer, 2010, pp. 198–205.

[56] C. Wan, J. Wang, G. Yang, H. Gu, and X. Zhang, "Wind farm micro-siting by gaussian particle swarm optimization with local search strategy," *Renewable Energy*, vol. 48, pp. 276–286, 2012.

[57] Y. Eroğlu and S. U. Seçkiner, "Design of wind farm layout using ant colony algorithm," *Renewable Energy*, vol. 44, pp. 53–62, 2012.

[58] M. Song, K. Chen, X. Zhang, and J. Wang, "The lazy greedy algorithm for power optimization of wind turbine positioning on complex terrain," *Energy*, vol. 80, pp. 567–574, 2015.

[59] F. G. Montoya, F. Manzano-Agugliaro, S. López-Márquez, Q. Hernández-Escobedo, and C. Gil, "Wind turbine selection for wind farm layout using multi-objective evolutionary algorithms," *Expert Systems with Applications*, vol. 41, no. 15, pp. 6585–6595, 2014.

[60] T. Kunakote, N. Sabangban, S. Kumar, G. G. Tejani, N. Panagant, N. Pholdee, S. Bureerat, and A. R. Yildiz, "Comparative performance of twelve metaheuristics for wind farm layout optimisation," *Archives of Computational Methods in Engineering*, vol. 29, no. 1, pp. 717–730, 2022.

[61] H. Yang, S. Gao, R.-L. Wang, and Y. Todo, "A ladder spherical evolution search algorithm," *IEICE Transactions on Information and Systems*, vol. 104, no. 3, pp. 461–464, 2021.

[62] L. Yang, S. Gao, H. Yang, Z. Cai, Z. Lei, and Y. Todo, "Adaptive chaotic spherical evolution algorithm," *Memetic Computing*, vol. 13, no. 3, pp. 383–411, 2021.

[63] H. Yang, S. Tao, Z. Zhang, Z. Cai, and S. Gao, "Spatial information sampling: another feedback mechanism of realising adaptive parameter control in meta-heuristic algorithms," *International Journal of Bio-Inspired Computation*, vol. 19, no. 1, pp. 48–58, 2022.

[64] X. Li, K. Wang, H. Yang, S. Tao, S. Feng, and S. Gao, "Paidde: A permutation-archive information directed differential evolution algorithm," *IEEE Access*, vol. 10, pp. 50 384–50 402, 2022.

[65] Y. Yu, S. Gao, M. Zhou, Y. Wang, Z. Lei, T. Zhang, and J. Wang, "Scale-free network-based differential evolution to solve function optimization and parameter estimation of photovoltaic models," *Swarm and Evolutionary Computation*, p. 101142, 2022.

[66] H. Gu and J. Wang, "Irregular-shape wind farm micro-siting optimization," *Energy*, vol. 57, pp. 535–544, 2013.

[67] L. Chen and E. MacDonald, "A system-level cost-of-energy wind farm layout optimization with landowner modeling," *Energy Conversion and Management*, vol. 77, pp. 484–494, 2014.

[68] J. Y. Kuo, D. A. Romero, and C. H. Amon, "A mechanistic semi-empirical wake interaction model for wind farm layout optimization," *Energy*, vol. 93, pp. 2157–2165, 2015.

[69] L. Amaral and R. Castro, "Offshore wind farm layout optimization regarding wake effects and electrical losses," *Engineering Applications of Artificial Intelligence*, vol. 60, pp. 26–34, 2017.

[70] S. M. Masoudi and M. Baneshi, "Layout optimization of a wind farm considering grids of various resolutions, wake effect, and realistic wind speed and wind direction data: A techno-economic assessment," *Energy*, p. 123188, 2022.

[71] X. Ju, F. Liu, L. Wang, and W.-J. Lee, "Wind farm layout optimization based on support vector regression guided genetic algorithm with consideration of participation among landowners," *Energy Conversion and Management*, vol. 196, pp. 1267–1281, 2019.

[72] D. H. Wolpert and W. G. Macready, "No free lunch theorems for optimization," *IEEE Transactions on Evolutionary Computation*, vol. 1, no. 1, pp. 67–82, 1997.

[73] Y.-K. Wu, P.-E. Su, Y.-S. Su, T.-Y. Wu, and W.-S. Tan, "Economics- and reliability-based design for an offshore wind farm," *IEEE Transactions on Industry Applications*, vol. 53, no. 6, pp. 5139–5149, 2017.

[74] J. Schepers, *ENDOW: Validation and improvement of ECN's wake model.* Energy Research Centre of the Netherlands ECN Petten, Netherlands, 2003.

[75] B. L. Du Pont and J. Cagan, "An extended pattern search approach to wind farm layout optimization," *Journal of Mechanical Design*, vol. 134, no. 8, 2012.

[76] S. Phatak and S. S. Rao, "Logistic map: A possible random-number generator," *Physical Review E*, vol. 51, no. 4, p. 3670, 1995.

[77] S. Das and P. N. Suganthan, "Problem definitions and evaluation criteria for cec 2011 competition on testing evolutionary algorithms on real world optimization problems," *Jadavpur University, Nanyang Technological University, Kolkata*, pp. 341–359, 2010.

[78] ——, "Differential evolution: A survey of the state-of-the-art," *IEEE Transactions on Evolutionary Computation*, vol. 15, no. 1, pp. 4–31, 2011.

[79] H.-W. Fang, Y.-Z. Feng, and G.-P. Li, "Optimization of wave energy converter arrays by an improved differential evolution algorithm," *Energies*, vol. 11, no. 12, p. 3522, 2018.

[80] Z. Xu, S. Gao, H. Yang, and Z. Lei, "SCJADE: Yet another state-of-the-art differential evolution algorithm," *IEEJ Transactions on Electrical and Electronic Engineering*, vol. 16, no. 4, pp. 644–646, 2021.

[81] N. H. Awad, M. Z. Ali, P. N. Suganthan, and R. G. Reynolds, "An ensemble sinusoidal parameter adaptation incorporated with l-shade for solving cec2014

benchmark problems," in *2016 IEEE Congress on Evolutionary Computation (CEC)*, 2016, pp. 2958–2965.

[82] X. Weng, A. A. Heidari, G. Liang, H. Chen, X. Ma, M. Mafarja, and H. Turabieh, "Laplacian nelder-mead spherical evolution for parameter estimation of photovoltaic models," *Energy Conversion and Management*, vol. 243, p. 114223, 2021.

[83] J. H. Holland, "Genetic algorithms," *Scientific american*, vol. 267, no. 1, pp. 66–73, 1992.

[84] Z. Lei, S. Gao, Z. Zhang, M. Zhou, and J. Cheng, "MO4: A many-objective evolutionary algorithm for protein structure prediction," *IEEE Transactions on Evolutionary Computation*, vol. 26, no. 3, pp. 417–430, 2022.

[85] Y. Sun, B. Xue, M. Zhang, G. G. Yen, and J. Lv, "Automatically designing cnn architectures using the genetic algorithm for image classification," *IEEE Transactions on Cybernetics*, vol. 50, no. 9, pp. 3840–3854, 2020.

[86] Z. Wang, S. Gao, J. Wang, H. Yang, and Y. Todo, "A dendritic neuron model with adaptive synapses trained by differential evolution algorithm," *Computational Intelligence and Neuroscience*, vol. 2020, Article ID 2710561, 2020.

[87] X. Wang, Y. Wang, K.-C. Wong, and X. Li, "A self-adaptive weighted differential evolution approach for large-scale feature selection," *Knowledge-Based Systems*, p. 107633, 2021.

[88] F. S. Gharehchopogh, B. Farnad, and A. Alizadeh, "A modified farmland fertility algorithm for solving constrained engineering problems," *Concurrency and Computation: Practice and Experience*, vol. 33, no. 17, p. e6310, 2021.